**University of Mosul**
**College of Electronics Engineering**
**Communication Engineering Department**

# Adaptive Modulation for the MIMO-OFDM System

## Mohammed Basil Shukur

(B.Sc. in Communication Engineering)

**M.Sc. Thesis**

**in**

**Communication Engineering**

**Supervised By**

## Dr. Younis M. Abbosh

**2015 A.D.**                                    **1436 A.H.**

# Adaptive Modulation for the MIMO-OFDM System

A Thesis Submitted

By

## Mohammed Basil Shukur
(B.Sc. in Communication Engineering)

To

The Council of the College of Electronic Engineering

University of Mosul

In Partial Fulfillment of the Requirements

for the Degree of Master of Science

in

## Communication Engineering

Supervised By

## Dr. Younis M. Abbosh

**2015 A.D.**                                                  **1436 A.H.**

## *Examination Committee Certification*

We the examining committee, certify that we have read this thesis entitled (**Adaptive Modulation for the MIMO-OFDM System**) and have examined the postgraduate student (**Mohammed Basil Shukur**) in its contents and that in our opinion; it meets the standards of a thesis for the degree of Master of Science in Communication Engineering.
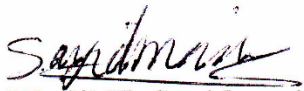
Signature: *Sayidmari*
Name: **Dr. Khalil H. Sayidmarie**
Academic Rank: Professor
(**Head of committee**)
Date:15 / 03 / 2015

Signature:
Name: **Dr. Bayez K. Al-Sulaifanie**
Academic Rank: Assistant Professor
(**Member**)
Date: 15 / 03 / 2015
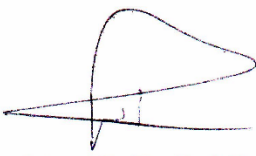
Signature:
Name: **Dr. Ibrahim Y. Dallal Bashi**
Academic Rank: Assistant Professor
(**Member**)
Date: 15 / 03 / 2015

Signature:
Name: **Dr. Younis M. Abbosh**
Academic Rank: Lecturer
(**Supervisor**)
Date: 13 / 03 / 2015

The college council, in its .................. meeting on    /    /2015, has decided to award the degree of Master of Science in Communication Engineering to the candidate.

Signature:
Name: **Dr. Khalid Khaleel Mohammed**
Academic Rank: Assistant Professor
(**Dean of the college**)
Date:    /    / 2015

Signature:
Name:
Academic Rank:
(**Council registrar**)
Date:    /    / 2015

## Supervisor's Certification

This is to certify that the work contained in the thesis entitled "Adaptive Modulation for the MIMO-OFDM System", by Mohammed Basil Shukur, has been carried out in Mosul University under my supervision in partial requirement of the M.Sc. degree in communication engineering.

Signature:
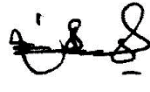
Supervisor: **Dr. Younis M Abbosh**
Date: **30** / 11 **/2014**

## Linguistic Advisor Certification

I certify that I have revised the M.Sc. thesis entitled "Adaptive Modulation for the MIMO-OFDM System", linguistically and that the language errors have been corrected.

Signature:

Linguistic Adviser's Name: Prof. Dr. Abbas Jawdat Rahim
Date: **25**/ **12**/2014

## Post-Graduate Committee Certification

In view of the recommendations of the supervisor and the linguistic adviser, I forward this thesis for debate.

Signature:

Committee Chairman Name:
Date:     /     /2014

## Department Head Certification

In view of the available recommendation, I forward this thesis for debate by the examining committee.

Signature:

Department Head's Name: Dr. Mahmod Ahmed Mahmod
Date:     /     /2014

## Publications

Some of the important results obtained in this work have appeared in the following publication:-

"Data Throughput Maximization Using Adaptive Modulation for Single Carrier Base Band Transmission System" International Journal of Emerging Technology and Advanced Engineering Volume 4, Issue 10, October 9-12-2014

# Acknowledgements

# Abstract

In the past few years, wireless communication technology has witnessed huge developments which have given rise to many new applications leading to transmitting and receiving high data rates without location or movement constraints.

In recent years, orthogonal frequency division multiplexing (OFDM) has proved to be one of the most multicarrier successful techniques. The OFDM technique carries out high data rates as well as spatial multiplexing so that multiple antennas can be used at the transmitter and at the receiver. This configuration of antennas is called Multiple Input Multiple Output (MIMO) antennas.

In addition to the MIMO and OFDM techniques, adaptive modulation is another important technique that is used to increase the data rate. The adaptive modulation can be carried out with accepted bit error rate (BER) and maximum data throughput on condition that the channel SNR and the Doppler frequency shift are well estimated. Therefore, this work has been conducted to investigate the best modulation scheme that can be used with the instantaneous Rayleigh fading channel corrupted by AWGN and for different speeds of the receiver. Three different communication systems have been considered in this project: the single carrier base band transmission system, the OFDM system and the 2*2 MIMO-OFDM system. Performances of these three systems were evaluated concerning BER and data throughput for different speeds of the receiver, and adaptation was decided accordingly. Switching to the best modulation scheme according to the instantaneous channel conditions, to achieve the desired BER, depends on the values of the signal to noise ratio (SNR) and the Doppler frequency shifts. This was achieved by using a look-up table constructed from the obtained results.

# Contents

# List of Figures

# List of Tables

# List of Abbreviations

| | |
|---|---|
| 3G | Third Generation |
| 4G | Fourth Generation |
| ADSL | Asymmetric Digital Subscriber Line |
| AMC | Adaptive Modulation and Coding |
| AMUD | Adaptive Multiuser Detection |
| ANSI's | American National Standard Institute's |
| AWGN | Additive White Gaussian Noise |
| BER | Bit Error Rate |
| BLER | Block Error Rate |
| BPSK | Binary Phase Shift Keying |
| BRANs | Broadband Radio Access Networks |
| *BW* | Bandwidth |
| CDMA | Code-Division Multiple Access |
| CP | Cyclic-Prefix |
| CQI | Channel Quality Indicator |
| CRC | Error Detection And Correction |
| DAB | Digital Audio Broadcasting |
| DFT | Discrete Fourier Transform |
| DMT | Discrete Multi-Tone |
| DVB | Digital Video Broadcasting |
| DVB-H | Digital Video Broadcasting for Handheld Terminals |
| DVB-T | Digital Video Broadcasting for Terrestrial Television |

| | |
|---|---|
| EESM | Exponential Effective SNR Mapping |
| ETSI's | European Telecommunication Standard Institute's |
| F.T | Fourier Transform |
| FDMA | Frequency-Division Multiple Access |
| FFT | Fast Fourier Transform |
| FLA | Fast Link Adaptation |
| GHz | Gigahertz |
| HSDPA | High-Speed Downlink Packet Access |
| ICI | Inter-Carrier Interference |
| IDFT | Inverse Discrete Fourier Transform |
| IFFT | Inverse Fast Fourier Transform |
| *Im* | Imaginary |
| ISI | Inter Symbol Interference |
| KHz | Kilohertz |
| km/h. | kilometer per hour |
| LLMS | Leaky Least Mean Square |
| LQI | link quality indicator |
| LTE | Long Term Evolution |
| MHz | Megahertz |
| MIMO | Multiple Input Multiple Output |
| MIMO-OFDM | Multiple Input Multiple Output-Orthogonal Frequency Division Multiplexing |
| MMSE | Minimum Mean Squares Error |
| M-QAM | Multi-array Quadrature Amplitude Modulation |
| OFDM | Orthogonal Frequency Division Multiplexing |

| | |
|---|---|
| OFDMA | Orthogonal Frequency Division Multiple Access |
| ORTHOMUX | Orthogonal Multiplexing |
| PAPR | Peak-to-Average Power Ratio |
| PDF | Power Spectral Density |
| PER | Packet Error Rate |
| PSAM | pilot symbol assisted modulation |
| PSK | Phase Shift Keying |
| QAM | Quadrature Amplitude Modulation |
| QoS | Quality of Service |
| QPSK | Quadrature Phase Shift Keying |
| *Re* | Real |
| SDM | space division multiplexing |
| SISO | Single Input Single Output |
| SNR | Signal to Noise Ratio |
| TDMA | Time- Division Multiple Access |
| TTL | Time to Live |
| UMTS | Universal Mobile Telecommunications System |
| VDSL | Very high Digital Subscriber Line |
| WCDMA | Wideband Code Division Multiple Access |
| WLANs | Wireless Location Area  Networks |
| ZF | Zero Forcing |

# List of Symbols

| | |
|---|---|
| $\circledast$ | convolution operator |
| $\alpha$ | angle between directions of the receiver velocity and the arriving signal |
| $\gamma$ | signal-to-noise ratio (SNR) per bit |
| $\lambda$ | wave length |
| $\Delta f$ | subcarrier bandwidth, subcarrier spacing |
| $S(v)$ | Doppler spectrum |
| $\sigma^2$ | prediction mean power of the multipath signal |
| $a_k^{(m)}$ | modulation symbol applied to the $kth$ subcarrier during the $mth$ OFDM symbol interval |
| $\dfrac{C}{BW}$ | Normalized channel capacity |
| c | speed of light |
| $E_b$ | Signal power |
| $F(f)$ | Fourier transform of Rayleigh coefficients |
| $f^*(t)$ | complex conjugate of Rayleigh coefficients |
| $f_c$ | carrier frequency |
| $f_d$ | Doppler spread |
| $f_s$ | sampling rate |
| H | 2*2 channel matrix |
| $H_{eq}(f)$ | Fourier transform of the impulse response of the equalizer |
| $h(t)$ | impulse response of the channel |
| $h_{eq}(t)$ | impulse response of the equalizer |

| | |
|---|---|
| $h_{ij}(t)$ | Channel impulse response |
| $J_o(\bullet)$ | zero order Bessel function |
| k | free space phase constant |
| $N$ | number of samples |
| $N_R$ | receiving antenna number |
| $N_T$ | transmitting antenna number |
| $N_0$ | Noise power |
| n(t) | noise |
| R($\Delta v$) | channel time correlation function |
| $\bar{s}$ | Vector representing two transmitted signals |
| $T_{cp}$ | length of the cyclic prefix |
| $T_o$ | channel coherence time |
| $T_s$ | sampling interval |
| V$\Delta$t | distance traversed |
| $\vec{v}$ | receiver velocity |
| x(t) | transmitted signal |
| y(t) | received signal |

# Chapter One

## Adaptive Modulation for the MIMO-OFDM System

### 1.1 Introduction

In the past few years, wireless technology has developed tremendously. This development has opened new applications of wireless communication without location or movement constraints. The maximum data rates for 4G network is 1GB/s for indoor and 100MB/s for environments [1].

These high data rates for indoor and outdoor environments cannot be achieved by using single-carrier systems, because at high data rates the problem of inter-symbol interference will arise and the period of one symbol interferes with that of another symbol. The data will be highly distorted, therefore the need for multicarrier transmission systems arises [2]. Multicarrier transmissions can be achieved by dividing the available bandwidth into a number of narrow bands called sub-bands. Each sub-band is modulated by a sub-carrier and transmitted simultaneously with other sub-carriers [3].

In recent years orthogonal frequency division multiplexing (OFDM) has proved to be one of the most successful techniques. In the context of wired environments, OFDM techniques are also known as Discrete Multi-Tone (DMT) transmissions and are employed in the American National Standard Institute's (ANSI) Asymmetric Digital Subscriber Line (ADSL) and Very high Digital Subscriber Line (VDSL) standards as well as in the European Telecommunication Standard

Institute's (ETSI). In the wireless scenario, OFDM has been used by many European standards such as Digital Audio Broadcasting (DAB), Digital Video Broadcasting for Terrestrial Television (DVB-T), Digital Video Broadcasting for Handheld Terminals (DVB-H), Wireless Location Area Networks (WLANs), and Broadband Radio Access Networks (BRANs) [4,5].

Before 1971 the use of the OFDM technique was limited to the military applications because it required a bank of sinusoidal subcarrier generators and demodulators. After 1971 Weinstein and Ebert [6] suggested that modulation and demodulation processes of the OFDM system can be implemented by using Inverse Discrete Fourier Transform (IFFT) at the transmitter and Discrete Fourier Transform at the receiver, which significantly reduces the complexity of the OFDM system [4,7].

The demand for high data rates does not depend on the ODFM technique only, but on using the OFDM with spatial multiplexing. In spatial multiplexing, multiple antennas are used at the transmitter and receiver to increase the data rate [8]. Spatial multiplexing is often described as the use of multiple input multiple output (MIMO) antennas. The multiple antennas in the spatial multiplexing are used to transmit multiple parallel data streams, so as to increase the data rate. The number of data streams is equal to the minimum number of transmitter or receiver antennas [9, 10].

Adaptive modulation is another important technique used to increase the data rate beside the MIMO and the OFDM techniques, to get maximum data throughput with accepted BER [11]. The adaptive

modulation is done by estimating the channel SNR and the Doppler frequency shift [12].

The main problem in wireless communication is the effect of the Rayleigh fading channel that degrades the BER performance for the wireless communication channel. The multipath fading and the interference with other users cause a time variant (SNR) in direct contrast with the Additive White Gaussian Noise (AWGN) channel where the channel characterized by a constant noise spectral density [13].

## 1.2 <u>Review of Literatures</u>

Ballard in 1966 [14] devised a new technique for multiplex communication, in which orthogonal pulse waveforms were transmitted as simultaneous subcarriers. Information signals were carried in the form of independent amplitude modulations of each subcarrier, and were extracted by means of waveform correlation. He named his new technique ORTHOMUX (orthogonal multiplexing), which offers the following advantages

    1) High spectrum efficiency.

    2) Maximum rejection of crosstalk and noise.

    3) Information response down to zero frequency.

    4) Mixed information rates.

    5) Simple, compact equipment.

    6) Modular flexibility.

The channel estimation can be done by inserting defined symbols at known instants of time. The inserted symbols are known as pilots. The pilots should be inserted periodically. The time period of the pilot should be smaller than the coherence time in order to track the channel variation. If the pilot time period is greater than the coherence time the estimator cannot track the channel variation. Cavers in 1991 [13] proposed a pilot symbol assisted modulation (PSAM). The channel effect on the amplitude and phase of the modulated symbols can be found by using PSAM. If there is no more one path between the transmitter and receiver, the channel effect on the received signal can be removed by multiplying the received signal by the inverse of the estimated channel parameters; therefore the original transmitted pulse shape will be recovered keeping the peak to its original average ratio.

The need for communication with high data rate and accepted BER led to looking for and investigating new techniques of digital communication, and to use the available bandwidth in efficient ways. Kim et.al. in 1997 [1] tried to increase the spectrum efficiency by using a good channel estimator with high-order modulation schemes.

Cho and Yoon in 2002 [4] proposed an adaptive modulation scheme which depends on link-quality indicator (LQI) reports that can be used to maximize the data throughput. The modulation scheme of the adaptive modulator is chosen to achieve a maximum data throughput with accepted BER. The modulation scheme of the adaptive modulator is chosen according to the channel state.

In 2002 Li et.al. [15] published a paper in which two link-adaptation methods were considered. In the first method, the fixed number of weak sub-carriers which are highly attenuated was left out to improve the BER performance. According to the second method, which depends on the channel quality of each sub-carrier, the modulation level on each sub-carrier was varied to adapt to the link condition in order to improve the system throughput. The analysis and simulation results proved that the proposed link adaptation and coding scheme is effective in improving system throughput compared with the system which has fixed modulation/coding.

Jing et.al. in 2003 [16] studied a communication system that employs both the MIMO-OFDM and adaptive modulation/coding technologies. In their work, the performance of different modulation schemes including fixed modulation/coding and adaptive modulation/coding were analyzed and compared by simulation. They also proposed an adaptive modulation/coding algorithm for the multi-user MIMO-OFDM system. This adaptive allocation algorithm assigns the sub-carriers and bits for users in the system with the minimum total transmission power and targeted BER based on the time-variant MIMO channel condition. Their computer simulation results demonstrate that the proposed algorithm is simple and can have a relative low transmission power compared with the fixed BPSK, QPSK and 16QAM modulation schemes.

Al-Tittinche in 2006 [17] implemented space division multiplexing (SDM) to transmit different signals simultaneously at the

same carrier frequency. The work detected the transmitted signals using many techniques such as zero forcing, minimum mean square error with and without decision feedback and maximum likelihood decoding. Moreover, the effect of increasing the number of transmit and receive antennas was investigated.

Faezah and Sabira in 2009 [18] considered only adaptive modulation and investigated the OFDM system performance of uncoded adaptive modulation using quadrature amplitude modulation (QAM) and phase shift keying (PSK). To further enhance the system, they tried to employ convolutional coding to the OFDM system. The obtained results show that significant improvements in terms of BER and throughput can be achieved, which demonstrates the superiority of the adaptive modulation schemes to the fixed transmission schemes.

In 2010 Martorell et.al [19] investigated the use of cross-layer fast-link adaptation (FLA) for WLANs employing a MIMO-OFDM physical layer. They also proposed a packet error rate (PER)-based FLA technique that, without loss of generality, makes use of the exponential effective SNR mapping (EESM). Channel estimation errors have also been considered, revealing the importance of good channel estimators in order for the FLA strategies to work satisfactorily.

Salih and Suliman in 2011 [20] proposed high-order modulation schemes which are used with good conditions of the channel. The lower-order modulation schemes (BPSK, QPSK) are used with bad conditions of the channel.

6

Oyetunji and Akinninranye in 2013 [9] investigated the performance of different digital modulation techniques in the additive White Gaussian Noise (AWGN) channel. The effect of multipath channels on bandpass modulation was also investigated by simulating a selective frequency fading channel with 6 rays in MATLAB environment for up to 20MHz bandwidth. Then they compared the practical results they got with the theoretical results.

In 2012 Makhtari et.al [21] investigated the performance evaluation of the OFDM Long Term Evolution (LTE) downlink physical layer according to the latest 3GPP specifications. The investigation was done by using an AGWN channel for static receiver and transmitter

In 2013 Harivikram et.al [22] designed an objective to minimize the error probability of an LTE (MIMO-OFDM) system and to bring the spectrum efficiency through adaptive modulation and coding rate.

Bhoyar et.al. in 2013 [23] presented a channel-estimation scheme based on the Leaky Least Mean Square (LLMS) algorithm proposed for the BPSK QPSK-PSK MIMO OFDM System. Then they analyzed the terms of the Minimum Mean Squares Error (MMSE) and BER which lead improved the SNR.

Sharma and Dalal in 2014 [24] published a paper in which simulation results were obtained for single input single output (SISO)-OFDM, MIMO-OFDM and adaptive multiuser detection (AMUD) MIMO-OFDM for 2*2, 3*3 and 4*4 antennas. In addition, capacity and BER results were obtained for different antenna configurations and different modulation techniques for SISO-OFDM, MIMO-OFDM and

AMUD MIMO-OFDM. They showed that AMUD MIMO-OFDM performs better when compared to SISO-OFDM and MIMO-OFDM in terms of BER and SNR.

### 1.3 Thesis Aims

The aims of the thesis are to optimize the convenient type of modulation scheme according to the instantaneous Rayleigh fading channel and speed of the receiver in an adaptive way. By using different channel predictions in adaptive modulation, look-up tables for prediction are searched when the signal passes through the high Doppler rates and the fast-fading channel in order to quickly specify the suitable modulation type.

### 1.4 Layout of the Thesis

This thesis consists of five chapters, the first of which is the introduction where a brief description of Adaptive Modulation for MIMO-OFDM System is provided.

Chapter Two: Gives the theoretical background of different channel effects and BER performance for M-array quadrature amplitude modulation (M-QAM) through the AWGN channel and the Rayleigh fading channel. Theoretical background of equalization and channel estimation, the OFDM wireless communication systems, advantages and disadvantages of OFDM techniques is given. Also the chapter explains cyclic-prefix

insertion, the MIMO-OFDM wireless communication systems, and an introduction to link adaptation (power and rate control).

In Chapter Three, three types of wireless communication systems are simulated: the single carrier wireless communication system, the OFDM wireless communication system, and the MIMO-OFDM wireless communication system.

In Chapter Four, the results are extracted from the simulated systems described in chapter three. The main results include the behavior of the system characterized by the BER according to the noise of the channel (AWGN), the Rayleigh fading and for different speeds of the receiver.

Chapter Five presents the conclusions and suggestions for future work.

# Chapter Two

## Theory of OFDM and MIMO systems

In this chapter, theoretical background for the baseband single carrier, OFDM and MIMO systems. Besides analyses of the behavior of signals through fading channels with Doppler effects and channel equalization techniques are stated.

## 2.1 THE SINGLE CARRIER WIRELESS COMMUNICATION SYSTEM

### 2.1.1 Additive White Gaussian Noise (AWGN)

Any received signal of a communication system is usually corrupted with Additive White Gaussian Noise (AWGN) that consists of many random independent components as shown in equation (2.1). AWGN is characterized by constant power spectral density [25].

$$y(t) = x(t) + n(t) \ldots\ldots\ldots\ldots\ldots (2.1)$$

where $x(t)$ is the transmitted signal, $n(t)$ is the noise, and $y(t)$ is the received signal, when the channel effects are excluded.

### 2.1.2 The Multipath Fading Channel

In wireless communication system, multipath effects cause the receiver to receive many copies of the transmitted wave, each of different time delay. The multipath effects are due to reflection, refraction, deflection and scattering of the original transmitted signal. Since the time delays between the received signal copies due to multi path effects are random, then destructive or constructive interference may occur. The

multipath fading results in inter symbol-interference (ISI). Equation (2.2) represents the effect of the multipath on the received signal strength.[9].

$$y(t) = x(t) \circledast h(t) + n(t) \quad \dots\dots\dots\dots\dots\dots (2.2)$$

where $h(t)$ impulse response of the channel.

Figure 2.1 shows block diagram of communication system model.
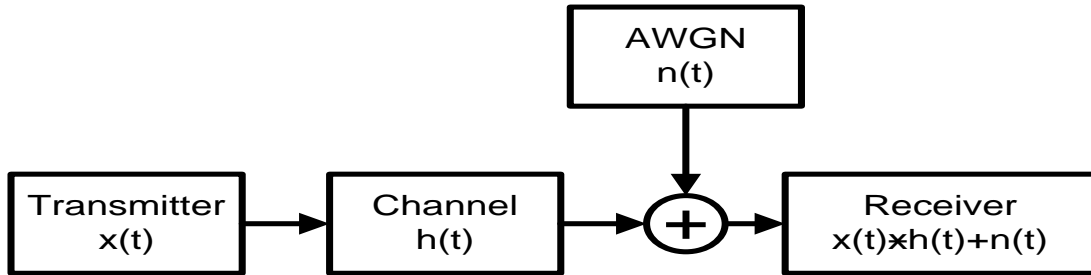


Figure 2.1: Communication system model through a channel with additive white Gaussian noise [9].

## 2.1.3 The Rayleigh Fading Channel

Rayleigh fading channel assumes there is no line of sight between the transmitter and the receiver, but a large number of the transmitted signal copies are received by the receiver. The probability density function (PDF) of the delays between the received copies of the transmitted signal is statically Rayleigh distribution. The following equation represents the Rayleigh PDF [26, 27]:

$$p(r_o) = \begin{cases} \frac{r_o}{\sigma^2} \exp\left[-\frac{r_o{}^2}{2\sigma^2}\right] & \text{for } r_o \geq 0 \\ 0 & \text{otherwise} \end{cases} \quad \dots\dots\dots\dots\dots\dots\dots (2.3)$$

where $\sigma^2$ is the predicted mean power of the multipath signal and $r_o$ is the Rayleigh random variable which represents in this study the relative delays.

### 2.1.4 Fast Fading versus Slow Fading Viewed In the Time Domain

The channel can be characterized as a fast fading channel if $T_o \leq T_s$, (where $T_o$ is the channel coherence time, and $T_s$ is the time duration of the transmitted symbol). If $T_o \geq T_s$ then the channel can be characterized as a slow fading channel. The fast fading channel $h(t)$ has low autocorrelation values, so that the channel characteristics change several times during the time duration of the transmitted symbol. The slow fading channel, on the other hand, has high autocorrelation values and the channel characteristics remain approximately constant during the symbol duration. Slow fading channel reduces the SNR more than fast fading one [16, 26].

### 2.1.5 The Maximum Doppler Frequency Shift (Jakes model)

The relative movement between transmitter and receiver leads to a frequency shift in the received signal. The received signal frequency shift is known as the Doppler shift. The Doppler shift for moving receiver and stationary transmitter can be calculated according to the following equation [24, 27]:

$$f_d = \frac{|\vec{v}|}{c} f_c \cos(\alpha) \ldots\ldots\ldots\ldots\ldots (2.4)$$

where $\vec{v}$ is the receiver velocity, $c$ is the speed of light, $f_c$ is the carrier frequency of the signal and $\alpha$ is the angle between the directions of the receiver velocity and the arriving wave. Equation (2.4) shows that a maximum +ve Doppler shift occurs when the receiver moves toward the transmitter, and a maximum –ve Doppler shift occurs when the receiver moves away from the transmitter [25].

The Doppler spectrum gives a clear idea about how fast the channel characteristics are changing with respect to time. The Doppler spectrum $S(f)$ is found by taking the Fourier transform of the channel time correlation function $R(\Delta v)$. Therefore, the Doppler spectrum is completely associated with the channel characteristics that vary with time. The following equation gives the normalized $R(\Delta v)$[26]:

$$R(\Delta v) = J_0(kV\Delta t) \quad\dots\dots\dots\dots\dots \quad (2.5)$$

where, $J_0(\bullet)$ is the zero order Bessel function of the first kind, $V\Delta t$ is the distance traversed, and $k = 2\pi/\lambda$ is the free space phase constant. A Doppler spectrum (Doppler PDF) is found by taking the Fourier transform of the equation [26, 28]:

$$S(f) = \frac{1}{\pi f_d \sqrt{1-(\frac{f-f_c}{f_d})^2}} \quad\dots\dots\dots\dots\dots \quad (2.6)$$

The Doppler spectrum of the equation is also called the Jakes spectrum. Figure 2.2 shows the duality relation between the multipath intensity profile (time varying channel) and the Doppler power spectrum.
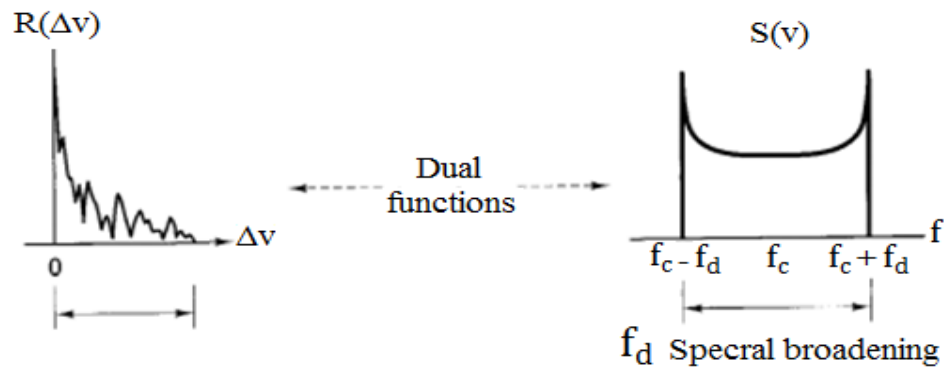


(a) Multipath intensity profile          (b) Doppler power spectrum

Figure 2.2: Relationship between the channel correlation and the power density function [26].

Due to the multipath effect, the transmitted signal travels over multiple paths to reach the receiver with different times and different angles. Each arriving component of the received signal is affected by a different Doppler shift statically subjected to the Jakes model [26]. The Doppler spread ($f_d$) is inversely proportional to the coherence time as shown in equation (2.7)

$$T_o = 0.423/\, f_d \quad \ldots\ldots\ldots\ldots\ldots\ldots \quad (2.7)$$

### 2.1.6 The BER performance for M-array quadrature amplitude modulation (M-QAM)

The data throughput for any communication system can be increased by increasing the bandwidth used to transmit data. Normally, in wireless communication systems, the bandwidth is specified by national and local licences. Due to this specification of the bandwidth, new technologies appear to increase the data throughput without increasing the bandwidth. One of these technologies is to use high-order modulation schemes. The high order modulation schemes use the available bandwidth in an efficient way [29].

Gray code constellation [30] is used to perform the square QAM modulation schemes. Cho and Yoon have derived in [4] an expression to show the BER performance of M-array QAM modulation schemes through the AWGN channel with respect to SNR as shown in equations (2.8), (2.9) and (2.10).

$$P_b = \frac{1}{\log_2(M)} \sum_{k=1}^{\log_2\sqrt{M}} P_b(k), \quad \dots\dots\dots\dots\dots\dots\dots\dots \quad (2.8)$$

$$P_b(k) = \frac{1}{\sqrt{M}} \sum_{i=0}^{(1-2^{-k})\sqrt{M}-1} \left\{ w(i,k,M)\,\mathrm{erfc}\left( (2i \right. \right.$$

$$\left. \left. + 1)\sqrt{\frac{3\log_2 M.\gamma}{2(M-1)}} \right) \right\}, \quad \dots\dots\dots\dots\dots\dots\dots\dots \quad (2.9)$$

where

$$w(i,k,M) = (-1)^{\left\lfloor \frac{i.2^{k-1}}{\sqrt{M}} \right\rfloor} \cdot \left( 2^{k-1} - \left\lfloor \frac{i.\,2^{k-1}}{\sqrt{M}} + \frac{1}{2} \right\rfloor \right) \quad \dots\dots\dots \quad (2.10)$$

where $\gamma = E_b/N_0$ denotes the SNR per bit, $M = 2^m$ , $m$ is appositive integer, and $k \in \{1,2,\dots,\log_2 I\}$ where $I$ is the size of I-channel in the M-QAM gray code constellation diagram.

## 2.1.7 The BER performance for M-array quadrature amplitude modulation (M-QAM) through the Rayleigh fading channel

For M-array QAM modulation schemes passing through a flat fading Rayleigh channel, an expression has been derived to find the BER performance through Rayleigh fading channel as shown in equations (2.11) and (2.12), respectively [29].

$$P_{Ray} = \frac{1}{\log_2(M)} \sum_{k=1}^{\log_2\sqrt{M}} P_{Ray}(k), \quad \dots\dots\dots\dots\dots\dots \quad (2.11)$$

15

$$P_{Ray}(k) = \frac{1}{\sqrt{M}} \sum_{i=0}^{(1-2^{-k})\sqrt{M}-1} \left\{ w(i,k,M)\,\text{erfc}\left( 1 - \frac{\sqrt{\dfrac{3(2i+1)^2\log_2 M.\gamma}{2(M-1)}}}{\sqrt{\dfrac{3(2i+1)^2\log_2 M.\gamma}{2(M-1)}+1}} \right) \right\}, \quad \text{...............} \quad (2.12)$$

where $\gamma = E_b/N_0$ denotes the SNR per bit, $M = 2^m$, $m$ is appositive integer, and $k \in \{1, 2, \dots, \log_2 I\}$ where $I$ is the size of I-channel in the M-QAM gray code constellation diagram.

## 2.1.8 Equalization and channel estimation

The problem of the ISI arises due to the multipath effects of mobile digital communication systems. The multipath effects cause a broadening in the received pulse shape with respect to time. This broadening in pulse shape causes interferences between the adjacent pulses and distort them. As the data rate increases, the ISI also increases and causes a higher BER at the receiver. So, ISI is the main problem that prevents the wireless communication system from transmitting data with high rates. Equalizer can be used to minimize the effects of ISI at the receiver. For the time varying channel, an adaptive equalizer is needed to track the channel characteristic variation and to ensure a high transmitting data rate with an accepted BER. If $x(t)$ is the original information signal

and $h(t)$ is the combined complex baseband impulse response of the channel, then the signal received by the equalizer is [31]

$$y(t) = x(t) \circledast h^*(t) + n_b(t) \ldots\ldots\ldots\ldots\ldots\ldots (2.13)$$

where $h^*(t)$ is the complex conjugate of $h(t)$, $n_b(t)$ is the baseband noise at the input of the equalizer, and $\circledast$ denotes the convolution operator. If the impulse response of the equalizer is $h_{eq}(t)$, then the output of the equalizer is [31]

$$\hat{d}(t) = x(t) \circledast h^*(t) \circledast h_{eq}(t) + n_b(t) \circledast h_{eq}$$

$$= x(t) \circledast g(t) + n_b(t) \circledast h_{eq}(t) \quad \ldots\ldots\ldots\ldots (2.14)$$

The aim of the equalizer is to get

$$H_{eq}(f)H^*(-f) = 1 \quad \ldots\ldots\ldots\ldots\ldots\ldots\ldots\ldots (2.15)$$

where $H_{eq}(f)$ and $H(f)$ are the Fourier transforms of $h_{eq}(t)$ and $h(t)$, respectively.
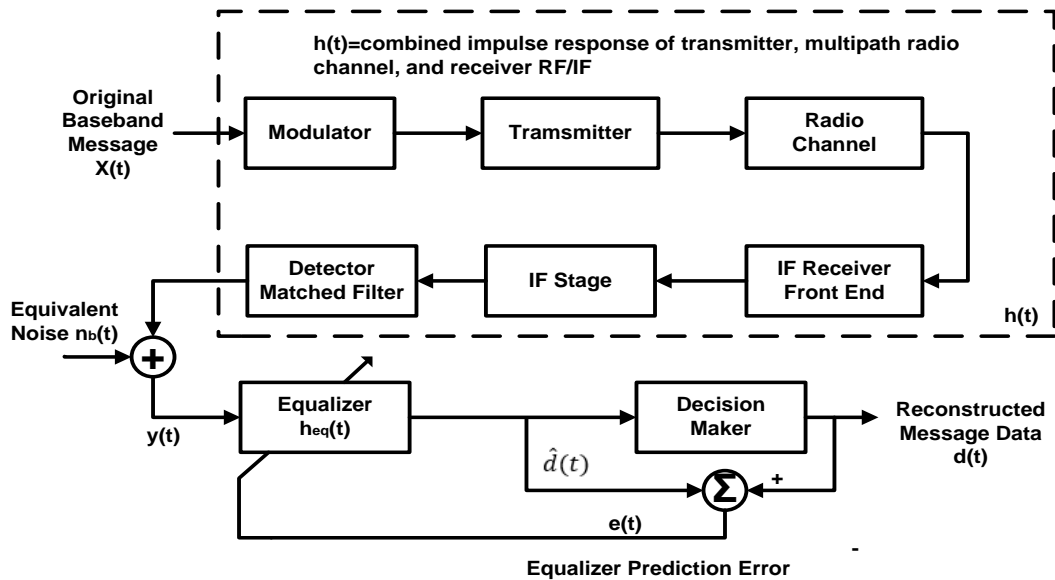


Figure 2.3: A simplified communication system block diagram using an adaptive equalizer at the receiver [31].

A flat fading channel can be characterized as a multipath channel which has only one path and represented as a single tab filter. Therefore, the convolution operation between the signal and channel impulse response can be converted into multiplication as shown in the following equation

$$y(t) = x(t) * h(t) + n_b(t) \dots\dots\dots\dots\dots (2.16)$$

## 2.2 The OFDM WIRELESS COMMUNICATION SYSTEM

### 2.2.1 Introduction to OFDM

OFDM stands for Orthogonal Frequency Division Multiplexing. The OFDM is the extension of the frequency division multiplexing (FDM) technique. The FDM technique uses a number of parallel narrow sub-band subcarriers to transmit parallel data streams within the available bandwidth. FDM, as compared with a single wide-band sub-carrier, which uses the whole bandwidth to transmit one stream of data, is shown in Figure 2.4 [32].
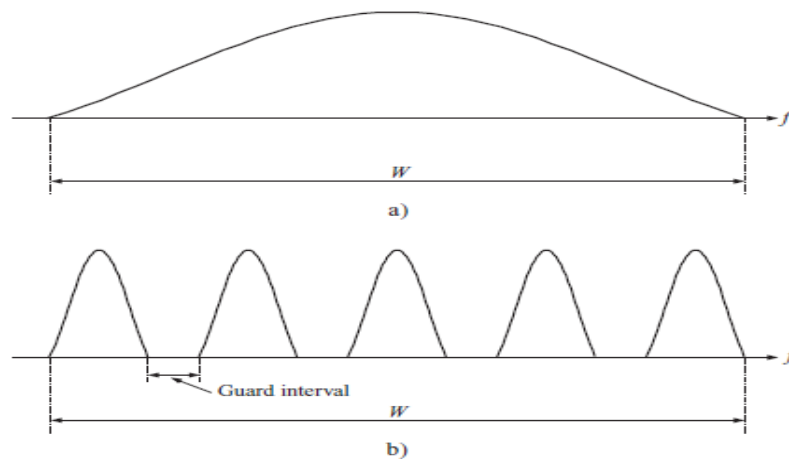


Figure 2.4: FDM principle. a) Wideband carrier b) FDM narrowband carriers [32].

## 2.2.2 The Basic Principle of OFDM

The OFDM technique is the basis for many modern communication systems such as the 3GPP Long Term Evolution as a downlink transmission scheme, WiMax and the Digital Video Broadcasting (DVB). The OFDM transmission can be characterized as a multicarrier transmission.

The basic characteristics of OFDM transmission are:

1- A number of narrow subcarriers are simultaneously transmitted to occupy the available bandwidth in an efficient way and sometimes the number of subcarriers may be huge and can reach a thousand subcarriers.

2- Usually the subcarrier spacing is $\Delta f = 1/T_u$ , where $T_u$ is the per-subcarrier modulation symbol time which is illustrated in Figure 2.5. The subcarrier spacing, therefore, equals the per-subcarrier modulation rate $1/T_u$.
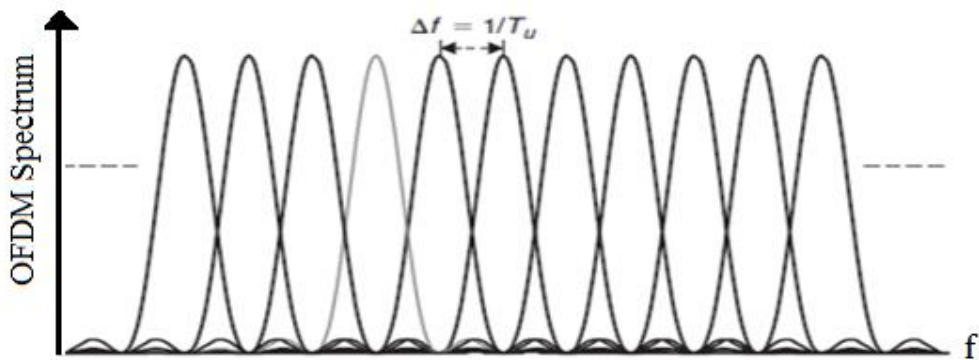


Figure 2.5: OFDM subcarrier spacing [33].

To describe how the OFDM symbol is generating, a bank of $N_c$ complex modulators are used to modulate $N_c$ complex symbols, where the

19

complex symbols are the output of the used modulation scheme (QPSK, 16QAM,…). The output of each modulator represents one OFDM subcarrier. Figure 2.6 shows how one OFDM symbol is generated.
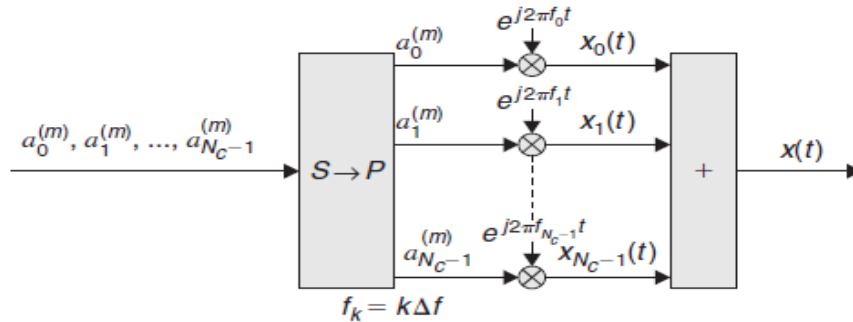


Figure valid for time interval $mT_u \leq t < (m+1)T_u$

Figure 2.6: OFDM modulation [33].

In complex baseband notation, a basic OFDM signal $x(t)$ during the time interval $mT_u \leq t < (m+1)T_u$ can thus be expressed as:

$$x(t) = \sum_{k=0}^{N_c-1} x_k(t) = \sum_{k=0}^{N_c-1} a_k^{(m)} e^{j2\pi k \Delta f t} \quad \text{............} \quad (2.17)$$

where $x_k(t)$ is the $kth$ modulated subcarrier with frequency $f_k = k * \Delta f$ and $a_k^{(m)}$ is the modulation symbol applied to the $kth$ subcarrier during the $mth$ OFDM symbol interval, i.e. during the time interval $mT_u \leq t < (m+1)T_u$. Equation (2.17) shows that to transmit one OFDM symbol through the channel, all the $N_c$ modulators simultaneously contribute during the symbol duration.

According to the application and the available and the allowable bandwidth, the number of subcarriers and their bandwidths can be

determined. The number of one OFDM symbol subcarriers may start from less than one hundred and may reach several thousands. As a result, the subcarrier spacing may range from few KHz to several hundred KHz. The subcarrier spacing is determined by the channel state that the system is working with, including the maximum estimated radio channel frequency selectivity (maximum expected time dispersion) and the maximum estimated rate of channel variation (maximum expected Doppler spread). After selection of the subcarrier spacing, the number of subcarriers is determined by the available bandwidth, taking into account guard bands to prevent OFDM symbols from interfering with each other.

The term Orthogonal Frequency Division Multiplex is due to the fact that two modulated OFDM subcarriers $x_{k_1}$ and $x_{k_2}$ are mutually orthogonal over the time interval $mT_u \leq t < (m+1)T_u$", i.e.

$$\int_{mT_u}^{(m+1)T_u} x_{k_1}(t)\, x_{k_2}^* \, dt =$$

$$\int_{mT_u}^{(m+1)T_u} a_{k_1} a_{k_2}^* e^{j2\pi k_1 \Delta f t} e^{-j2\pi k_2 \Delta f t} \, dt = 0 \ \text{ for } k_1 \neq k_2 \ \ldots \ldots \ldots \ (2.18)$$

The OFDM demodulation process can be basically achieved by using a bank of parallel correlators. The number of correlators should be equal to the number of subcarriers contributing to producing one OFDM symbol, one correlator for each subcarrier. Figure 2.7 shows the basic principle of the OFDM demodulation.
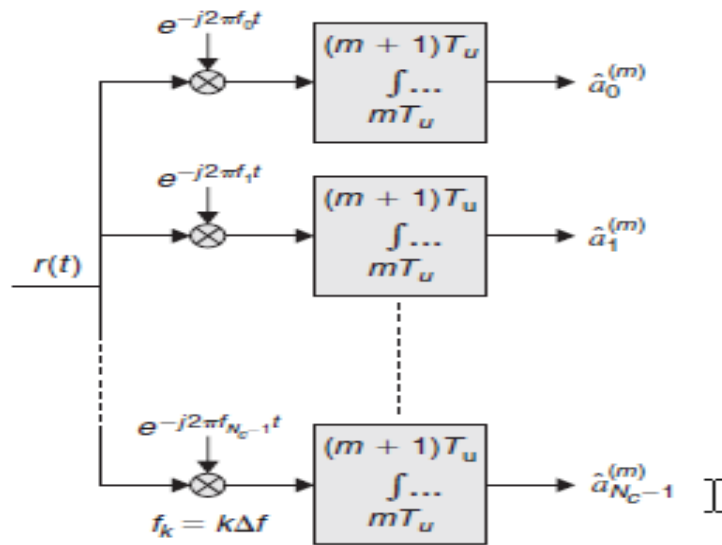
Figure 2.7: Basic scheme for OFDM demodulator [33].

For an ideal case, two OFDM subcarriers do not cause any interference with each other after demodulation due to the orthogonality between the subcarriers according to equation (2.18) [33].

### 2.2.3 The Advantages and disadvantages of The OFDM technique

OFDM technique shows many advantages over other widely known wireless techniques, such as Frequency-Division Multiple Access (FDMA), Time- Division Multiple Access (TDMA) and Code-Division Multiple Access (CDMA) [32].

1- In OFDM the radio channel is divided into many narrow-bands with low-rates and frequency-non-selective sub-channels (sub-carriers), which leads to parallel transmit multiple symbols, meanwhile a high spectral efficiency is maintained.

22

2- Each subcarrier in the OFDM system can be used to transmit data for a different user resulting in a simple multiple access scheme which is known as Orthogonal Frequency Division Multiple Access (OFDMA).

3- The OFDMA allows for different media to be transmitted simultaneously on the same radio link such as video, graphics, speech, text or other kind of data. The quality of service (QoS) and the type of service determine the media used with the OFDMA system.

4- Depending on the channel state, the OFDM system uses different modulation schemes (QPSK, 16QAM …..) for each group of subcarriers or even for each user. The choice of a modulation scheme depends on the channel quality and the number of active users. For example, the high-order modulation schemes are used for users who are close to the base station because a good channel quality is available, whereas low order modulation schemes are used for the users who are far from the base station or on the urban areas where the number of active users is huge because of the bad channel conditions.

5- The OFDM system shows high operating performance from the viewpoint of high data throughput even though time varying (frequency selective) channel is considered.

6- Besides the mentioned advantages of the OFDM system, the OFDM system is described by its low complex implementation in the transmitter and receiver sides. For example, complex equalizers at the receiver need to be used for the classical single carrier system in

order to decrease the effect of the Inter-Symbol Interference (ISI) introduced by multi-path fading. By contrary, only a cyclic prefix is added to the OFDM symbol to exhibit a high resilience against the ISI.

-The disadvantages of OFDM may be:

1- The increased values in Peak-to-Average Power Ratio (PAPR) as compared with that of the single-carrier system.

2- Because of the high value of PAPR, the OFDM system needs a large, linear-range amplifier at the system transmitter output.

**3-** "OFDM is sensitive to carrier frequency offset, resulting in Inter-Carrier Interference (ICI)".

## 2.2.4 OFDM implementation using IFFT/FFT processing

Although OFDM modulation and demodulation can be achieved by using a bank of parallel modulators and correlators, respectively (Figures 2.6 and 2.7 show the schemes for the basic principle of the OFDM system), it is difficult in actual implementation to get large numbers of modulators and correlators that can work synchronously. In addition, the subcarrier spacing $\Delta f$ which is equal to the per-subcarrier symbol rate $1/T_u$ leads to huge structure implementation. These problems are resolved after the invitation of the IFFT/FFT where the IFFT/FFT circuit can be used instead of the bank of modulators/correlators, respectively. Of course, the IFFT/FFT circuits are much easier to implement and more economic.

To prove that the IFFT/FFT can be used instead of modulators/correlators, and since $f_s = \frac{1}{T_s} = N * \Delta f$ ; where $f_s$ is the sampling rate, $N$ is the number of samples, $\Delta f$ is the subcarrier bandwidth, and $T_s$ is the sampling time, then parameter $N$ should be chosen so that the sampling theorem is sufficiently fulfilled. As $N_c * \Delta f$ can be seen as the nominal bandwidth of the OFDM signal, $N$ should exceed $N_c$ with a sufficient margin. According to these assumptions, the time-discrete OFDM signal can be expressed as [33]

$$x_n = x(nT_s) = \sum_{k=0}^{N_c-1} a_k e^{j2\pi k \Delta f n T_s} = \sum_{k=0}^{N_c-1} a_k e^{j2\pi kn/N}$$

$$= \sum_{k=0}^{N_c-1} a_k' e^{j2\pi kn/N} \quad \ldots \ldots \ldots \ldots \ldots \ldots \ldots . (2.19)$$

Where

$$a_k' = \begin{cases} a_k & 0 \le k < N_c \\ 0 & N_c \le k < N \end{cases}$$

Thus, the sequence $x_n$, i.e. the sampled OFDM signal, has the size-$N$ Inverse Discrete Fourier Transform (IDFT) of the block of modulation symbols $a_0, a_1, \ldots, a_{N_c-1}$ extended with zeros to length N. Therefore, the OFDM system modulation can be implemented by using IDFT with a digital to analog converter as shown in Figure 2.8.
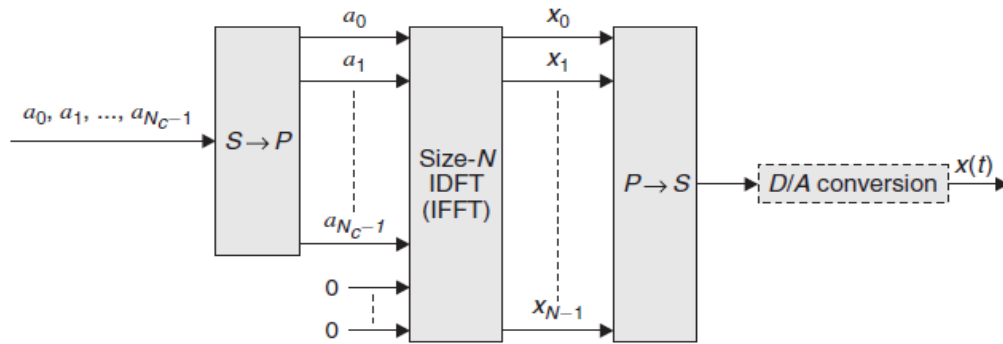
Figure 2.8: OFDM modulation by means of IFFT processing [33].

By choosing the size of the IDFT to be equal to $2^m$ where $m$ is an integer value, the OFDM modulation can be implemented by means of the implementation-efficient radix-2 Inverse Fast Fourier Transform.

Similar to the OFDM modulation, the OFDM demodulation can be achieved by using FFT instead of a bank of parallel correlators and by using a sampler with a sampling rate of $f_s = 1/T_s$, as shown in Figure 2.9 [33].
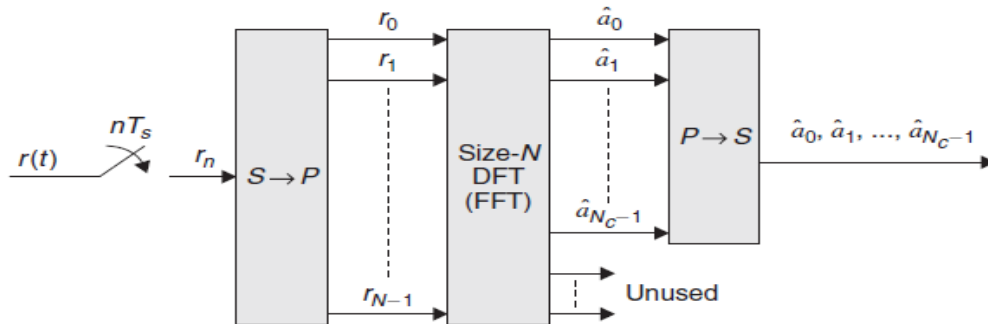


Figure 2.9: OFDM demodulation by means of FFT processing [33].

## 2.2.5 Cyclic-prefix insertion

In the ideal case when the received OFDM symbol is uncorrupted due to channel effect, the OFDM symbol can be demodulated without any interference between subcarriers. To understand the subcarrier

orthogonality in equation (2.17), the modulated subcarriers $x_k(t)$ during the demodulator integration interval $T_u = 1/\Delta f$ consist of an integer number of periods as exponents of complex exponentials. In general, however, the channel effect cannot be ignored and in the case of the time dispersive channel, the orthogonality between the subcarriers will be lost. The subcarrier orthogonalities are lost in the case of the time dispersive channel, because the demodulator correlation interval for one path will overlap with the adjacent OFDM symbol boundary of another path. Figure 2.10 shows the problem of the time dispersive channel.
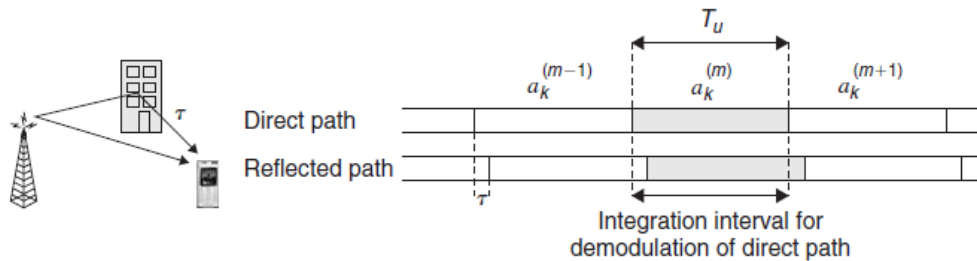


Figure 2.10: Time dispersion and corresponding received-signal timing [33].

To overcome the problem of the interference between subcarriers due to the time dispersive channel and to get an OFDM signal insensitive to the time dispersive channel, a cyclic-prefix insertion is used. As shown in Figure 2.11, by cyclic-prefix insertion the data in the last part of the OFDM symbol has to be copied and inserted at the beginning of the symbol which leads to increase the length of the OFDM symbol from $T_u$ to $T_u + T_{cp}$, where $T_{cp}$ is the length of the cyclic prefix. Therefore OFDM symbol rate is reduced due to the CP insertion in the symbol [34]. Figure 2.11 shows in its lower part that the subcarriers are still orthogonal to each other if the correlation at the receiver side is still only achieved over a time

interval $T_u = 1/\Delta f$. In the case of a time-dispersive channel, if the span of the time dispersion is shorter than the cyclic- prefix length then the subcarrier orthogonally still implies [33].
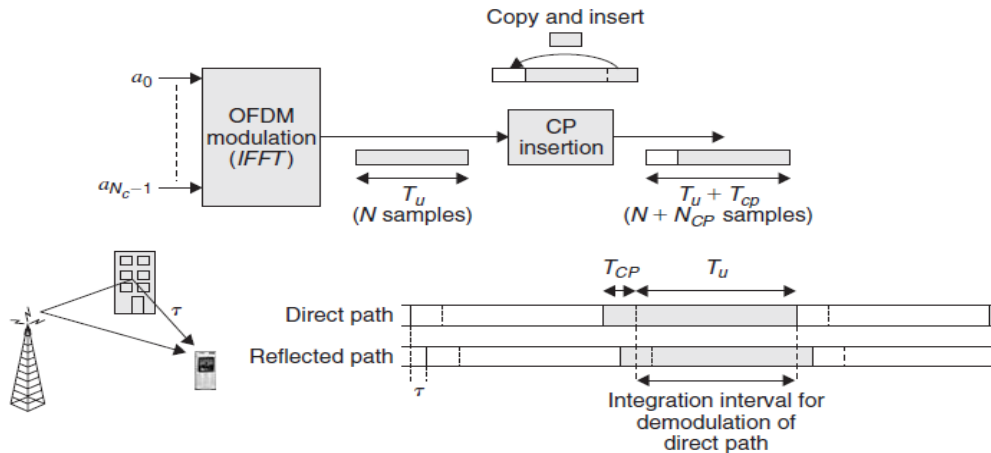


Figure 2.11: Cyclic-prefix insertion [33].

The cyclic prefix should be added to the OFDM symbol before transmitting it through the channel. Since the cyclic prefix data contains iterated information, it should be cancelled at the receiver before the demodulation of the OFDM symbol (OFDM demodulation is done by using DFT/FFT). The cancellation of the cyclic prefix is done in the digital phase of the demodulator because at the first stage of the OFDM system receiver an analog to digital is used. The disadvantages of using cyclic prefix insertion is that a fraction of the received signal power which is equal to $T_u/(T_u + T_{cp})$ is actually utilized by the OFDM demodulator, and as a result the complement fraction of this power will be lost at the demodulation. In addition, there will be a loss of the same fraction in bandwidth and as a result the OFDM symbol rate is reduced without reducing the overall signal bandwidth.

In practice, cyclic prefix insertion can be achieved in discrete form by copying the last $N_{cp}$ samples of the IFFT output samples, which equal $N$, and paste them at the beginning, so the number of samples is increased from $N$ to $N + N_{cp}$. At the receiver, the added samples for cyclic prefix are discarded before demodulation of the OFDM symbol by means of DFT/FFT processing [33]. Figure 2.12 shows the whole OFDM system that is implemented by using IFFT/FFT.
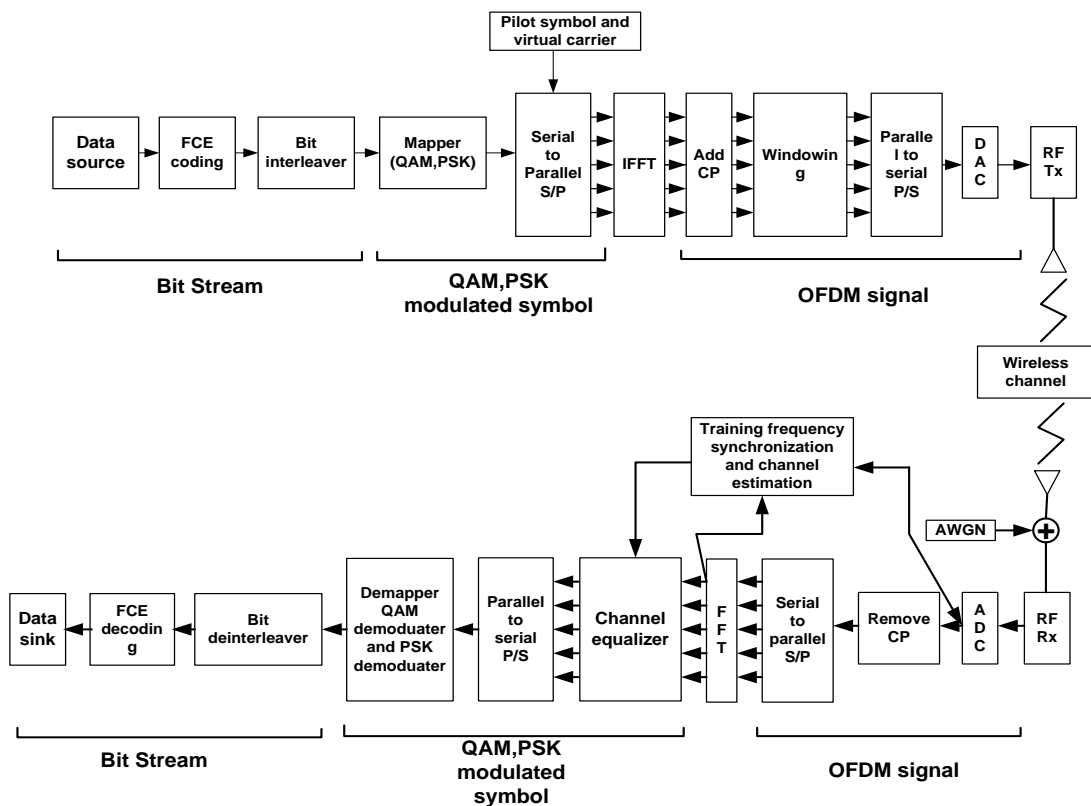


Figure 2.12: Block diagram of transmitter and receiver in an OFDM system [35].

## 2.2.6 User-multiplexing and multiple-access scheme of OFDM

In the OFDM, the whole bandwidth can be allocated for one user, and the bandwidth can be used as a user multiplexing or multiple access as shown in Figure 2.13.

29
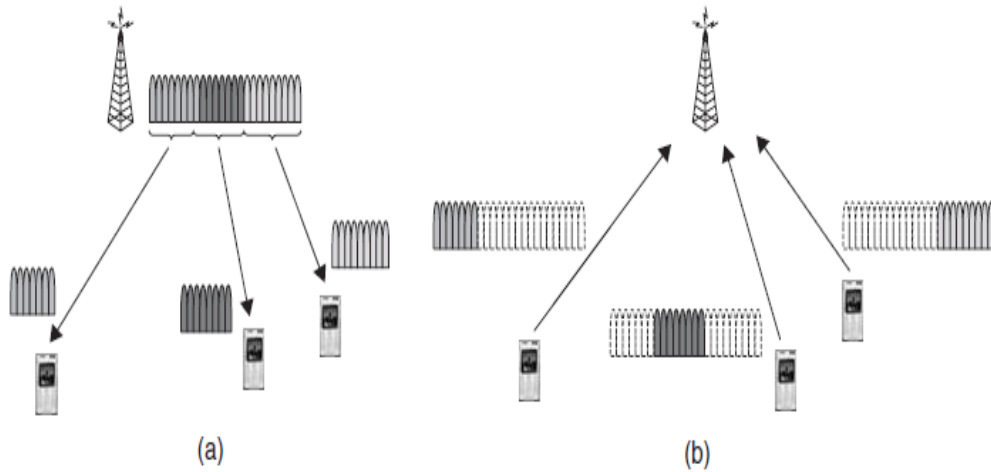
Figure 2.13: OFDM as a user-multiplexing/multiple-access scheme (a) downlink and (b) uplink [33].

Figure 2.13.a shows the downlink case (user multiplexing case), where all the OFDM subcarriers (the whole bandwidth) are divided into subsets of subcarriers. Each subset of the subcarriers is allocated for one mobile receiver. In the uplink direction (Figure 2.13.b), on the other hand OFDM is used as user multiplexing or multiple access, where the OFDM symbol bandwidth is divided into different subsets of the OFDM subcarriers which are used for data transmission from different mobile terminals. The OFDM system, in the case of multiple access is known as the Orthogonal Frequency Division Multiple Access (OFDMA). Figure 2.13 shows that the subcarriers that are transmitted to/from each mobile terminal have adjacent distributions in the frequency domain. The distribution of the subcarriers can also possibly be changed to distributed subcarriers as shown in Figure 2.14. The advantage of using distributed subcarriers, as shown in Figure 2.14, is to spread the bandwidth of the subcarriers allocated for each mobile terminal and as a result, to get additional frequency diversity [33].
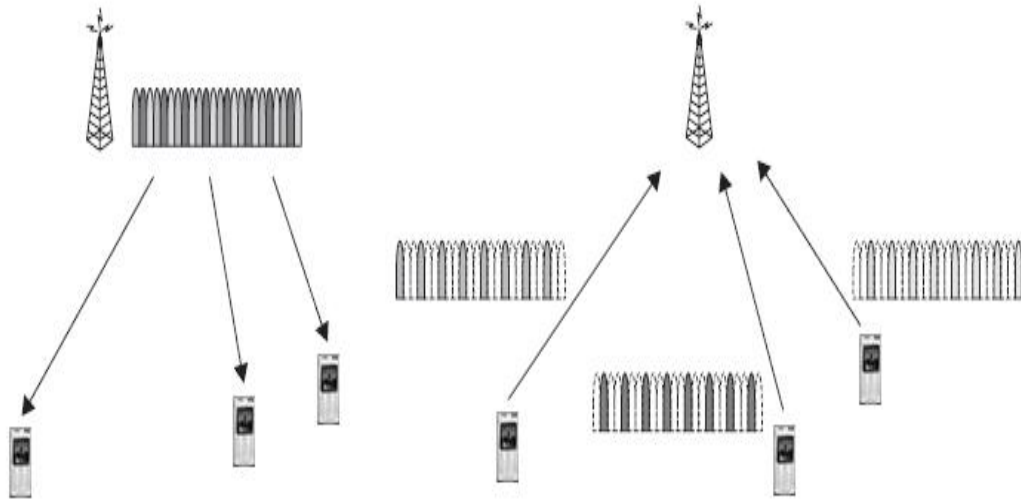
Figure 2.14: Distributed user multiplexing [33].

## 2.3 The MIMO-OFDM WIRELESS COMMUNICATION SYSTEM

### 2.3.1 Introduction to MIMO

The Multiple-Input, Multiple-Output (MIMO) technique is capable to support significantly higher data rates as compared with the Universal Mobile Telecommunications System (UMTS) and the High-Speed Downlink Packet Access (HSDPA) based 3G networks. As shown in Figure 2.15, a MIMO system can exploit both the transmitter and the receiver diversity since information is transmitted through different paths. In comparison with the Single-Input, Single-Output (SISO) systems, the MIMO systems have the following two advantages [32]:

**1.** A significant increase in the capacity and the spectral efficiency of the system.

**2.** A dramatic reduction of the effects of fading due to the increased diversity.
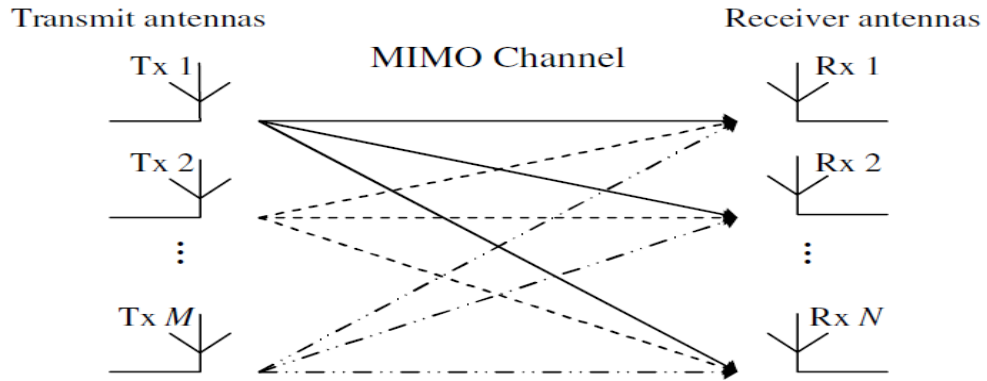
Figure 2.15: Configuration of *M* transmitter antennas and *N* receiver antennas in a general MIMO system [32].

## 2.3.2 The Basic Principles of MIMO System

The multiple antennas system can be used to improve the SNR at the receiver. The SNR improvement is proportional to the number of the transmitting and receiving antennas for the system. Concerning for $N_T$ transmitting antennas and $N_R$ receiving antennas, the gain in the SNR is proportional to the product of $N_T * N_R$ [33]. The gain acquired from increasing the SNR lies in the increase of the data throughput in the same ratio, on condition that the bandwidth is unlimited. Generally, however, the bandwidth is limited, therefore, increasing the number of antennas over some numbers does not introduce additional gain in terms of data rate (the data rate will reach saturation unless the bandwidth increases). To understand the saturation in the data rate, first assume a single antenna system is used and its normalized channel capacity expression is given in equation (2.20)

$$\frac{C}{BW} = \log_2\left(1 + \frac{S}{N}\right) \dots\dots\dots\dots\dots\dots (2.20)$$

32

where, the SNR can be increased by increasing the number of antennas by means of beam forming, and the SNR growth is proportional to $N_T * N_R$.

Let us assume that the $SNR$ is equal to $x$, then in mathematics approximation $\log_2(1 + x)$ is proportional to $x$ for small $x$ according to Taylor series expansion, therefore, for the low SNR, the capacity growth is linearly proportional to the SNR. However, for a large value of $x$, $\log_2(1 + x) \approx \log_2(x)$, and for large values of the SNR, the capacity grows logarithmically with the SNR. However, for the MIMO system the channel capacity is [33]:

$$\frac{C}{BW} = \log_2\left(1 + \frac{N_R}{N_L} * \frac{S}{N}\right) \dots \dots \dots \dots \dots \dots \dots (2.21)$$

where $N_L = \min\{N_T, N_R\}$, $N_T$ and $N_R$ are the number of transmitters and receivers, respectively.

Because there are $N_L$ parallel channels, the channel capacity for each one is given as in equation (2.21) and the overall channel capacity of such a system is given in the following equation [33]

$$\frac{C}{BW} = N_L * \log_2\left(1 + \frac{N_R}{N_L} * \frac{S}{N}\right)$$

$$= \min\{N_T, N_R\} * \log_2\left(1 + \frac{N_R}{\min\{N_T, N_R\}} * \frac{S}{N}\right) \dots \dots (2.22)$$

Equation (2.22) shows that under certain conditions, the channel capacity is proportional to the number of antennas on condition that there is no saturation in the data rate.

To understand the basic principle of how multiple parallel channels work, consider a 2*2 antenna system as shown in Figure 2.16, two antennas for transmitter and two antennas for receiver,.
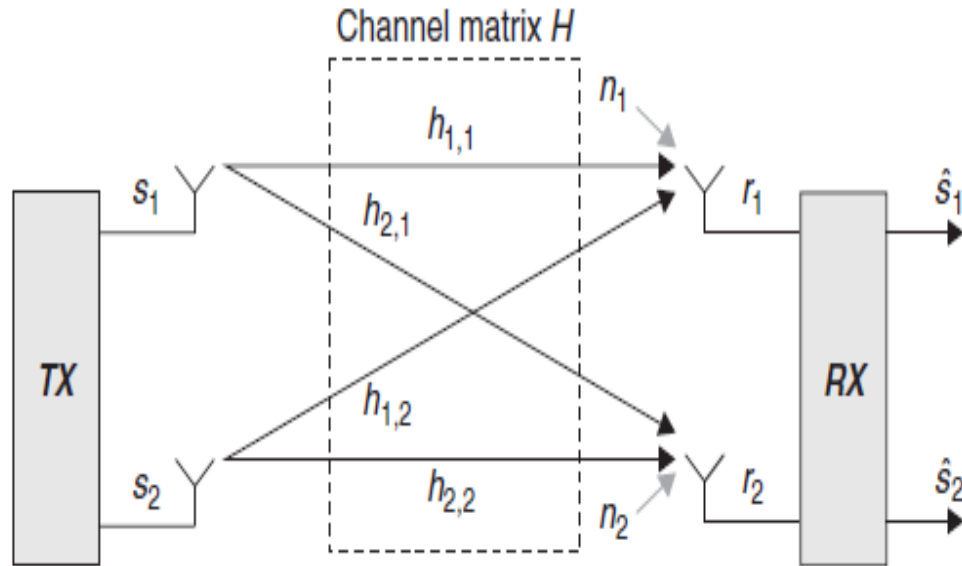


Figure 2.16: 2*2 antenna configuration [33].

In addition, assume that the transmitted signal is passing through a flat fading channel, frequency non-selective channel (there is no radio channel time dispersion), and additive white noise. Therefore, the received signal can be expressed in the following equation.

$$\bar{r} = \begin{pmatrix} r_1 \\ r_2 \end{pmatrix} = \begin{pmatrix} h_{1,1} & h_{1,2} \\ h_{2,1} & h_{2,2} \end{pmatrix} \cdot \begin{pmatrix} s_1 \\ s_2 \end{pmatrix} + \begin{pmatrix} n_1 \\ n_2 \end{pmatrix} = H \cdot \bar{s} + \bar{n} \ \dots \dots \dots \dots \dots (2.23)$$

where H is the 2*2 channel matrix and the vector $\bar{s}$ represents the two transmitted signals. At receiver the two transmitted signals $s_1$ and $s_2$ can be recovered perfectly without interfering between them on condition that there is no noise effect on the signals and the channel matrix H is invertible as shown in Figure 2.17.

34
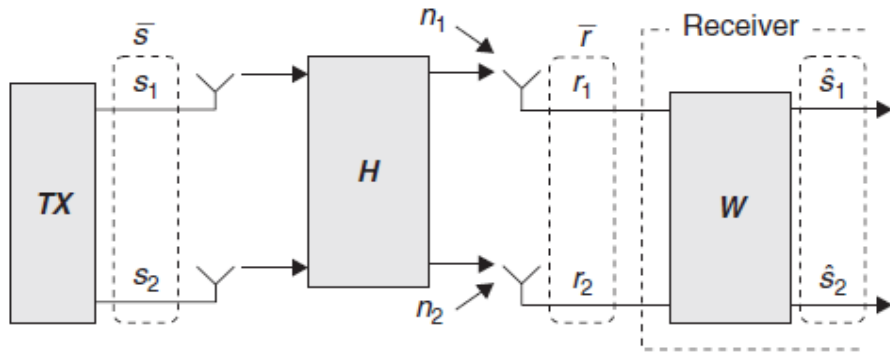
Figure 2.17: Linear reception/demodulation of spatially multiplexed signals [32].

There is no way to get rid of the white noise effect. Therefore, to recover the transmitted signals at the receiver the noise should be taken into account as shown in the following equation [33].

$$\begin{pmatrix} \hat{s}_1 \\ \hat{s}_2 \end{pmatrix} = W \cdot \bar{r} = \begin{pmatrix} S_1 \\ S_2 \end{pmatrix} + H^{-1} \cdot \bar{n} \dots \dots \dots \dots \dots \dots \dots \ (2.24)$$

where $W = H^{-1}$ .

In the MIMO systems, the maximum number of signals can be transmitted by spatial multiplexing equaling to $N_L$ and $N_L = \min\{N_T, N_R\}$. Practically, the following remarks are to be considered for optimum work of the MIMO system [33]:

1- The maximum number of transmitting signals simultaneously is equal to $N_T$ where $N_T$ is the number of the transmitting antennas.

2- In a MIMO system of $N_R$ receiving antennas, the maximum number of the interfering signals that can be suppressed, is $N_R - 1$ and therefore a maximum of $N_R - 1$ signals can be spatially multiplexed. It should be noted that the order of the spatial multiplexing is less than $N_L$ given.

35

3- The MIMO system does not work for spatial multiplexing in the case of very bad channel conditions (low SNR at the receiver), instead the transmitting and the receiving antennas should work for beam forming to increase the SNR at the receiver.

4- In a more general case, the order of the spatial-multiplexing is determined from the channel matrix properties whose size is $N_T *$ $N_R$. Extra antennas are used for beam forming rather than increasing the order of spatial multiplexing. Pre-coder-based spatial multiplexing is usually used to achieve combined spatial multiplexing and beam forming.

### 2.3.3 MIMO-OFDM

The three basic parameters used for describing the quality of any wireless link are, the data rate, the transmission range, and the transmission reliability. In the ordinary wireless communication systems, there is always a tradeoff between these three parameters. For example, increasing the data rate demands a degradation in the transmission range or in the transmission reliability or in both. Therefore, to improve any of the parameters, the other two parameters should be degraded. However, these three parameters can be improved simultaneously. Furthermore, a straightforward matrix algebra can be invoked for processing the MIMO-OFDM signals, so that the implementation of MIMO assisted OFDM becomes more efficient. Figure 2.18 shows the whole MIMO-OFDM system [32].

36
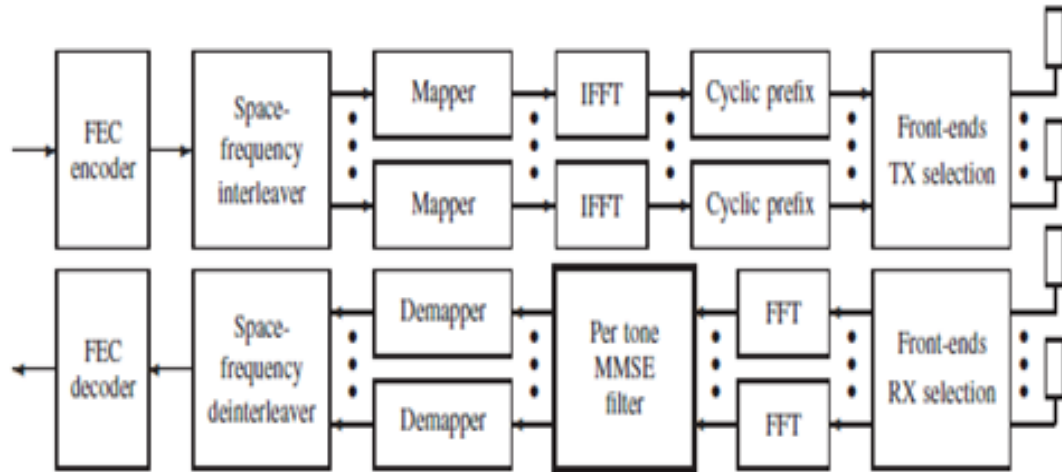
Figure 2.18: MIMO-OFDM transceiver block diagram [32].

## 2.4 Link Adaptation

### 2.4.1 Introduction to Link Adaptation

The idea of link adaptation is based on getting a maximum data throughput with an acceptable BER (or with an acceptable block error rate (BLER)) [27], which depends on the state of the channel. The channel state is determined by the receiver side then transmitted back to the transmitter side every time to live (TTL). The process of the channel state transmission from the receiver to the transmitter is known as the channel quality indicator (CQI) report. The CQI is determined by the received SNR at the receiver. After receiving the CQI report by the transmitter side, the modulation and the code scheme of the transmitted data will be changed accordingly. This means that the data rate may be changed with each received CQI report according to the link adaptation algorithm which is pre-identified. Moreover, the capability of the receiver data processing time and the memory speed should be taken into account by the link adaptation algorithm [32].

37

### 2.4.2 Link adaptation: Power and rate control

In some wireless communication applications, a power controller is used to adjust the transmitted signal power in order to get an approximately constant SNR at the receiver. A constant SNR means that the power controller is used to compensate the channel fading effects. In poor channel conditions, the power controller transmits high power and vice-versa. The constant SNR at the receiver leads to a nearly constant BER which is needed in many communication systems such as WCDMA and CDMA2000. Figure (2.19.a) shows a power control signal. However, in many wireless communication systems there is no need for a constant data rate at the receiver. The data throughput of such systems is set to be maximum without increasing the transmission bandwidth. To achieve a high data throughput with an accepted BER, a data rate controller at the transmitter is needed. The data rate controller is used to control the data throughput according to the channel conditions state. For good channel conditions, high-order modulation schemes are used to achieve a high data throughput and high spectral efficiency. For poor channel conditions, low-order modulation schemes are used to achieve an accepted BER and to maintain the link between the transmitter and the receiver. Figure (2.19.b) shows a rate control signal.
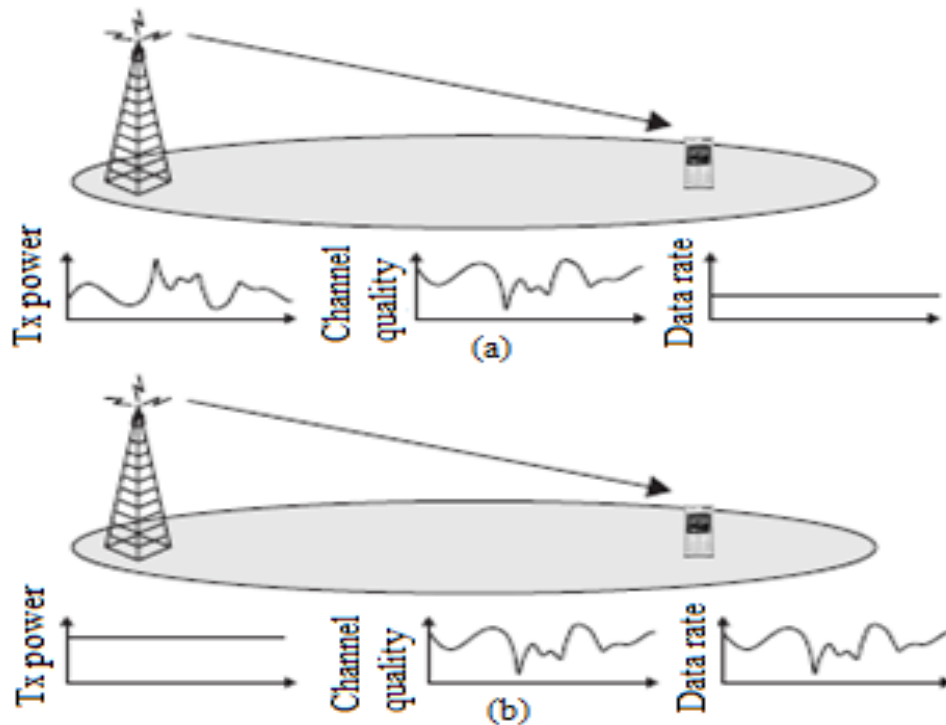
Figure 2.19: (a) Power control and (b) rate control.

Many researches have proved that rate control is more efficient than power control. As shown in Figure 2.19, a power amplifier in rate control always transmits in full power. On the other hand, the transmitting power of the power amplifier is mostly less than its maximum in power control transmission. In practice, the radio-link data rate is controlled by adjusting the modulation scheme and/or the channel coding rate. For good radio-link conditions, although the SNR at the receiver is high, there is a limitation that the data rate is dependent on the bandwidth of the radio link. Therefore, it is preferable to use higher-order modulation, for example 16QAM or 64QAM, together with a high code rate. But, for poor radio-link conditions, QPSK and low-rate coding are used. Accordingly, rate control link adaptation is sometimes named Adaptive Modulation and Coding (AMC) [33, 36].

# Chapter Three

# System Design, Simulation and Analyses

## 3.1 Introduction

In this chapter three types of wireless communication systems are simulated: The single-carrier wireless communication system, the OFDM wireless communication system, and the MIMO-OFDM wireless communication system.

## 3.2 The SINGLE-CARRIER WIRELESS COMMUNICATION SYSTEM

For a single carrier base band transmission system, totally $10^7$ random bits have been generated by using MATLAB function which is random binary sequence generator. The generated bits have been divided into 100 frames each of which contains $10^5$ bits. Six modulation types (BPSK, QPSK, 16QAM, 32QAM, 64QAM and 128QAM) have been used to modulate the randomly generated bits. All the calculated BERs are in physical layer and without any error correction. The modulated symbol duration of (66.7μsec) was chosen so that the symbol bandwidth was much less than the coherence bandwidth. The carrier frequency was set to 2.6GHz and the maximum allowable speed of receiver equipment is 160 km/h, so the maximum Doppler shift frequency becomes 385.185Hz. The generated symbols have been transmitted through the AWGN channel and the Rayleigh flat fading channel with the effect of AWGN. Each symbol has been transmitted separately through these two channels. At the receiver, an ideal channel estimation has been done to find the Rayleigh

fading channel parameters. The ideal Rayleigh fading channel parameters have been used with a single tab equalizer (zero forcing equalizer) to compensate the effect of Rayleigh fading channel on the received symbol. After that the received symbols were demodulated by a proper demodulation scheme which matches the modulation scheme that was used at the transmitter side to get the received bits. From the received signal, the BER performance was calculated.

Two different speeds of the receiver equipment have been chosen to experience the Doppler frequency shift effect on the received signal strength. In the first case, the receiver was assumed to move in a crowded traffic so that its speed does not exceed 10 km/h. The effects of such a speed are expected to be like those when the receiver is in a static situation where the signal experiences a flat fading multipath effect. In the second case, the receiver equipment was assumed to move at a speed of 160 km/h as a maximum speed of the moving vehicle.  Figure 3.1 shows the effects of the two speeds on the received signal strength.
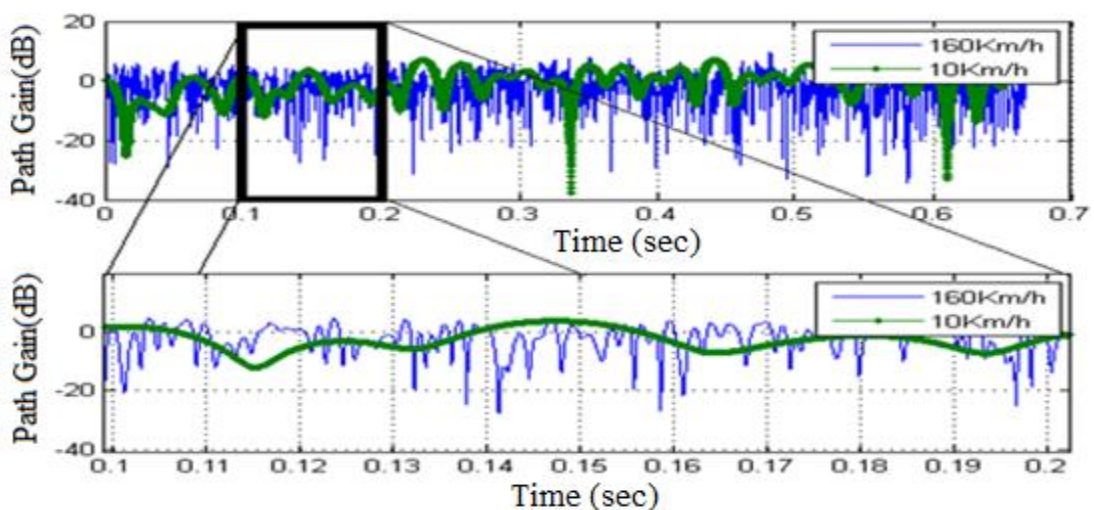


Figure 3.1: Path gain for Rayleigh fading channel and for two speeds of the receiver 10 km/h and 160 km/h.

41

For high moving speed, Figure 3.1 shows that, the received signal has severe fluctuations in the signal power strength (i.e. fast fading) due to effect of the high value of the Doppler frequency shift. For low moving speed of the receiver equipment, on the other hand, the signal has slow fading in the signal power strength.

In the case of the practical system, the Rayleigh fading channel parameters have been estimated by assuming 10% of the transmitted data as pilot bits. The pilot bits are inserted between the transmitted data. Therefore 10% of the Rayleigh faded channel parameters can be estimated at equal time spaces. The remaining 90% of the Rayleigh fading channel parameters are interpolated as shown in Figure 3.2.
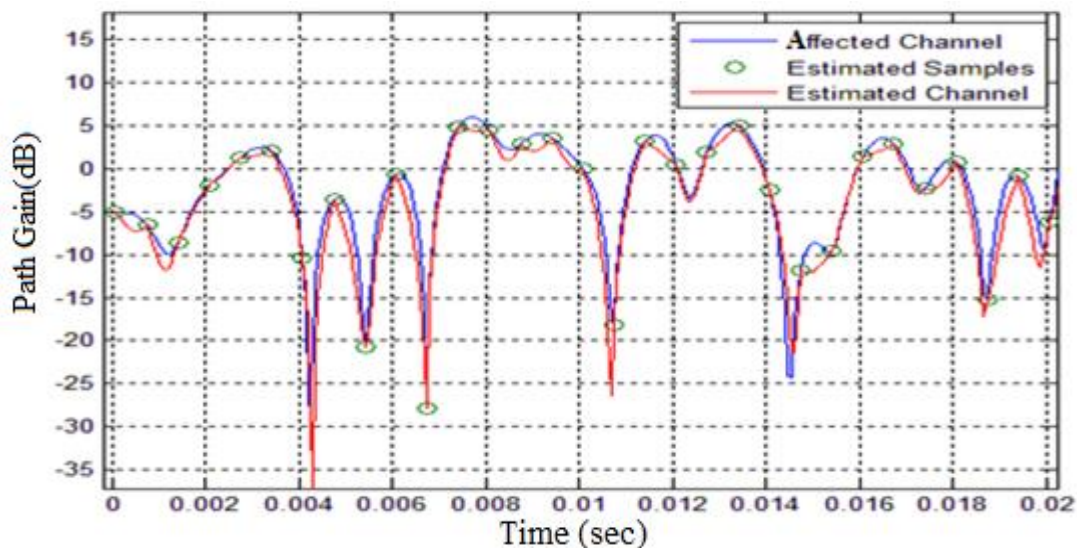


Figure 3.2: Difference between actual channel and estimated channel.

The practical effect of the Rayleigh fading channel, the samples of the estimated Rayleigh fading channel and the estimated Rayleigh fading channel are shown in Figures 3.3 and 3.4. The two figures are plotted for two different speeds of the receiver and they show this for only

42

one transmitted frame. The estimated channels in the two cases are interpolated to functions of 9th degree.
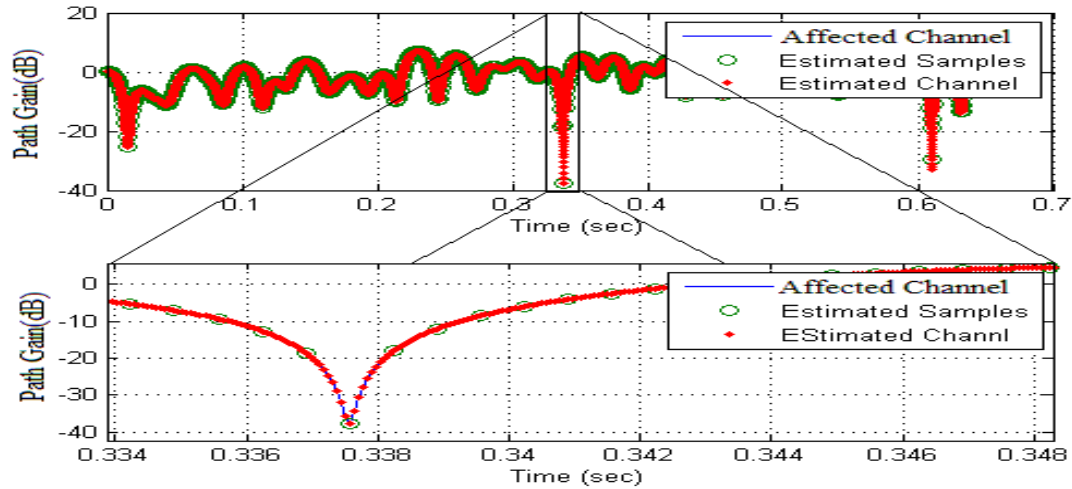


Figure 3.3: Channel estimation by using 10% of data as a pilot for 10 km/h receiver speed.
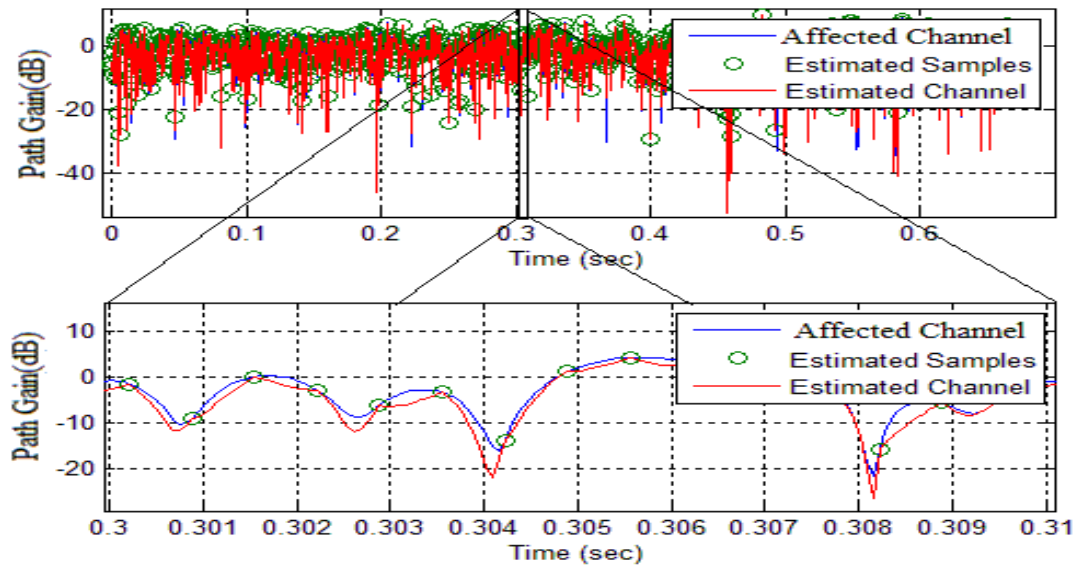


Figure 3.4: Channel estimation by using 10% of data as a pilot for 160 km/h receiver speed.

Figure 3.3 shows that at 10 km/h moving speed of the receiver equipment, the actual and the practical estimated Rayleigh fading channels are approximately the same. Figure 3.4 shows that at 160 km/h moving

43

speed of the receiver equipment there is a difference between the actual and the estimated Rayleigh fading channels, which causes a degradation and limitation in the BER performance of the received signal. The difference between the actual and the estimated Rayleigh fading channels at 160 km/h speed is due to the high Doppler effect which causes a high fluctuation in the actual Rayleigh fading channel as shown in Figure 3.4. In other words, when the receiver equipment speed is 160 km/h, the number of transmitted pilots is not enough to estimate the actual Rayleigh fading channel accurately.

## 3.3 The OFDM WIRELESS COMMUNICATION SYSTEM

### 3.3.1 The OFDM Symbol Generation

Two OFDM symbols are generated by using MATLAB. The first symbol is generated by using the multicarrier OFDM system. The multicarrier OFDM system is implemented by using a number of modulators which is equal to the number of the OFDM symbol subcarriers. The hardware implementation of the multicarrier OFDM system is very difficult because there is need for a huge number of modulators, in addition to the difficulty to synchronize these modulators with each other, although the multicarrier OFDM system seemed to be easily implemented by the software program. In practice the multicarrier OFDM needs to be generated and compared with the OFDM symbol that is generated by a single-carrier method (IFFT method). To implement the multicarrier OFDM system in MATLAB, sixty-four modulators are used to modulate 64 different complex symbols that are obtained from three different

modulation schemes. The first modulation scheme is BPSK with a zero phase shift, the second is also BPSK but with a phase shift of $\pi/5$ and finally modulating the data with the QPSK modulation scheme. The number 64 has been chosen because the size of the IFFT should be equal to $2^m$. The frequency hopping between adjacent modulators is set to $15KHz$ and the symbol duration is $66.7\mu sec$ ($BW = 2/66.7\mu sec = 30KHz$). The frequency hopping and the symbol duration have been chosen such that orthogonality between subcarriers is achieved. The spectrum of the multicarrier OFDM symbol is plotted by taking the Fourier Transform ($F.T$) of each modulator output and sums the results as shown in the following figure.
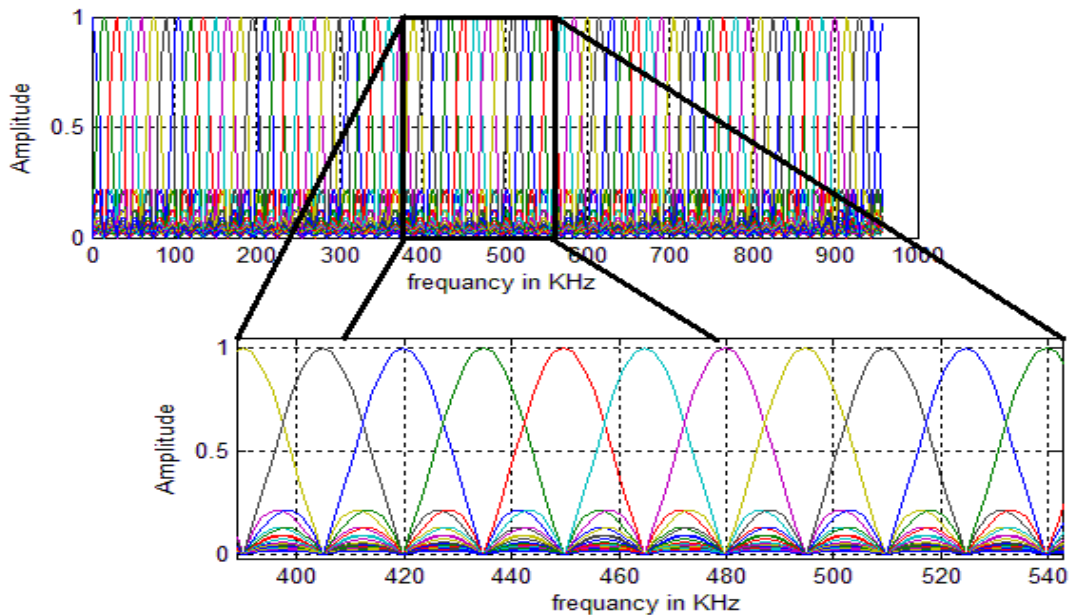


Figure 3.5: Spectrum of orthogonal subcarriers.

Figure 3.5 shows that the bandwidth needed to transmit 64 complex symbols over one OFDM symbol is $960KHz$ ($15KHz * 64$). To produce one multicarrier OFDM symbol, the outputs of the modulators are

45

summed. The duration of the generated multicarrier OFDM symbol becomes $66.7 \mu sec$.

The second set of OFDM symbols have been generated for the three modulation schemes as mentioned before, by using a single-carrier OFDM system (using IFFT instead of modulators). The hardware implementation of a single carrier OFDM system is easier than a multicarrier OFDM system because it replaces the modulators and summation by IFFT and the parallel to serial convertor. The time spaces between the output samples of the parallel to serial convertors determine the OFDM symbol duration and as a result determine the subcarrier bandwidth. The time space between the samples that are the outputs of parallel to serial was set to $1.0587 \mu sec$ ($66.7 \mu sec / (64 - 1)$) in order to get an OFDM symbol duration of $66.7 \mu sec$. Figures 3.6, 3.7 and 3.8 show the results of the multicarrier and single carrier for different modulation schemes.
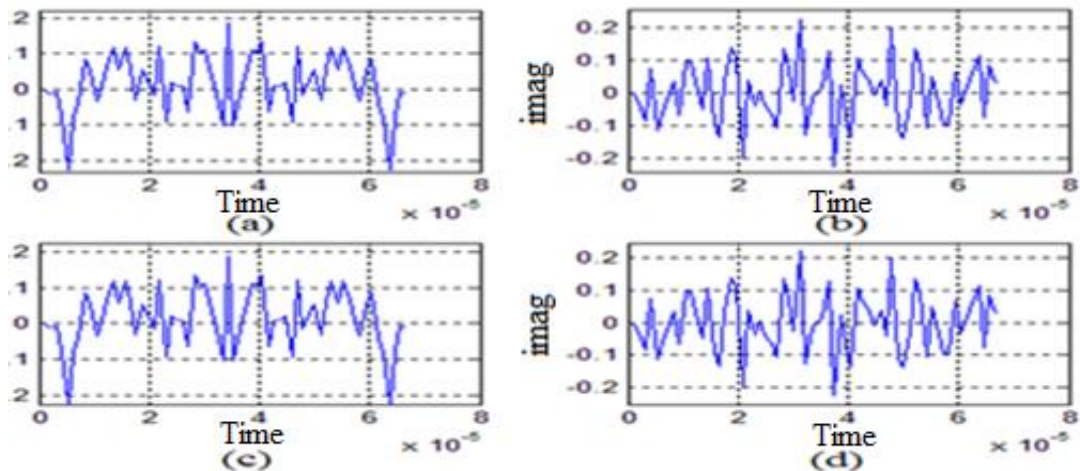


Figure 3.6: Comparison between the multicarrier and single carrier OFDM symbol for BPSK modulation with zero phase shifts and for the same transmitted bits where, (a) and (b) are for multicarrier, (c) and (d) are for single carrier.

46

Figure 3.6 shows the real and imaginary parts of the ODFM symbol that are generated by using multicarrier and single carrier methods. In this figure, the modulation used is BPSK with a zero phase shift (i.e. real values of 1and -1). The signal results of the two methods are obviously identical and each of them contains 64 complex samples with a duration of 66.7μsec. Figure 3.6 shows that the second half of the complex OFDM symbol is the complex conjugate of the first half except the first and middle points, since the first point represents the dc value and the middle point has no conjugate because the number of output points is even (the first point is the DC value, so there remain 63 samples which are divided into two groups of 31 samples each; the values of one group are the complex conjugates of those of the other group and the remaining one point in the middle is strictly real so that it is a complex conjugate of itself). The output of the IFFT and the FFT is a complex conjugate if their inputs are real values. Figure 3.7 shows that the multicarrier and single-carrier OFDM symbols of BPSK modulation with π/5 phase shift are the same.
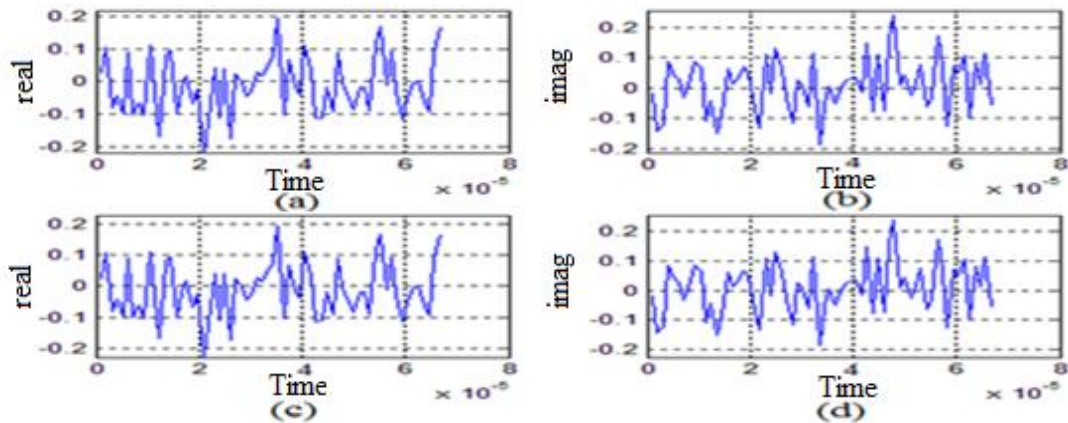


Figure 3.7: Comparison between the multicarrier and single carrier OFDM symbol for BPSK modulation with π/5 phase shifts and for the same transmitted bits where (a) and (b) are for multicarrier, (c) and (d) are for single carrier.

47

The difference between Figure 3.6 and Figure 3.7 is that each generated OFDM symbol in Figure 3.6 consists of complex values such that the first-half values are conjugates of the second half of the symbol, whereas the generated OFDM symbol in Figure 3.7 has complex values without conjugates. Therefore, there is no need for transmitting the conjugates of the multicarrier OFDM symbol and the time needed to transmit the symbol in Figure 3.6 becomes half of the time required to transmit a single-carrier OFDM symbol as in Figure 3.7.

Except for the BPSK modulation with zero phase shift, all the other modulation scheme outputs are in complex form without conjugates. Figure 3.8 shows a comparison between the multicarrier and single carrier OFDM symbol for QPSK modulation with zero phase shifts and for the same transmitted bits (simulated for 64 subcarriers).
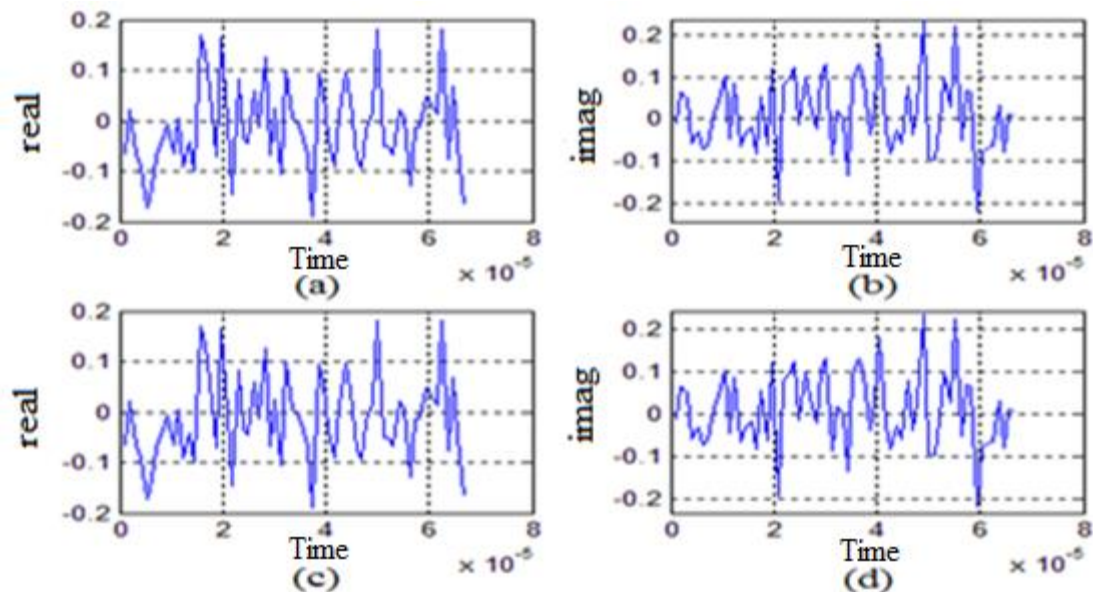


Figure 3.8: Comparison between the multicarrier and single carrier OFDM symbol for QPSK modulation with $\pi/5$ phase shifts and for the same transmitted bits where (a) and (b) are for multicarrier, (c) and (d) are for single carrier.

Figures 3.7 and 3.8 show a general case of the generated OFDM symbol that is modulated by IFFT and also show that the results are in complex form. Therefore, the whole OFDM symbol (real and imaginary parts) should be transmitted to the receiver side. Because the sine and cosine waves are perpendicular to each other, each of them is used simultaneously to modulate the real and imaginary parts of the OFDM symbol separately. Usually, the real part is up converted by using the sine carrier and the imaginary part is up converted by using the cosine carrier. Figure 3.9 shows the power spectrum of the OFDM symbol for the case of 64 QPSK modulated symbols. The spectrum is plotted by taking ( $20log_{10}abs\{(F.T(real\ or\ imag\ of\ (x(t))))\}$ where $x(t)$ is the complex OFDM symbol and F.T is the Fourier transform. Figure (3.10.a) is for the real part, and Figure (3.10.b) for imaginary part.
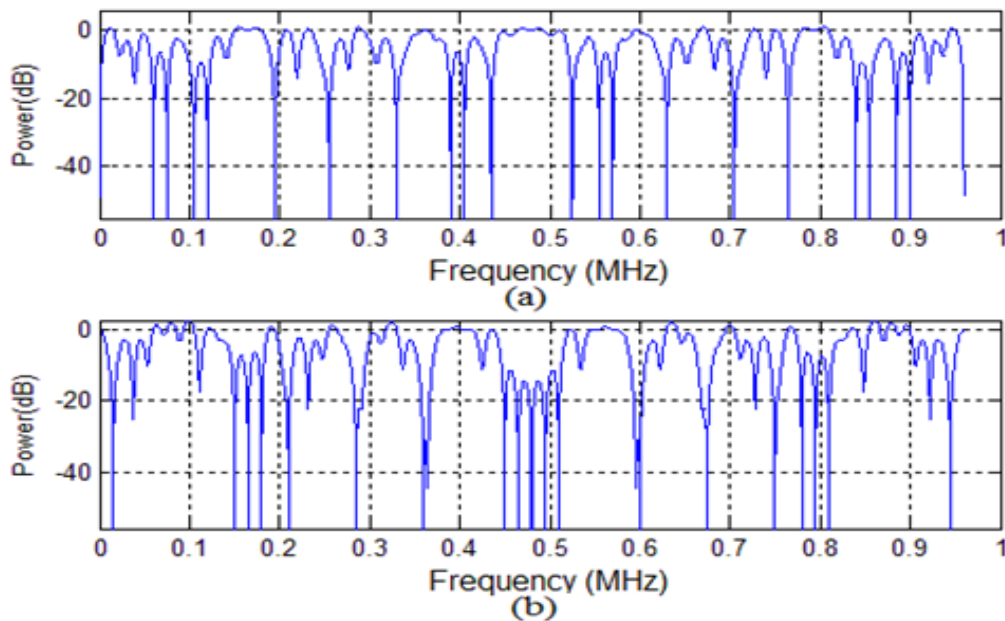


Figure 3.9: Spectrum of $x(t)$ as output of OFDM in QPSK (a) Real part spectrum (b) imaginary part spectrum.

49

Figure 3.9 shows that the bandwidth required to transmit the real part and the imaginary part is the same and equal to $960\ KHz\ (15KHz*64)$ where 64 is the number of symbols.

For 128 complex symbols and for QPSK modulation, the obtained OFDM symbol is shown in the following figure:
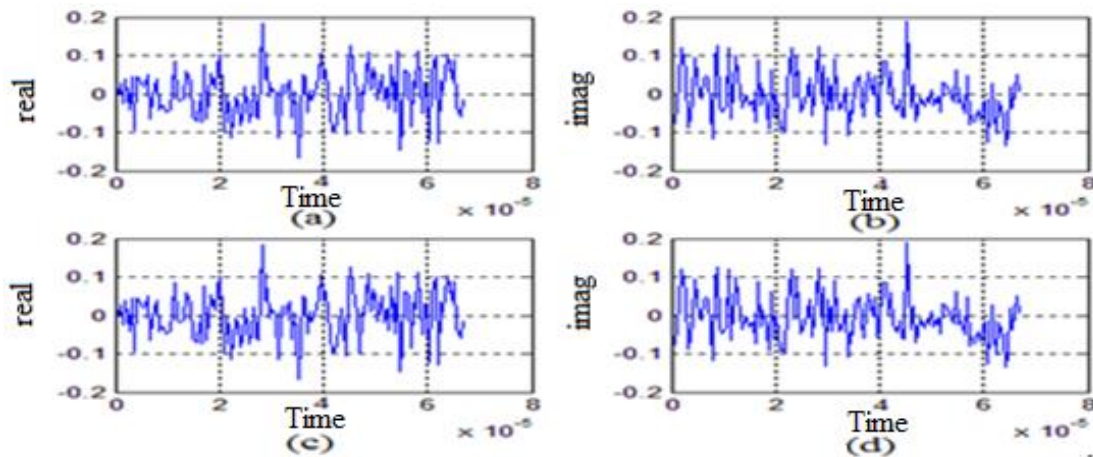


Figure 3.10: Comparison of the multicarrier and single carrier OFDM symbol in QPSK for the same transmitted bits (simulated for 128 subcarriers) where (a) and (b) are for multicarrier, (c) and (d) are for single carrier.

Figure 3.10 shows that the OFDM symbol time duration in the case of 128 modulated QPSK symbols is the same as the OFDM symbol time duration in the case of 64 modulated QPSK symbols as in Figure 3.8. The difference in time domain is the number of samples where in Figure 3.10 it is twice the number of samples in Figure 3.8. The other difference between the two cases is the bandwidth as shown in Figure 3.11, which shows that the bandwidth needed for the 128 symbols is twice the bandwidth needed for 64 symbols. Since the imaginary part spectrum bandwidth is the same as the real part spectrum bandwidth, there is no need for plotting it in Figure 3.11.
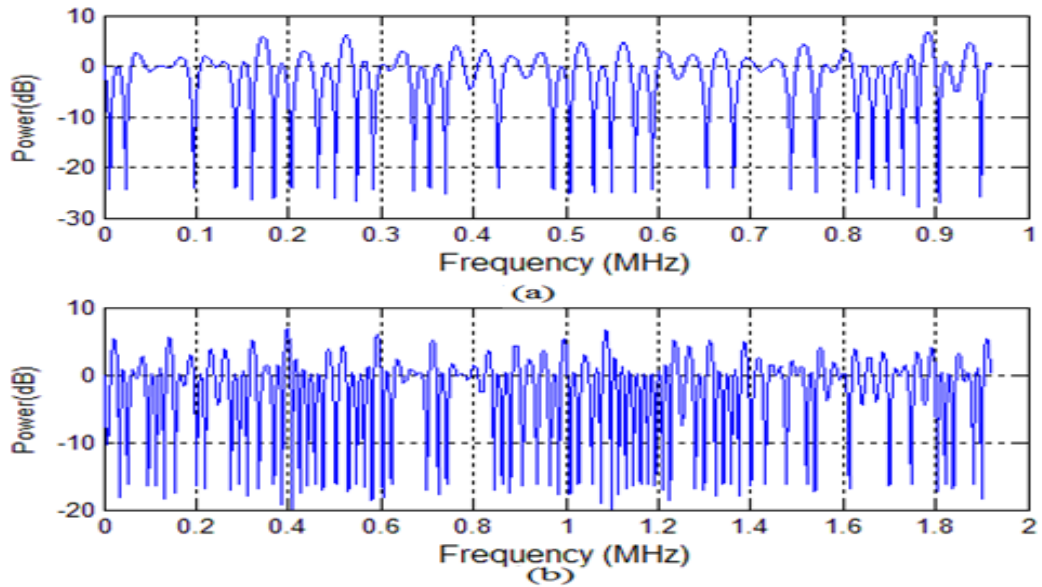
Figure 3.11: Real values spectrum comparison for two OFDM symbols (a) for 64 QPSK symbols and (b) for 128 QPSK symbols.

The work that has been done for the OFDM system until this point analyses and shows how the OFDM symbol is generated for 64 or 128 symbols (considered as a small number in real the world). In the next chapter, the LTE protocols are used in real the world and therefore 2048 symbols are taken into account.

### 3.3.2 LTE Time domain of the OFDM symbol without CP

According to the LTE protocol [37], the available bandwidth is $20MHz$, the subcarrier spacing is $15KHz$ the number of subcarriers is 1200 subcarriers, and the carrier frequency is $2.6GHz$. Two carriers are used to modulate the OFDM symbols, the sine carrier is used to modulate the real part and the cosine carrier is used to modulate the complex part, or vice-versa. Each OFDM subcarrier is modulated with a different complex

51

symbol (QPSK, 16QAM, 32QAM, 64QAM, 128QAM or 256QAM). The modulation process of the subcarriers is done by using IFFT of size 2048 ($2^{11}$). The first 424 and the last 424 IFFT inputs are zeros padded in order to get a symmetric zero padding. The remaining 1200 inputs of the IFFT are connected to the complex modulated symbols that are produced from the used modulation scheme. According to the IFFT size, the OFDM symbol consists of 2048 complex samples which are obtained after the parallel to serial convertor. The number of transmitted OFDM real samples is 2048. The number of transmitted OFDM imaginary samples is 2048. Therefore, two signals are transmitted simultaneously. Figure 3.12 shows the transmitter structure of the OFDM system. The time space between each of the adjacent OFDM samples is $0.0326$ $\mu sec$ ($66.7$ $\mu sec$/ ($2048 - 1$)), so the overall OFDM symbols duration is $66.7$ $\mu sec$. In practice, the output samples are passed through LPF before converting them from digital to analog and to get their final shapes, then they are up converted and transmitted through the channel. In the MATLAB there is no need to use the LPF because the MATLAB program processes the signal in digital form. The bandwidth occupied by the OFDM symbol is $18MHz$ ($1200 * 15KHz$). The remaining $2MHz$ is used as a guard band. Figure 3.13 shows a normalized ODFM symbol in time domain before channel and noise effects. In this case, there is also no cyclic prefix insertion. In this present work, the scaling is always applied and has no effect on the system performance because a percentage noise is added to the signal to get the desired SNR at the receiver.
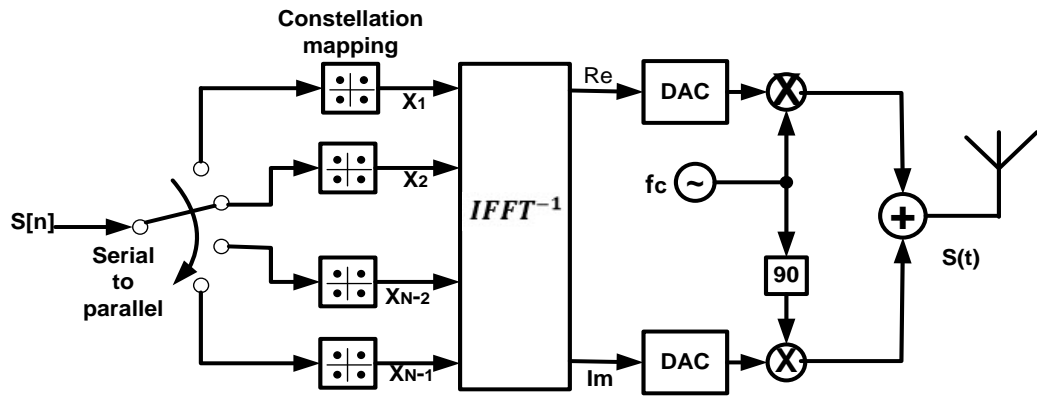
Figure 3.12: Transmitter structure of the OFDM system.
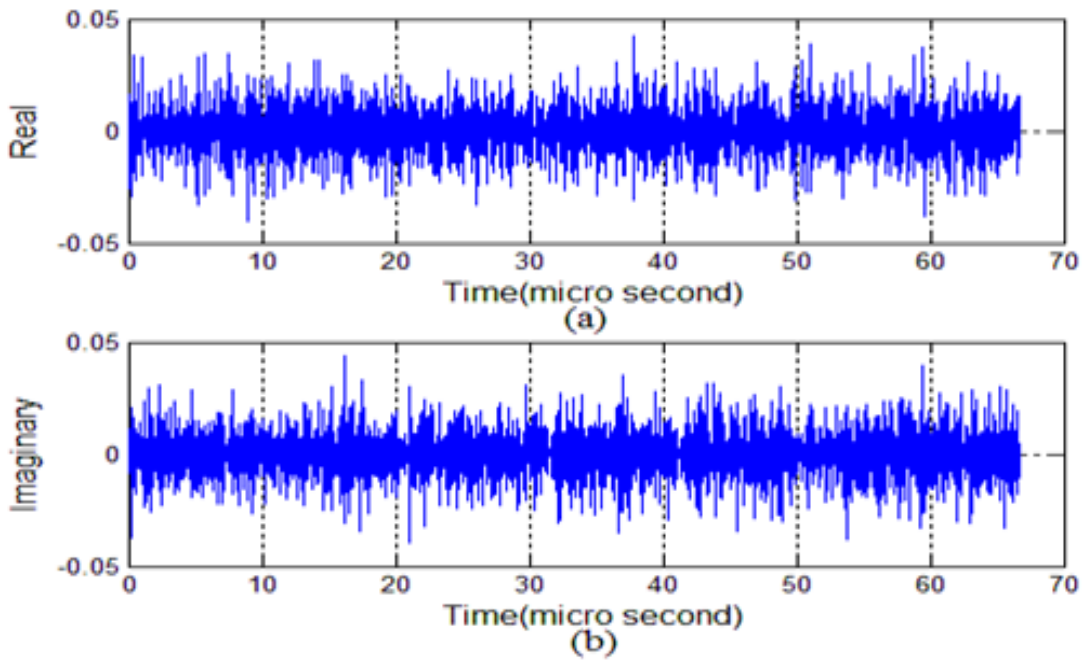


Figure 3.13: Transmitted OFDM symbol for QPSK modulation and without cyclic prefix (a) real part (b) imaginary part.

To show the spectrum of the previous OFDM signal, the signal applied to Fast Fourier Transform has a size larger than the IFFT size used in the transmitter side. Figure 3.14 shows the spectrum of the OFDM symbol in the base band where absolute values are applied.

53
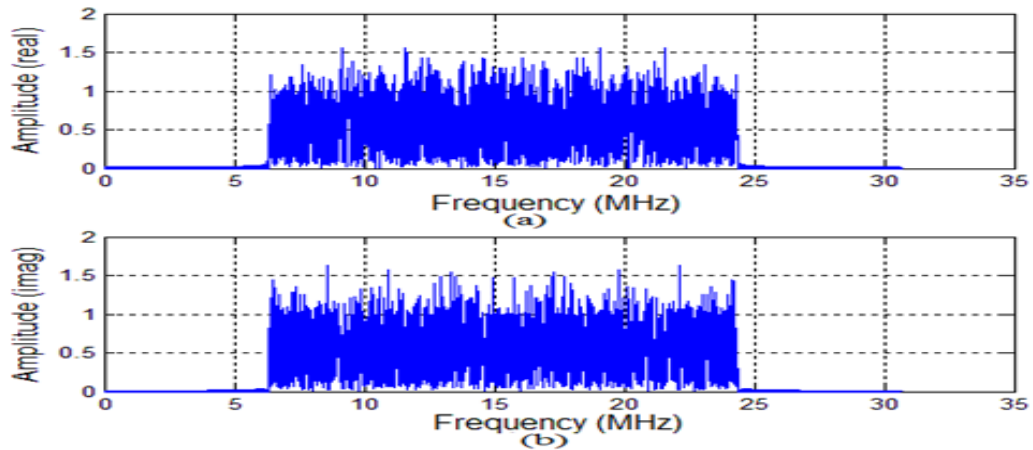
Figure 3.14: Amplitude spectrum of the transmitted OFDM symbol for QPSK modulation without CP (a) real part (b) imaginary part.

To have a clear idea about the OFDM symbol spectrum, the power spectral of the OFDM symbol is plotted by taking the $(20log_{10}abs\{((F.T(real(x(t)))))\})$ and $(20log_{10}abs\{((F.T(imag(x(t)))))\})$ where $x(t)$ is the complex OFDM symbol and F.T is the Fourier transform. Figure 3.15 shows the power spectrum of one OFDM symbol.
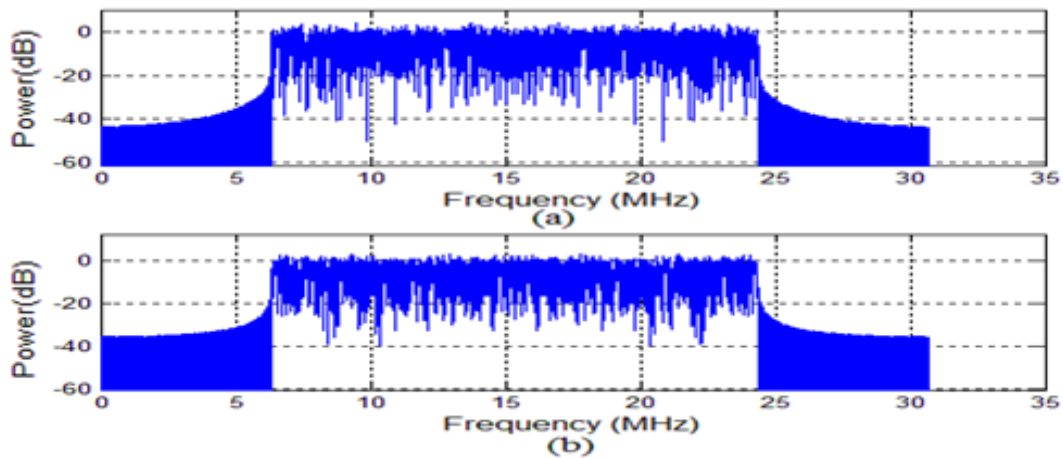


Figure 3.15: Power spectrum of the transmitted OFDM symbol without CP (a) real part (b) imaginary part.

54

Figures 3.14 and 3.15 show that the bandwidth of the real and imaginary parts is the same. To determine the bandwidth of the transmitted OFDM symbol, one can use the real or the imaginary part only. Figure 3.16 shows the real part OFDM symbol bandwidth in zooming.
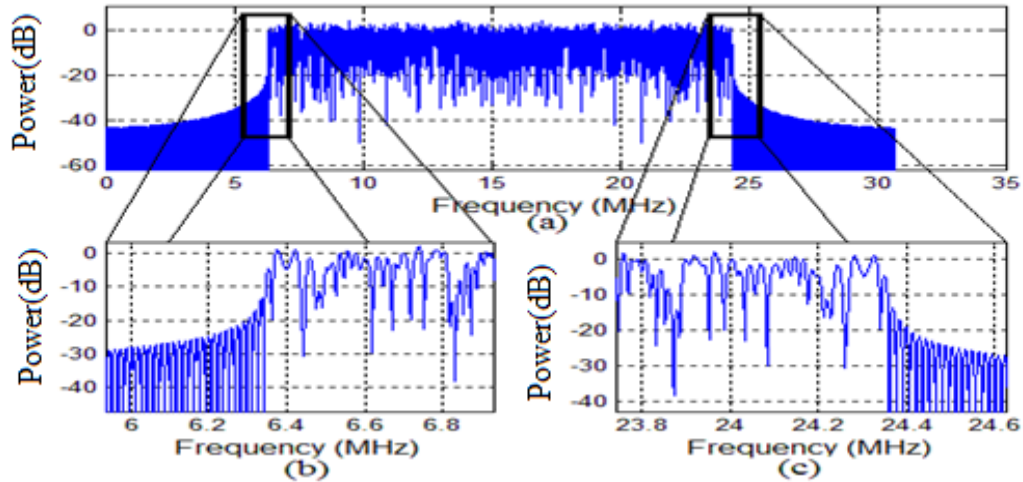


Figure 3.16: OFDM symbol bandwidth (a) without zooming (b), (c) with zooming.

Figure 3.16 shows that the OFDM bandwidth is 18MHz (6.43MHz-24.3MHz). The power spectrum outside the mentioned range is fast decaying from 0dB to around -40dB. In practice, a band pass filter is also used to attenuate the frequencies outside the specified bandwidth range in order to reduce the interference with the adjacent bands. In the present work, the band pass filter is not considered since there is no interference with adjacent spectra because the MATLAB software assumes that there are no other communication systems.

The pattern of the zero padding to the IFFT is very important. For the symmetric zero padding at the two sides of the inputs of the IFFT, the OFDM symbol subcarriers are orthogonal to each other because

55

18MHz is needed to transmit one complex OFDM symbol which contains 1200 complex symbols (Figure 3.16).

Another form of symmetric zero padding is obtained when the complex input symbols are divided into two groups of 600 complex symbols (1200/2). The first group is applied to the first 600 IFFT inputs and the second group is applied to the last 600 IFFT inputs. The remaining 848 middle inputs out of the 2048 point size of the IFFT are zero padded. The power spectrum of the second zero padding form is shown in Figure 3.17.
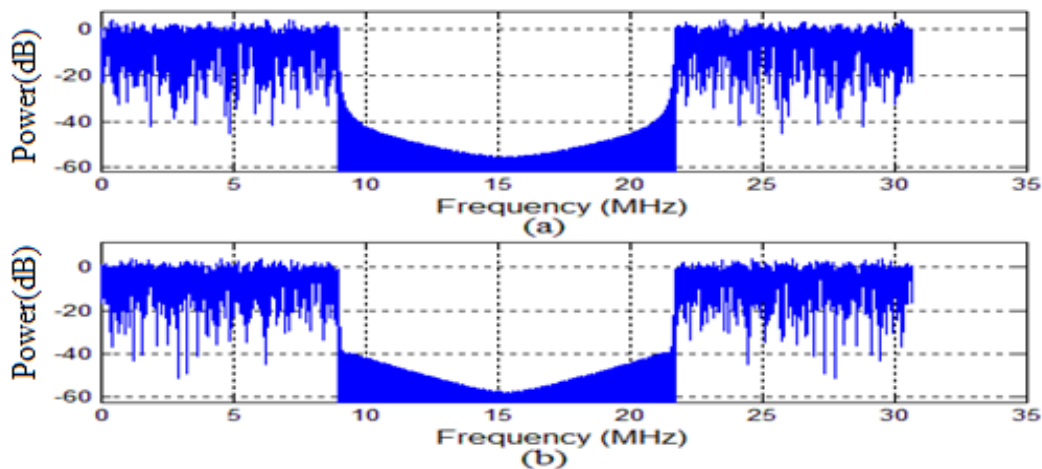


Figure 3.17: The power spectrum for the second zero padding form (a) for real part (b) for imaginary part.

Figure 3.17 (a) or (b) shows the bandwidth needed to transmit the OFDM symbol which is 18MHz and is divided into two equal parts separated by a gap of 12.72MHz ($848 * 15$KHz). According to Figure 3.17, the second type of zero padding cannot be used because the available bandwidth according to the LTE protocol is continuous through the 20MHz as in Figure 3.16.

The third type of zero padding is asymmetric where the complex input symbols are applied to the first 1200 IFFT inputs. The remaining 848 are zero padded. The fourth type of zero padding is also asymmetric but the complex input symbols are applied to the last 1200 IFFT inputs. The remaining 848 are zero padded. The OFDM symbol power spectra for the two asymmetric cases are shown in Figures 3.18 and 3.19.
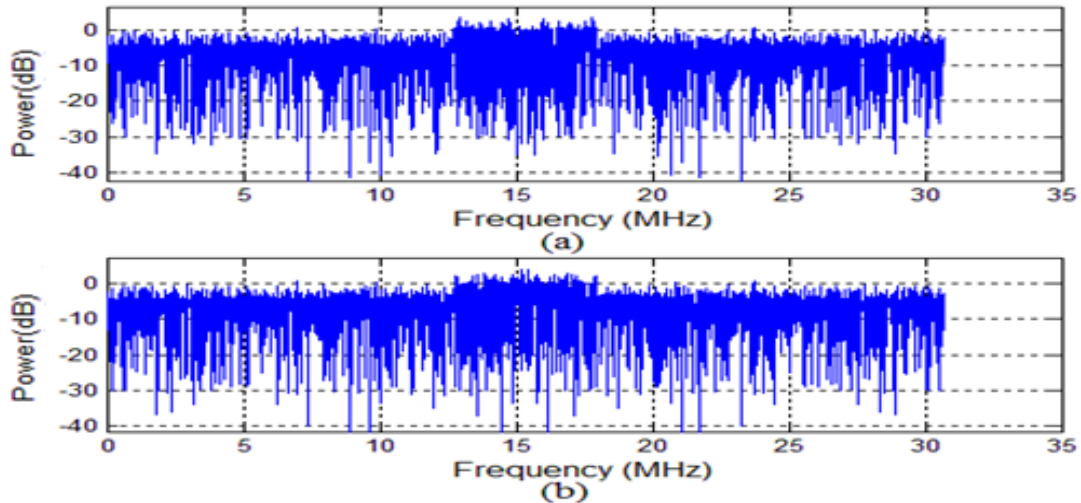


Figure 3.18: The power spectrum for the third zero padding form (a) for real part (b) for imaginary part.
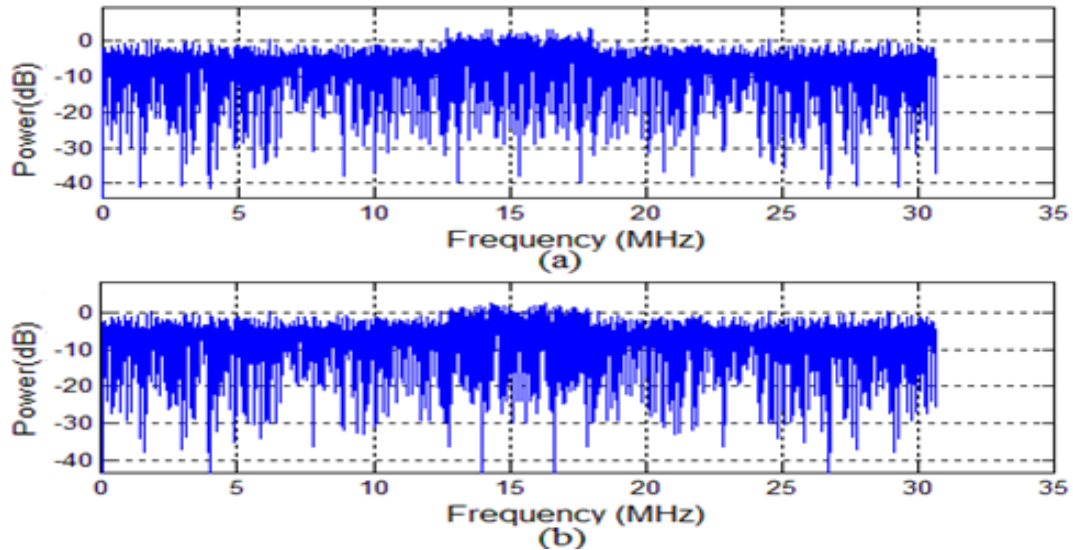


Figure 3.19: The power spectrum for the fourth zero padding form (a) for real part (b) for imaginary part.

57

Figures 3.18 and 3.19 show that the subcarriers orthogonality of the OFDM symbols, which are produced from the third and fourth zero padding methods, are lost. Therefore, in these two cases the bandwidth needed to transmit the 1200 complex symbols is 30.72MHz ($2048 *$ $15KHz$) as shown in Figures 3.18 and 3.19. In addition, the band pass filter cannot be used to restrict the bandwidth of the transmitted OFDM symbols to18MHz because the components outside the range 6.43MHz to 24.3MHz have high power. Therefore, the third and fourth methods for zero padding are band wasting and inefficient to use.

One can conclude that the best and most applicable method for the IFFT zero padding to generate the OFDM symbol is the first method (symmetric zero padding at the two sides of the IFFT inputs). One can conclude that the spectrum bandwidth of the real part and the imaginary part is the same.

### 3.3.3 Cyclic prefix insertion

Although the OFDM system is used to eliminate the problem of the ISI there is an ISI in the initial part of the OFDM symbol only. The solution to this problem is to copy the last part of the OFDM symbol and insert it at the beginning of it; this process is known as cyclic prefix insertion (CP). The cyclic prefix added to the OFDM symbol at the transmitter should be removed at the receiver. In the present work, the CP duration is chosen to be $4.7\mu sec$ according to the LTE protocol. After CP insertion, the OFDM symbol duration becomes 71.4 $\mu sec$ ($66.7\mu sec +$ $4.7\mu sec$). The CP insertion is done by taking the last 144 samples

$(4.7\mu sec/0.0326\mu sec)$ of the OFDM symbol and inserting them at the beginning of the OFDM symbol as shown in Figure 3.20.
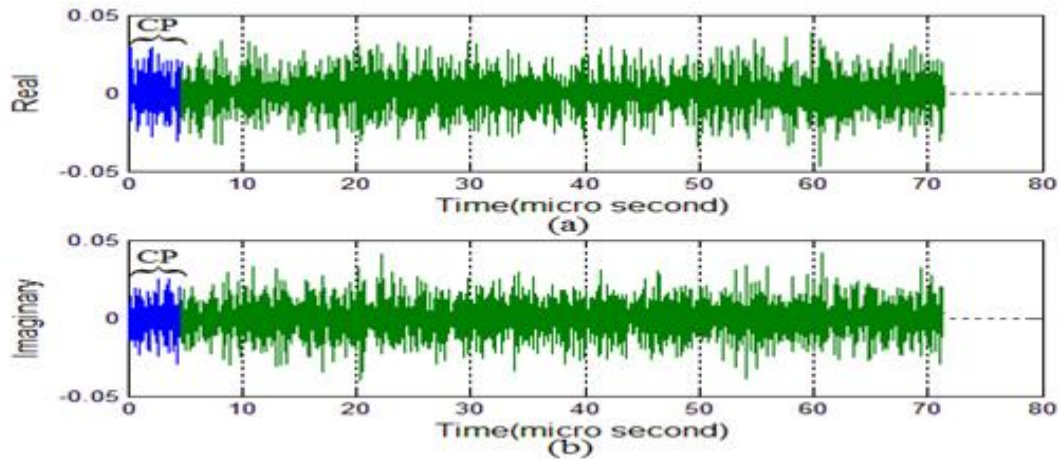


Figure 3.20: CP insertion in the transmitted OFDM symbol (a) real part (b) imaginary part.

The power spectrum of the OFDM symbol after adding the CP is shown in Figure 3.21:
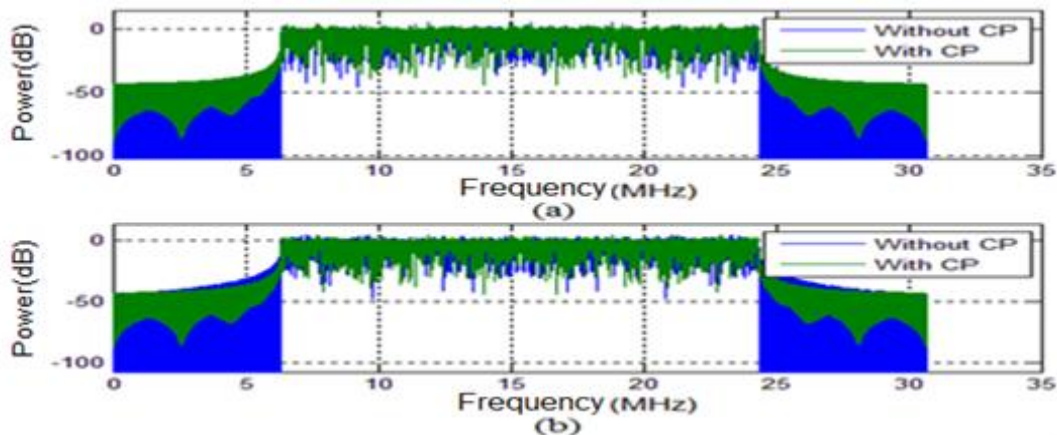


Figure 3.21: Power spectrum of the transmitted OFDM symbol (a) real part (b) imaginary part.

To see the details of the power spectrum of the OFDM symbol, zooming was done on parts of the graph before adding the CP and after

adding it. Figure 3.22 shows that zooming only the real part of the complex OFDM symbol is considered in the graph since the imaginary part has the same details.
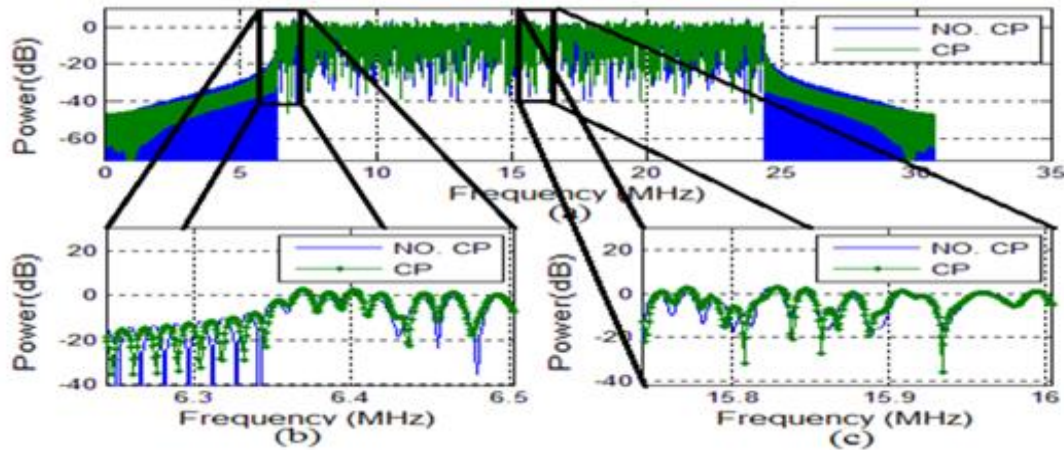


Figure 3.22: (a) Power spectrum of the OFDM symbol before adding CP and after adding it (b), (c) zoomed of the beginning and the end of (a).

It is obvious from Figures 3.21 and 3.22 that the bandwidth needed to transmit one OFDM symbol before and after adding CP is the same. Figure 3.23 shows the bandwidth of the CP part of the OFDM symbol.
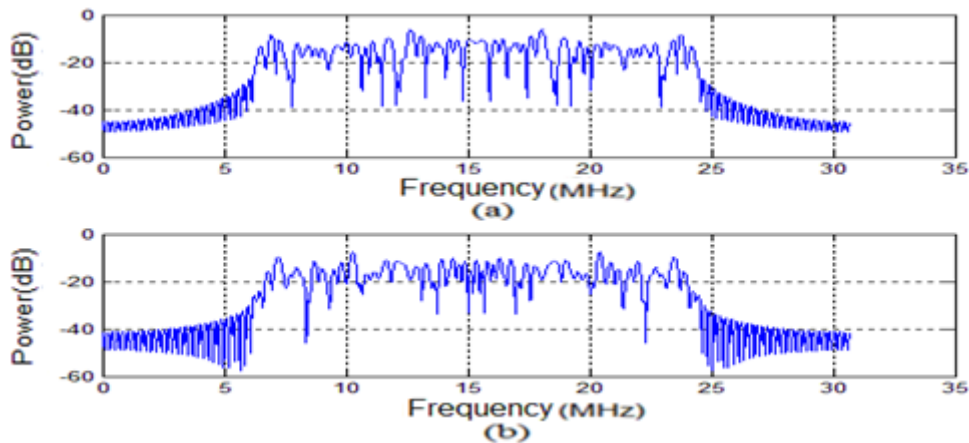


Figure 3.23: Power spectrum of the CP part of the transmitted OFDM symbol (a) real part (b) imaginary part.

60

Figure 3.23 shows that the CP added to the OFDM symbol has the same bandwidth of the OFDM symbol before adding the CP. Therefore, the added CP does not introduce an extra bandwidth to the transmitted OFDM symbol.

After generating the ODFM symbol, it is up converted to the desired frequency then passed through the channel. In the computer simulation, it is difficult to generate a signal with a high frequency (2.6 GHz), which means generating a large number of samples to form the signal. This large number of samples also needs a huge buffer size and a very high-speed data processor. In the MATLAB program, scaling can be used to overcome the problem of high frequencies by dealing with the signal in the baseband. In MATLAB, there is a function used to generate the Rayleigh flat fading channel effects taking into account the used carrier frequency and the Doppler effects. The scaling is done by multiplying the baseband OFDM symbol by the generated Rayleigh flat fading channel for the desired carrier frequency (in this project 2.6GHz). In practice, the channel is convoluted with the signal to produce a signal convolving the channel parameters. The convolution process can be achieved by multiplication if the signal is assumed to be transmitted on a flat fading channel with a delay spread of less than 1% of the signal length, which is considered in the present work [38]. In addition, Matlab software considers this rule for the flat fading channel.

### 3.3.4 Channel effect on the received OFDM symbol

### 3.3.4.1 Channel characterization

The effect of the channel on the received OFDM symbol is characterized by multiplying the transmitted complex OFDM symbol samples by the Rayleigh coefficients, then adding the effect of the AWGN. The Rayleigh coefficients are generated softwarely by one of the MATLAB functions. The inputs to the function that generates the Rayleigh coefficients are the carrier frequency (which is equal to 2.6GHz), the symbol duration (which is equal to $66.7 \ \mu sec$), the Doppler frequency, the number of multipath (which is equal to 1 in this case), the coefficient gains normalized to 1 and a control key of the Rayleigh coefficients in order to restart the Rayleigh coefficients for each new symbol. The generated Rayleigh coefficients are in complex form. The number of the Rayleigh coefficients is equal to the number of samples of one OFDM symbol. The OFDM symbol duration is $66.7 \ \mu sec$ (excluding CP) because only one path is assumed between the transmitter and the receiver. In this case, adding CP to the OFDM symbol does not enhance the system performance and can be cancelled. In this project, the transmitter is assumed as a base station and the receiver is assumed as a mobile, therefore, the Doppler effects are associated with the speed and the direction of the receiver. AWGN is considered to have its effects on the signal distorted by the Rayleigh fading channel. The AWGN channel is generated by using a MATLAB function which measures the signal power and adding the AWGN in such a way so that the desired SNR can be achieved at the receiver. The generated AWGN coefficients are in complex form with a

real part and an imaginary part that are generated independently according to the AWGN statistics. The number of generated AWGN channel samples is equal to the number of the samples for one OFDM symbol. The AWGN channel is regenerated on each new OFDM symbol. To show the channel effects on the received OFDM symbol, two speeds of the receiver are considered, 10 and 100 km/h.

**3.3.4.2 Effect of 10 km/h receiver speed on the received OFDM symbol**

For 10 km/h receiver speed, the Rayleigh fading channel variations for one OFDM symbol are shown in Figure 3.24. Figure (3.26.a) represents the path gain and it is plotted by taking $20log_{10}(|h(t)|)$ where $h(t)$ is the impulse response of the channel. Figure (3.26.b) represents the phase delay and it is plotted by taking

$tan^{-1}(Im(h(t))/Re(h(t)))$.
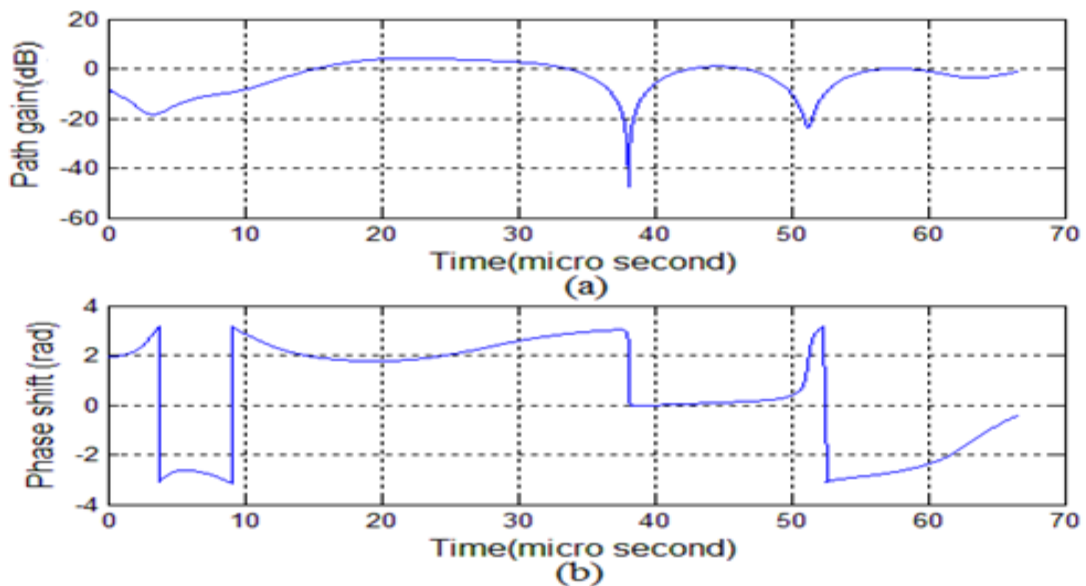


Figure 3.24: Rayleigh fading channel variation for 10 km/h speed of receiver (a) path gain (b) phase shift.

The effect of the Rayleigh fading channel on the received OFDM symbol before adding the AWGN is shown in Figure 3.25. Figure (3.27.a) shows the transmitted OFDM symbol before and after multiplying it by the Rayleigh channel coefficients. Figure 3.25 (b), (c) shows the zoomed parts of Figure 3.25.a.
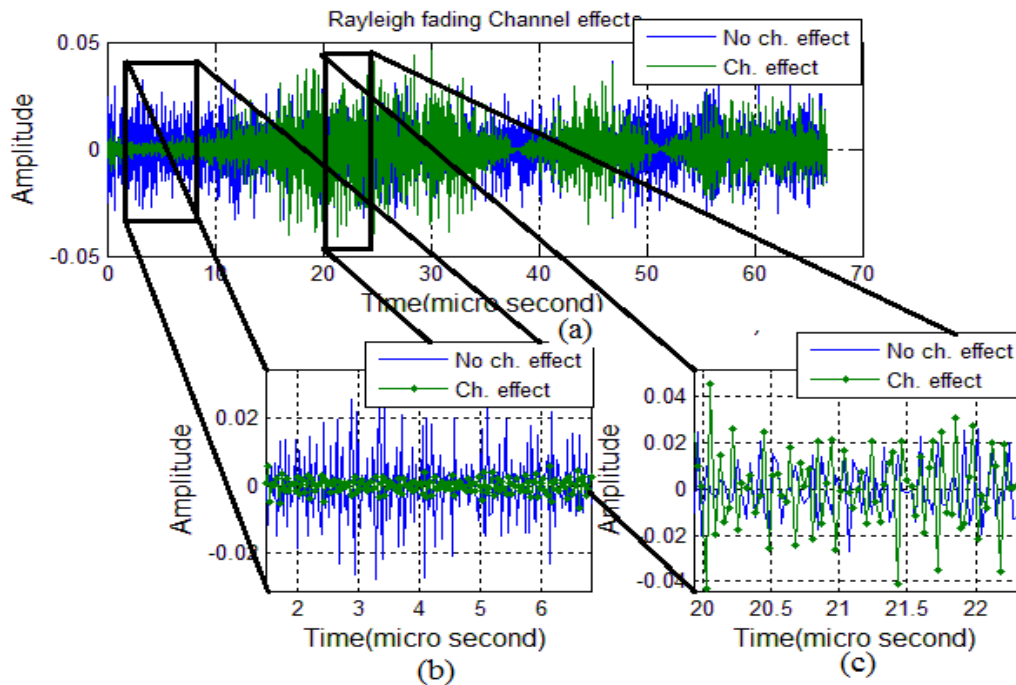


Figure 3.25: Transmitted OFDM symbol without channel effect and with Rayleigh channel effect (a) the whole OFDM symbol (b), (c) zoomed parts.

Figures (3.24a) and (3.25.a) show that the OFDM symbol severely fades at some parts due to destructive interference; see for example, the region from 0μ$sec$ to 15μ$sec$ or from 34μ$sec$ to 42μ$sec$. Meanwhile, during some parts of the OFDM symbol, the signal may have high gain due to constructive interference; see for example the region from 16μ$sec$ to 33μ$sec$. Figure 3.25 (b), (c) shows two different parts of the

transmitted OFDM symbol where in (b) a destructive interference occurs and in (c) a constructive interference occurs.

Figure 3.26 shows the power spectrum of the OFDM symbol before and after the Rayleigh effects for a 10 km/h speed of the receiver.
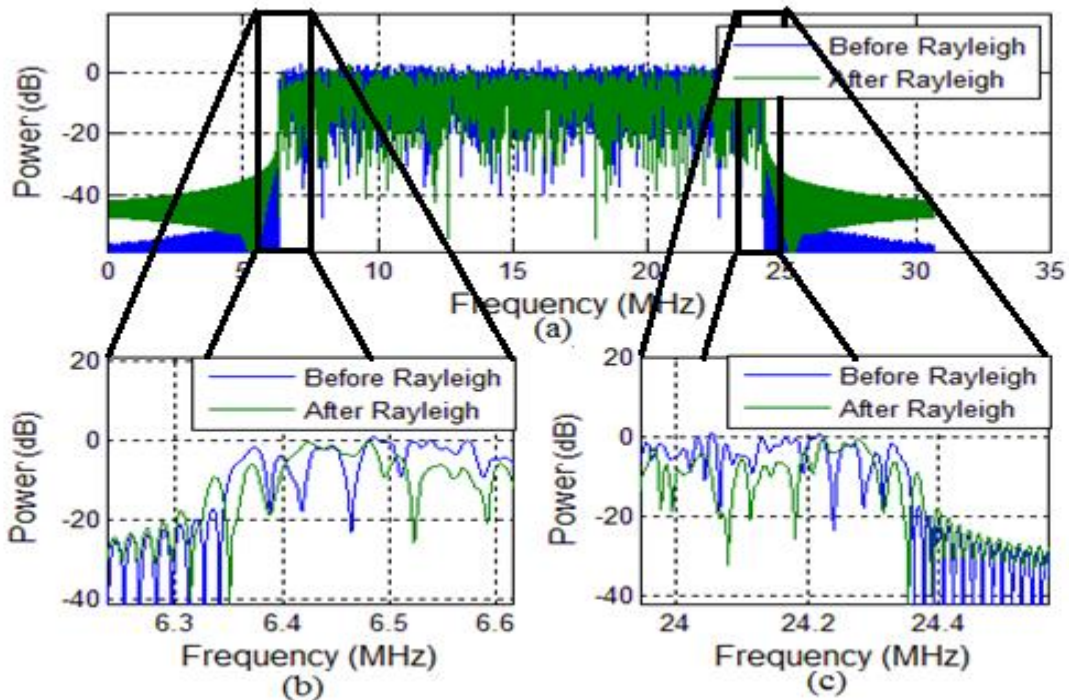


Figure 3.26: (a) OFDM symbol spectrum bfore Rayleigh effcect and after Rayeigh effect and for 10 km/h receiver speed. (b), (c) zoomed of the beginning and the end of (a).

Figure 3.26 shows the spectrum of the OFDM symbol affected by a Rayleigh channel with a receiver speed of 10 km/h. It is different from the spectrum of the signal without a Rayleigh channel effect. The Doppler effect results in broadening the spectrum bandwidth. The bandwidth broadening in the spectrum shown in Figure 3.26 is small because the speed of the receiver is low.

## 3.3.4.3 Effect of 100 km/h receiver speed on the received OFDM symbol

For 100 km/h receiver speed, the Rayleigh fading channel variations for one OFDM symbol is shown in Figure 3.29.
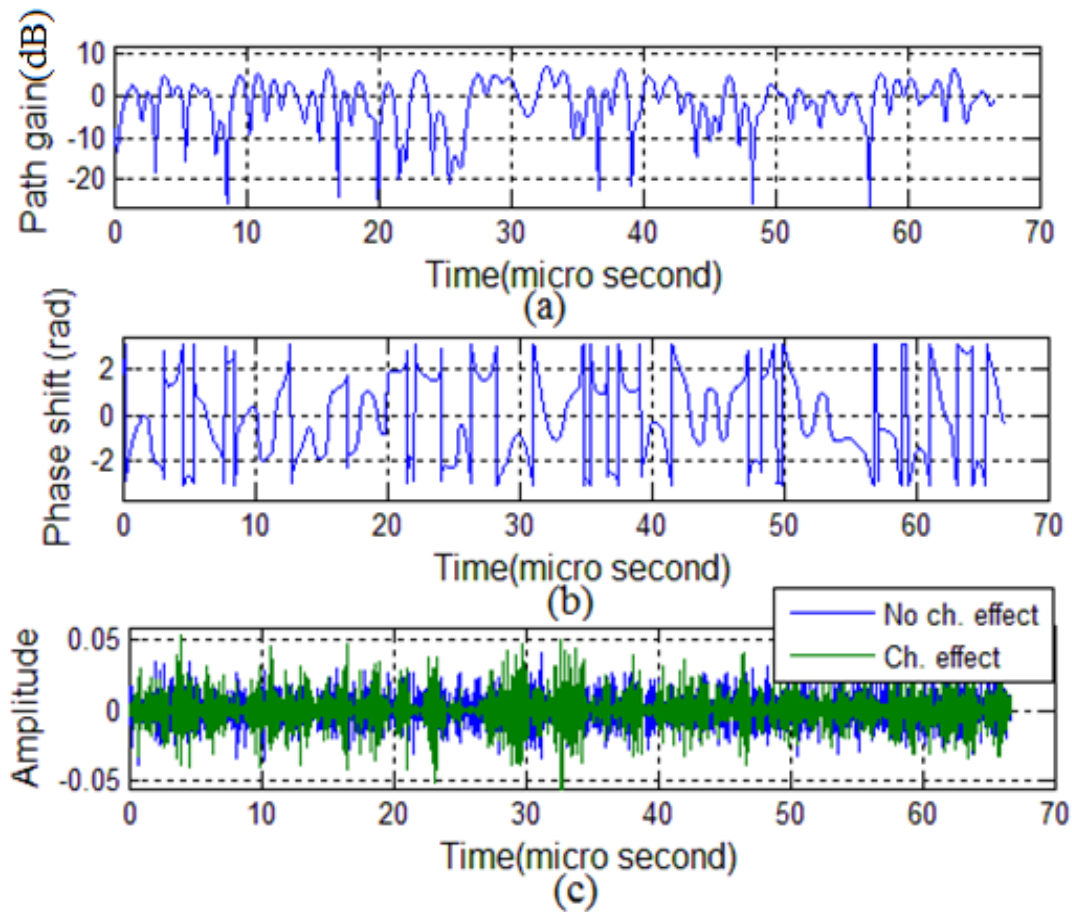


Figure 3.27: Rayleigh fading channel state for 100 km/h speed of receiver (a) path gain (b) phase shift (c) channel effect on the symbol.

Figures 3.24 and 3.27 (a), (b) show that when the speed of the receiver increases, the fluctuations of the Rayleigh channel for the same period of time also increases. The increasing fluctuations in channel make the channel estimation at the receiver less accurate, which leads to

degrading the system performance as mentioned in Chapter One. The spectrum of the OFDM symbol affected by the Rayleigh fading channel for100 km/h speed of the receiver is shown in Figure 3.28.
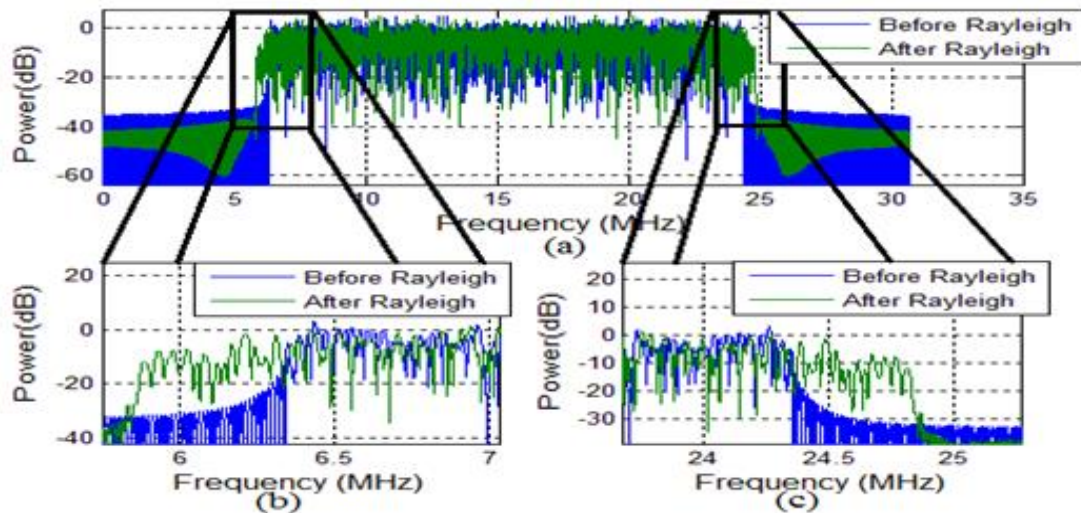


Figure 3.28: (a) OFDM symbol spectrum before Rayleigh effect and after Rayeigh effect and for 100 km/h receiver speed. (b), (c) zoomed of (a).

Figure 3.28 (b) and (c) shows the broadened OFDM symbol spectrum due to the Doppler effects. The conclusion that may be drown from Figures 3.26 and 3.28 is that the broadening in spectrum is proportional to the speed of the receiver. From the spectrum broadening, the speed of the receiver can be calculated so that it can be used later as an input parameter to determine the best modulation scheme that can be used with the instantaneous channel state.

### 3.3.4.4 Effect of AWGN on the received OFDM symbol

The other effect of channel on the received signal is the AWGN, which is added to the signal after considering the effect of the Rayleigh fading channel. As mentioned previously, the value of the AWGN that is

added to the signal is determined by the desired SNR value. Figures 3.29, 3.30 and 3.31 show the effect of the 0dB, 10dB and 20dB SNR on the received OFDM symbols, respectively.
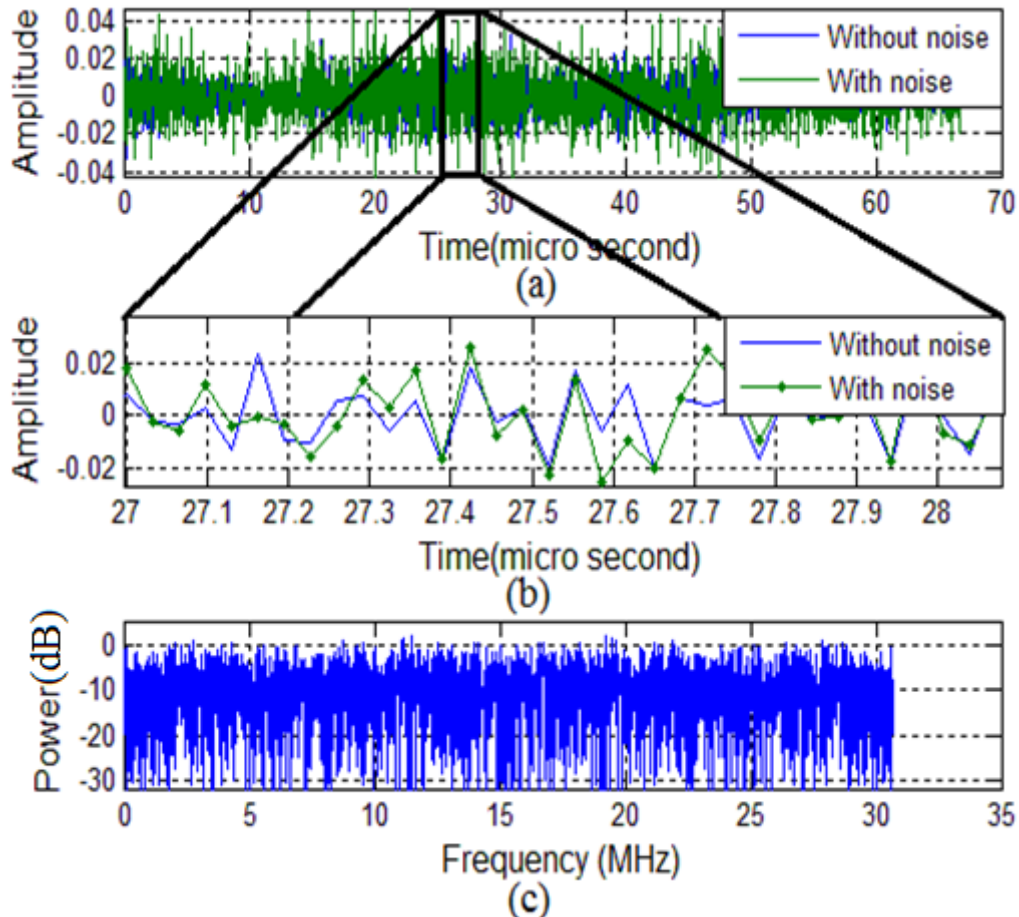


Figure 3.29: (a) AWGN channel effect on the received OFDM symbol with Rayleigh channel effect to achieve 0dB SNR at the receiver (b) zoomed part of signal (c) the spectrum of the noise over 30MHz bandwidth.

Figure 3.29 (a) and (b) shows the effect of noise on the OFDM symbol in time domain. Figure 3.29 (c) shows that the power spectrum of noise is around 0dB, which means the signal power is equal to the noise power.
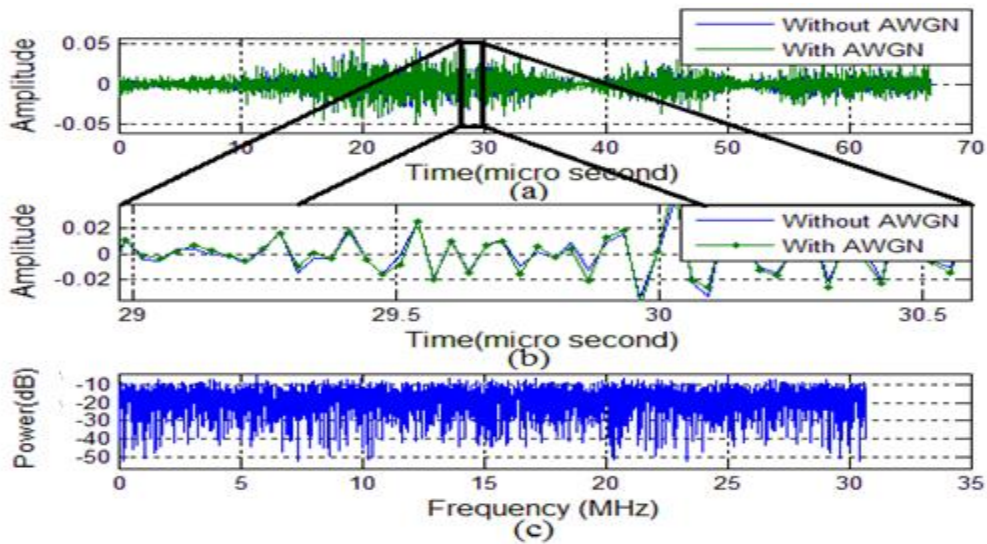
Figure 3.30: (a) AWGN channel effect on the received OFDM symbol with Rayleigh channel effect to achieve 10dB SNR at the receiver (b) zoomed part of signal (c) the spectrum of noise over 30MHz bandwidth.
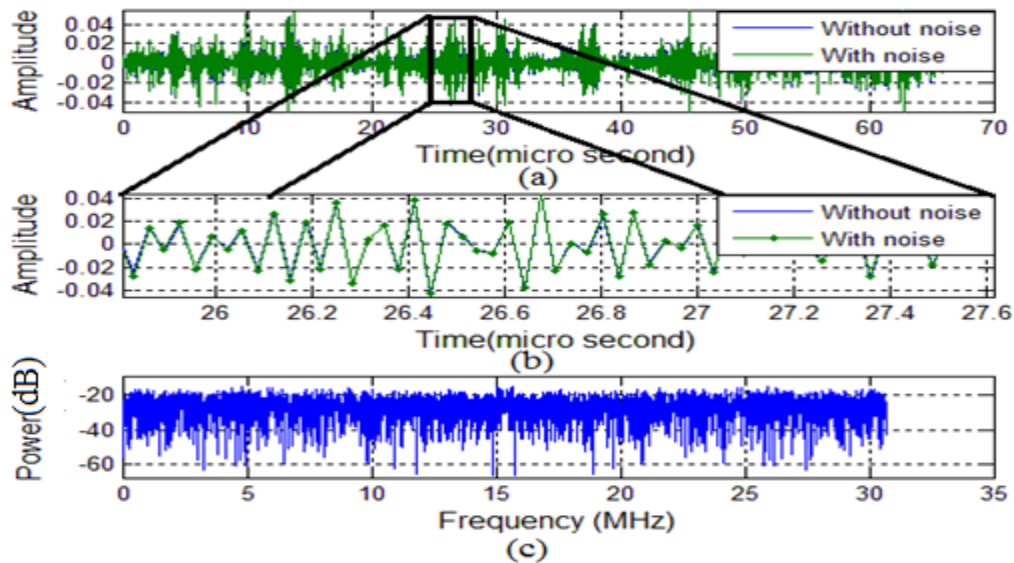


Figure 3.31: (a) AWGN channel effect on the received OFDM symbol Rayleigh channel effect to achieve 20dB SNR at the receiver (b) zoomed part of signal (c) the spectrum of noise over 30MHz bandwidth.

Figure (3.30 c) shows that the noise power is 10 dB below the signal power. Figure (3.31 c) shows that the noise spectrum power is 20 dB below the signal power. Figure (3.29 b), Figure (3.30 b) and Figure

69

(3.31 b) show that the noisy samples are similar to the samples without noise as the value of the SNR increases.

### 3.3.5 OFDM receiver

In the OFDM receiver, a single tab equalizer is used to compensate the Rayleigh fading channel effects. A single tab equalizer in the OFDM system receiver can be used instead of the multi-tab equalizers because the idea of the OFDM system is to convert the transmitted signal into a multiple of narrow band subcarriers. Each narrow band subcarrier is affected by a flat fading channel. As mentioned previously the transmitted OFDM symbol consists of a real part and an imaginary part, each of which is transmitted separately with a sine or cosine wave. Figures 3.32, 3.33 and 3.36 show the recovered real part OFDM symbol after the equalizer with ideal channel estimation and for 0dB, 10dB and 30dB SNRs, respectively. The imaginary part equalization process is similar to the real part equalization process.
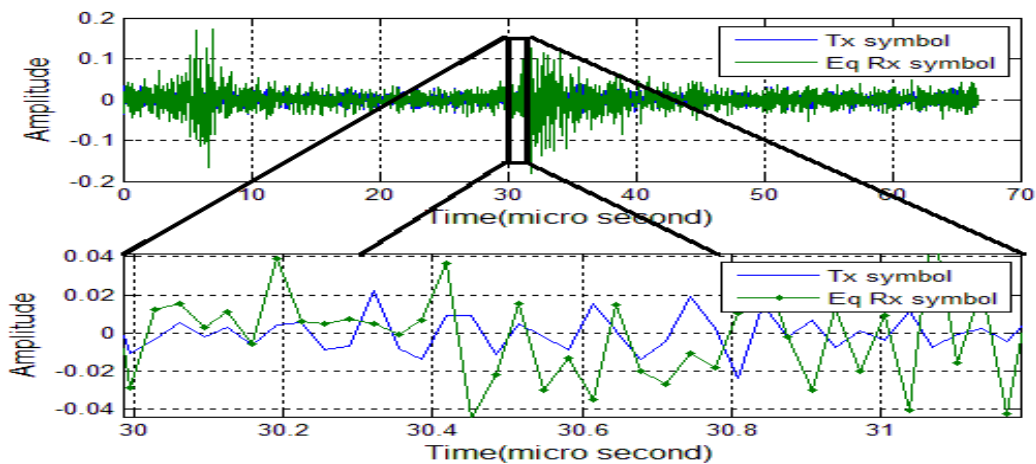


Figure 3.32: Received equalized OFDM symbol for 0dB SNR at the receiver.
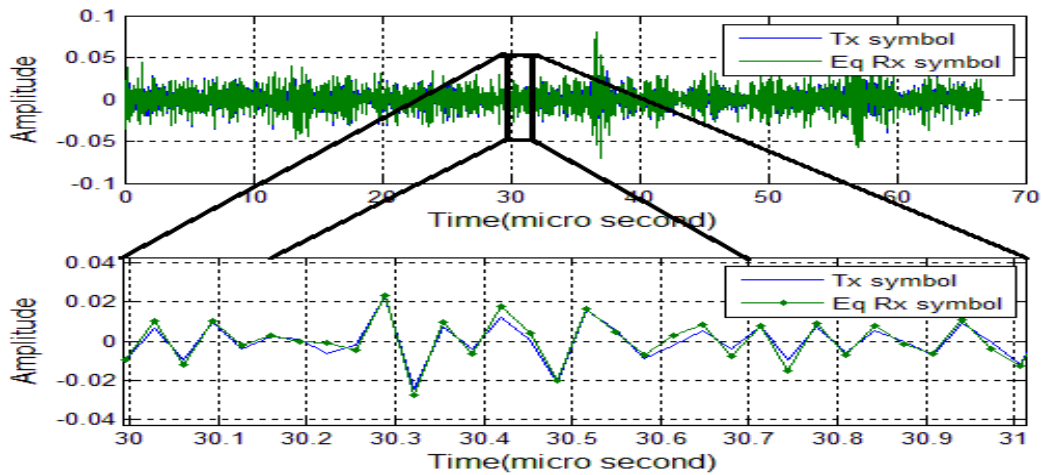
Figure 3.33: Received equalized OFDM symbol for 10dB SNR at the receiver.
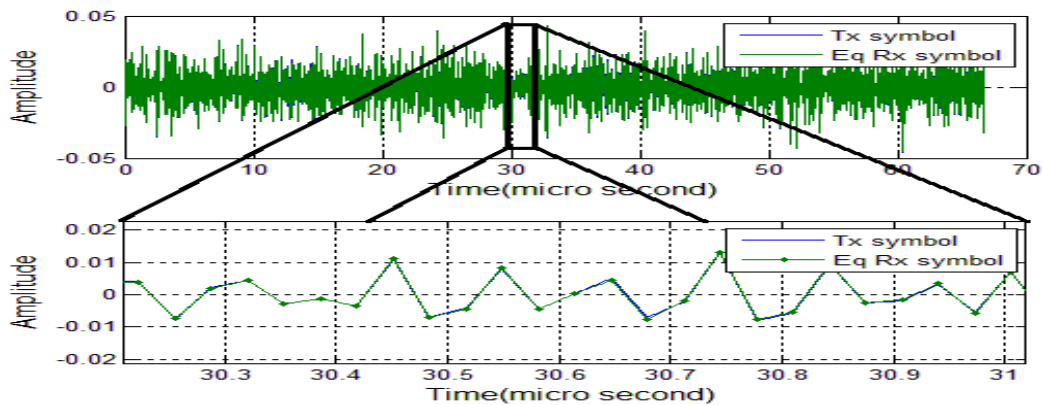


Figure 3.34: Received equalized OFDM symbol for 30dB SNR at the receiver.

After the equalization of the real part and the imaginary part, the two equalized parts are summed to reproduce the transmitted complex OFDM symbol of size 2048 complex samples affected by the noise. The recovered complex OFDM symbol is applied to a Fourier Transformation of size 2048, which is similar to the transmitting side where the modulated symbols are applied to an Inverse Fourier Transform of size 2048. In addition, the first 424 and the last 424 complex samples of the FFT output

71

are ignored since in IFFT these samples are considered as zeros. However the ignored samples may have small complex values rather than zeros because the samples may be corrupted by AWGN. The remaining samples are 1200 containing all the transmitted information but corrupted with noise. The 1200 complex samples are then applied to a proper demodulation scheme (QPSK, 16QAM, 32QAM, 64QAM, 128QAM or 256QAM). The selected demodulation scheme in the receiver side to recover the transmitted data in the binary form is the same modulation scheme used in the transmitter side.

## 3.4 THE MIMO-OFDM WIRELESS COMMUNICATION SYSTEM

### 3.4.1 Introduction

The benefit of using MIMO-OFDM is to increase the data throughput without increasing the used bandwidth. The idea of the MIMO-OFDM is to transmit a multiple of OFDM symbols from multiple antennas simultaneously, with the same frequency band (spatial multiplexing). The MIMO system used in this work is 2*2 MIMO (two transmit antennas and two receive antennas). The OFDM symbol specifications used to assist MIMO are mentioned in Chapter Two (according to the LTE protocol). In this work, the MIMO antennas are used for transmitting two parallel streams of data but for beam forming.

### 3.4.2 The MIMO-OFDM system transmitter

Since two transmitting antennas are used, two ODFM symbols can be transmitted simultaneously. Each OFDM symbol is generated by

using the IFFT method which produces complex OFDM symbols. Therefore, the whole OFDM symbol (i.e. the real and the imaginary parts) should be transmitted to the receiver side. The two transmitted OFDM symbols are shown in Figures 3.35 and 3.36.
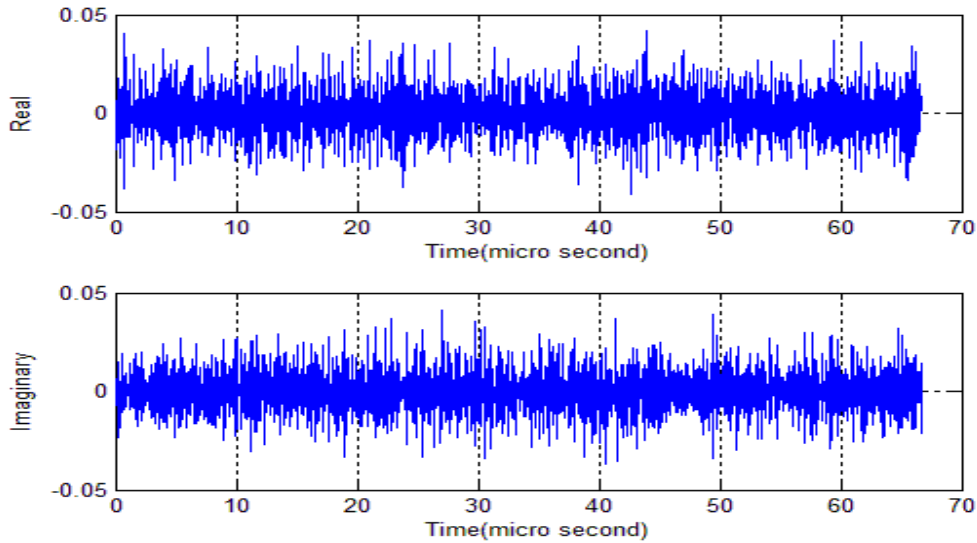


Figure 3.35: Transmitted OFDM symbol from antenna 1 (a) real part (b) imaginary part.
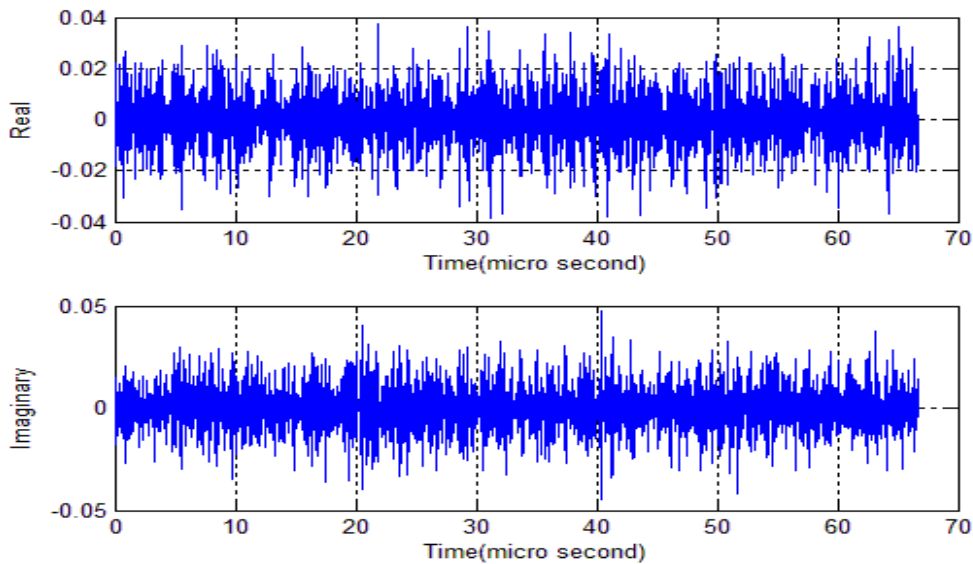


Figure 3.36: Transmitted OFDM symbol from antenna 2 (a) real part (b) imaginary part.

73

The bandwidth of the two transmitted OFDM symbols, for the 2*2 MIMO-OFDM system, are similar to those of the OFDM symbols transmitted see section 3.3.2, (Figures 3.14 and 3.15), therefore they are not plotted here.

### 3.4.3 The MIMO channel effect on the two transmitted OFDM symbols

The m*n-MIMO system requires m*n independent channels to be simulated where m represents the number of transmit antennas and n represents the number of receive antennas. Since a 2*2 MIMO-OFDM system has been used, four Rayleigh flat fading channels should be simulated simultaneously in whichever every receive antenna should be connected to every transmit antenna with one of the four simulated Rayleigh flat fading channels. Figure 3.37 represents the path gains of the four channels between the transmitter and the receiver where the receiver speed is 20 km/h (the effect of the speed on the received signal is explained in the previous chapter). Each path gain is plotted by taking $20log_{10}(|h_{ij}(t)|)$ where $h_{ij}(t)$ is the complex Rayleigh flat fading channel coefficients, the subscript $i$ represents the transmit antenna number and the subscript $j$ represents the received antenna number. Figure 3.38 shows the phase delays of the four Rayleigh fading channels. Each phase delay is plotted by calculating $tan^{-1}(Im(h_{ij}(t))/Re(h_{ij}(t)))$.
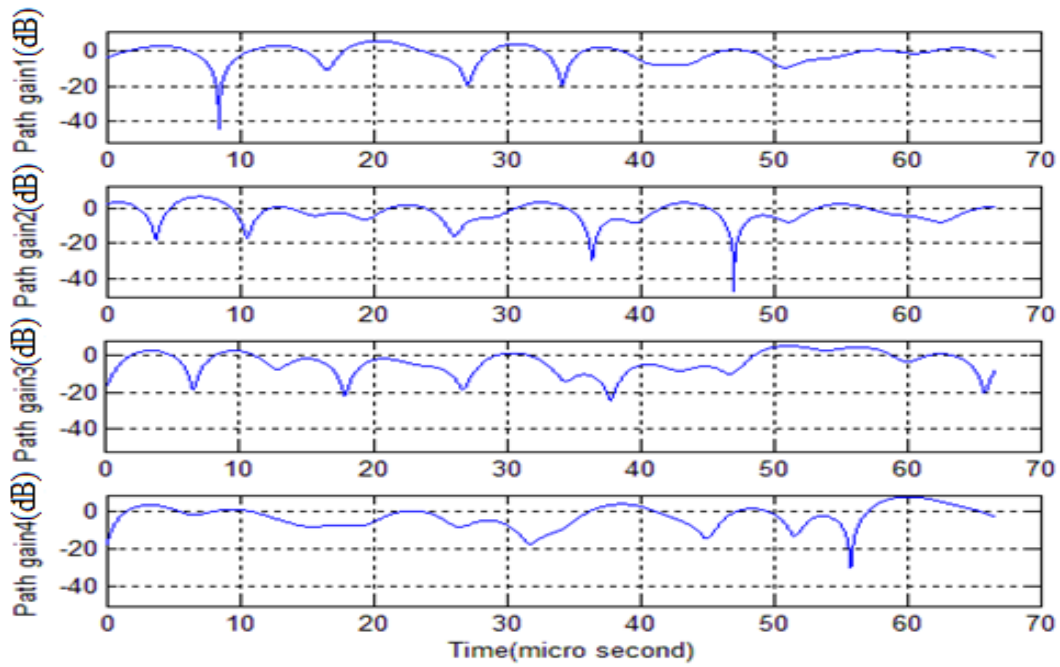
Figure 3.37: Path gains of the Rayleigh fading channel variations for 20 km/h speed of the receiver and for the four paths between the transmitter and receiver.
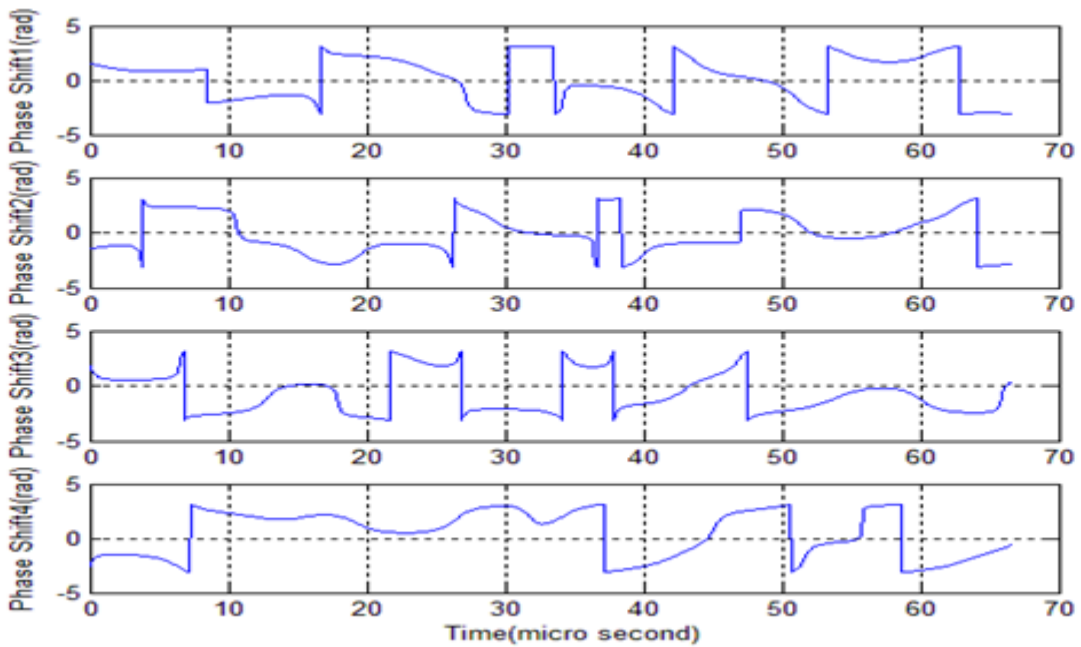


Figure 3.38: Phase shift of the Rayleigh fading channel variations for 20 km/h speed of the receiver for the four paths between the transmitter and receiver.

In the time domain, since the effect of the Rayleigh channel on the OFDM symbol is flat fading, the effect of the channel can be represented as a multiplicative effect (as mentioned in the previous chapter). The transmitted OFDM symbol from transmitter antenna 1 will be received by the receiver antenna 1 and the receiver antenna 2. Therefore, this symbol will be affected by two different Rayleigh flat fading channels (two different paths) in a multiplicative way, then the AWGN will be added to each path separately. Moreover, the transmitted OFDM symbol from transmitter antenna 2 will be received by the receiver antenna 1 and the receiver antenna 2. This symbol will be affected by two different Rayleigh flat fading channels (two different paths) in a multiplicative way, then the AWGN will be added to each path separately. In practice the added noise power for each of the four paths may be different but in the present work equal noise powers are assumed to be added to all channels.

### 3.4.4 The MIMO-OFDM system receiver

At the receiver, two complex signals are received, signal1 is received from antenna 1 and signal 2 is received form antenna 2. Each received signal is obtained by adding the two transmitted OFDM symbols which are distorted by the Rayleigh flat fading and AWGN. The value of the AWGN that is added to the signal is determined by the desired SNR value. By assuming that a high value of SNR is achieved, the signal received by antenna 1 is shown in Figure 3.39, and the signal received by antenna 2 is shown in Figure 3.40.
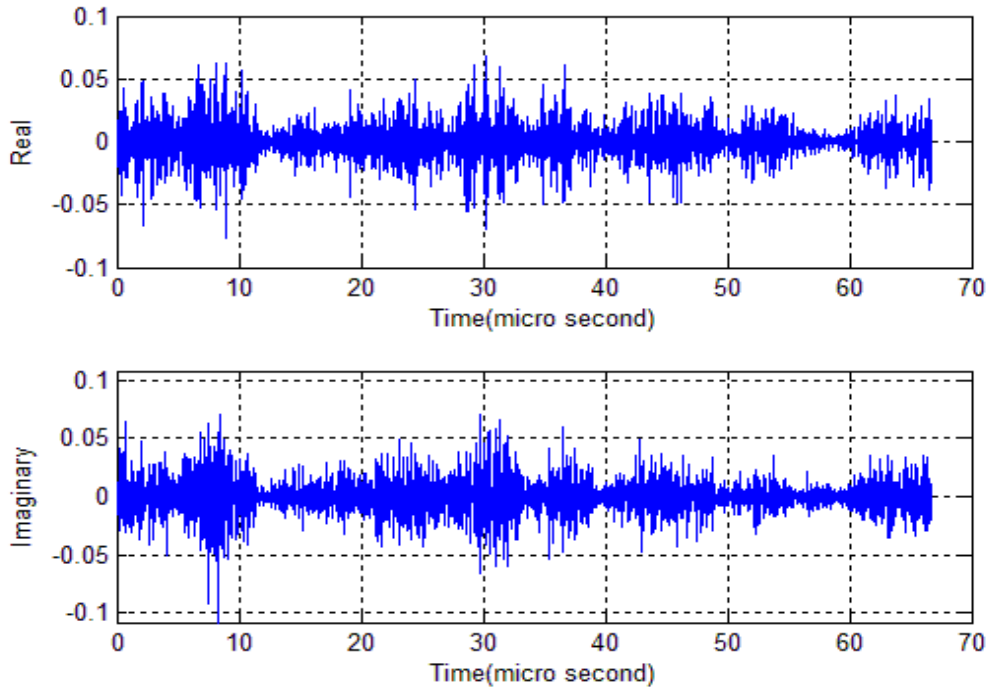
Figure 3.39: Received signal at receiver antenna 1 (a) real part (b) imaginary part.
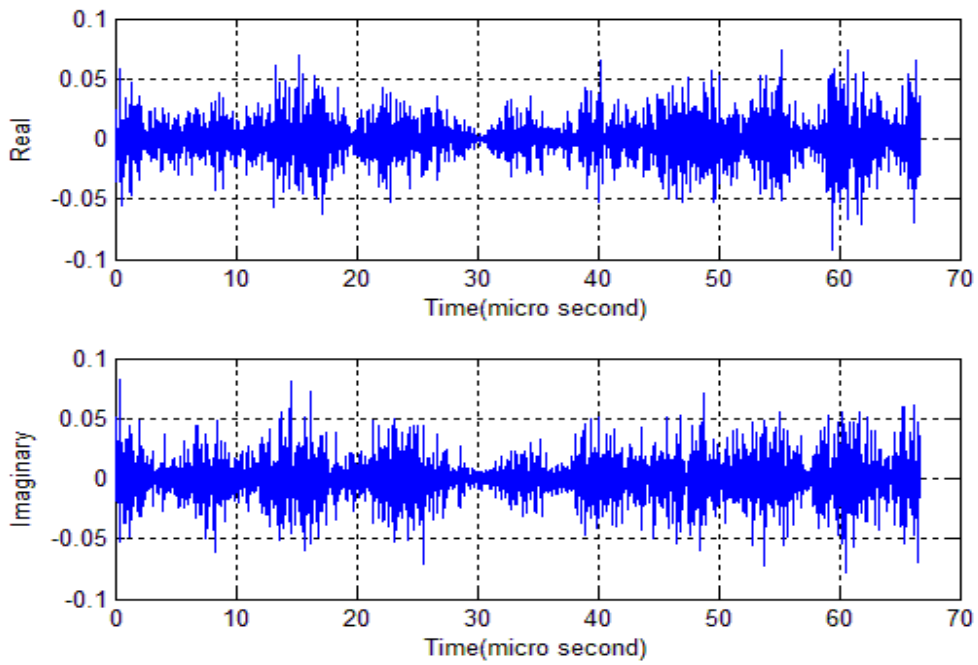


Figure 3.40: Received signal at receiver antenna 2 (a) real part (b) imaginary part.

The power spectra of the two complex received signals are plotted in Figures 3.41 and 3.42.
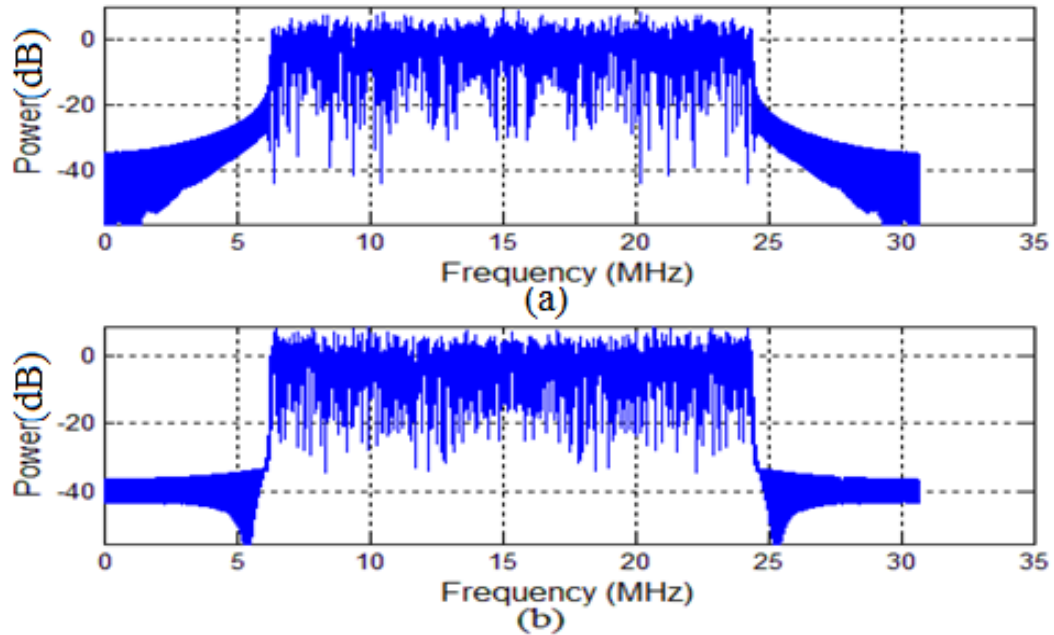


Figure 3.41: Power spectrum of the received signal at receiver antenna 1 (a) real part (b) imaginary part.
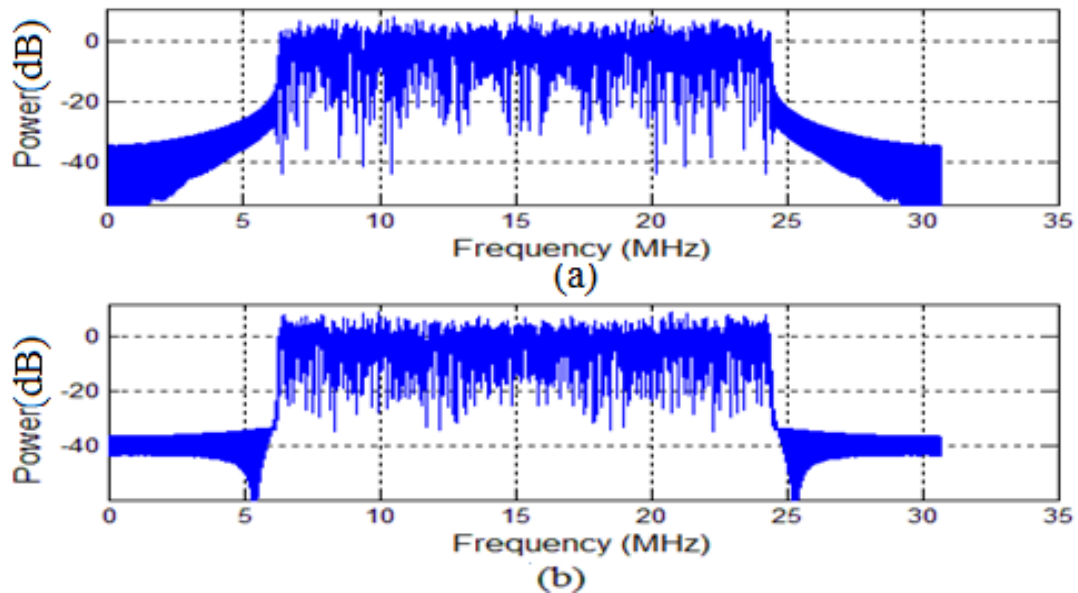


Figure 3.42: Power spectrum of the received signal at receiver antenna 2 (a) real part (b) imaginary part.

Figures 3.41 and 3.42 show that the bandwidth of the power spectrum of the two received signals, by antenna 1 and by antenna 2, is the same as that of the transmitted OFDM symbols without using MIMO (Chapter Two). The two received signals can be expressed by the following equation [33]

$$\bar{r} = \begin{pmatrix} r_1 \\ r_2 \end{pmatrix} = \begin{pmatrix} h_{1,1} & h_{1,2} \\ h_{2,1} & h_{2,2} \end{pmatrix} \cdot \begin{pmatrix} s_1 \\ s_2 \end{pmatrix} + \begin{pmatrix} n_1 \\ n_2 \end{pmatrix} = H \cdot \bar{s} + \bar{n} \quad \dots\dots\dots\dots \ (3-1)$$

Where the vector $\bar{r}$ represents the two received signals, H is the 2*2 channel matrix and the vector $\bar{s}$ represents the two transmitted signals. At the receiver, the two transmitted signals $s_1$ and $s_2$ can be recovered by using a MIMO single tab zero forcing equalizer (ZF) on condition that the channel matrix H is invertible. In this project, assuming that 10% of the transmitted data are transmitted as pilots, only 10% of the Raleigh channel coefficients are known at the receiver and the remaining channel coefficients are interpolated. Equation (3-2) shows the mathematical representation of the MIMO single tab zero forcing equalizer [33].

$$\begin{pmatrix} \hat{s}_1 \\ \hat{s}_2 \end{pmatrix} = W \cdot \bar{r} = \begin{pmatrix} s_1 \\ s_2 \end{pmatrix} + H^{-1} \cdot \bar{n} \qquad \dots\dots\dots\dots\dots\dots \ (3-2)$$

where $W = H^{-1}$ .

Figures 3.43, 3.44 and 3.45 show the recovered real parts, of the transmitted OFDM symbol from antenna 1 after the equalizer for 0dB, 20dB and 40dB SNRs, respectively. The imaginary part equalization process is similar to the real part equalization process.
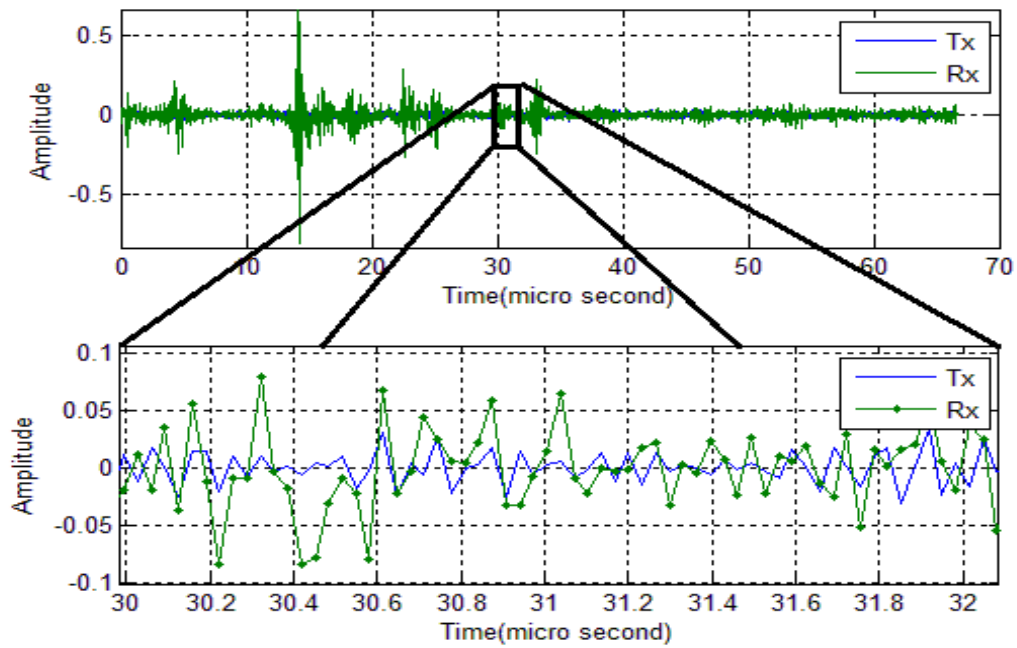
Figure 3.43: Amplitude of received equalized OFDM symbol which is transmitted from antenna 1 for 0dB SNR at the receiver.
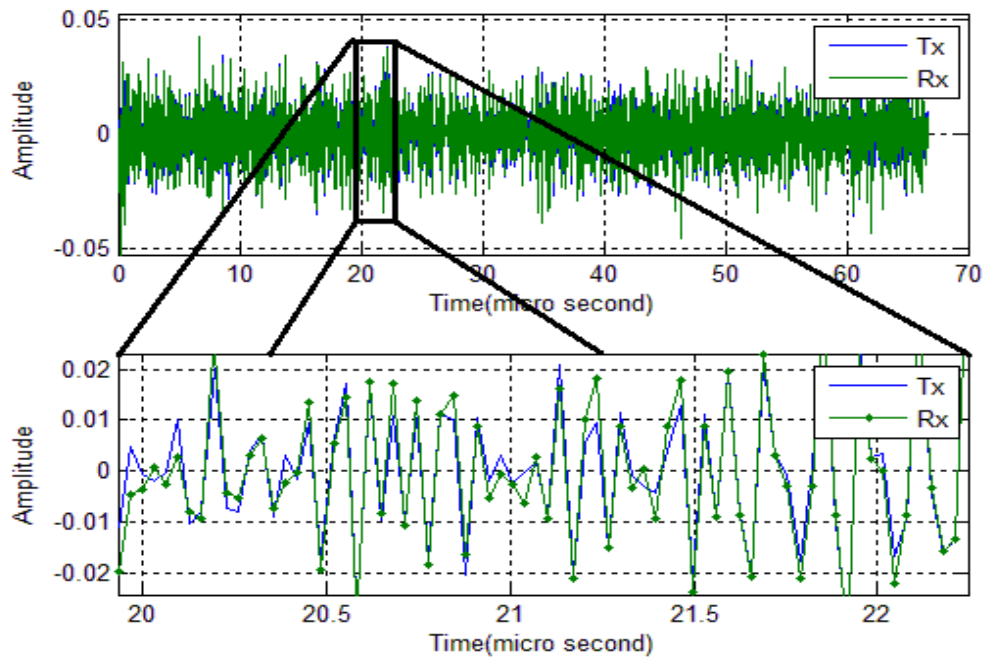


Figure 3.44: Amplitude of received equalized OFDM symbol which is transmitted from antenna 1 for 20dB SNR at the receiver.
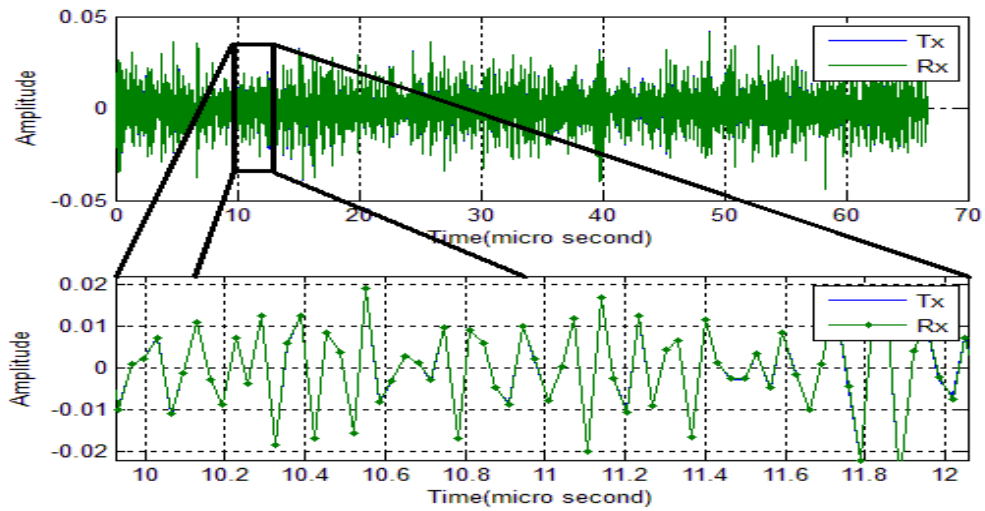
Figure 3.45: Amplitude of received equalized OFDM symbol which is transmitted from antenna 1 for 40dB SNR at the receiver.

Figures 3.46, 3.47 and 3.48 show the recovered real parts of the transmitted OFDM symbol from antenna 2 after the equalizer for 0dB, 20dB and 40dB SNRs, respectively. The imaginary part equalization process is similar to the real part equalization process.
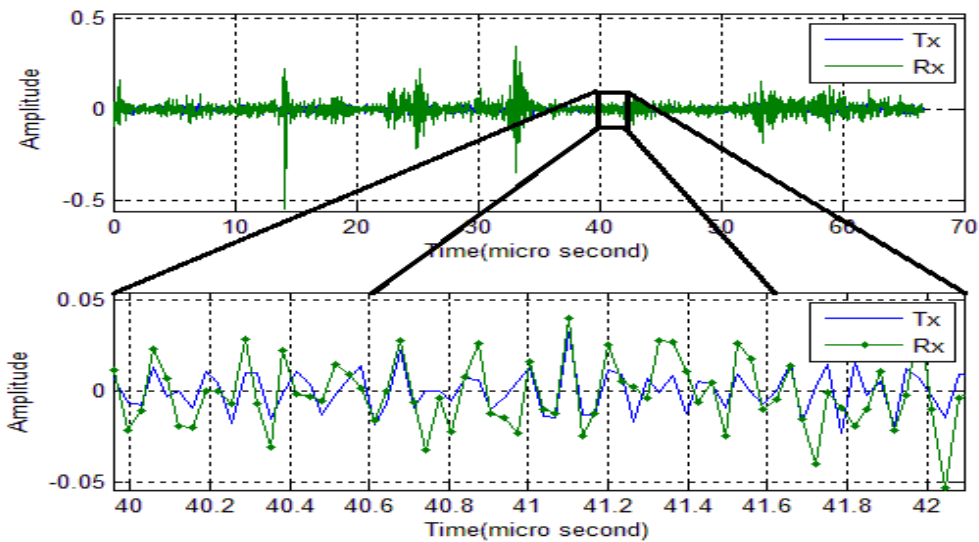


Figure 3.46: Amplitude of received equalized OFDM symbol which is transmitted from antenna 2 for 0dB SNR at the receiver.

81
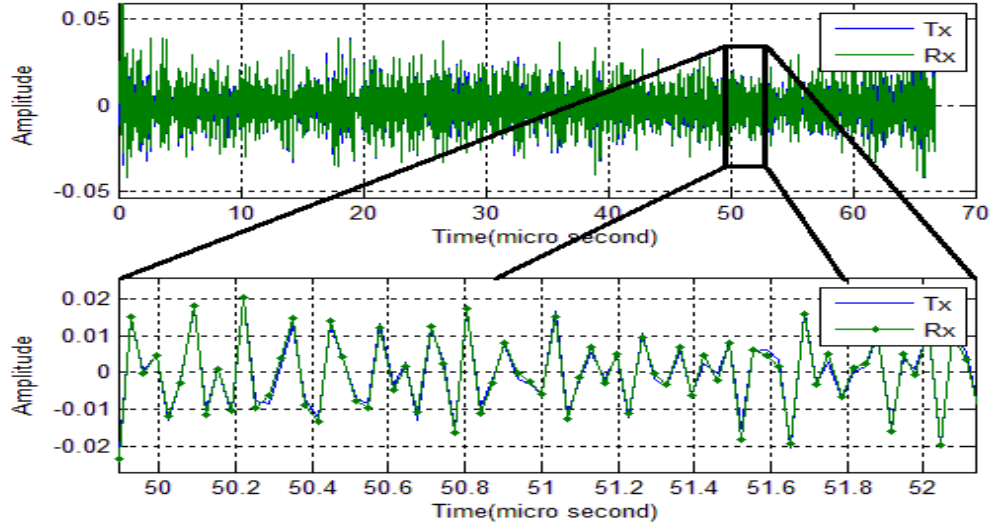
Figure 3.47: Amplitude of received equalized OFDM symbol which is transmitted from antenna 2 for 20dB SNR at the receiver.
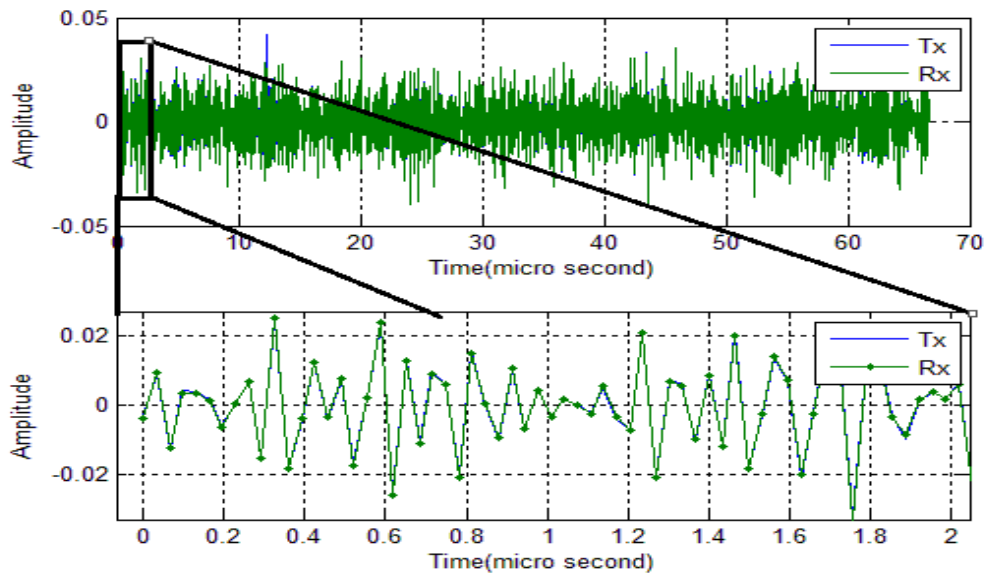


Figure 3.48: Amplitude of received equalized OFDM symbol which is transmitted from antenna 2 for 40dB SNR at the receiver.

Figures 3.43-3.48 show that the detected symbols for high SNR (good channel conditions) are more accurate than the detected symbols in low SNR (bad channel conditions).

# Chapter Four

# Results and Discussions

## 4.1 Introduction

The results in this chapter are extracted from the simulated system described in Chapter Three. The results mainly include the behavior of the system characterized by the BER according to the noise of the channel (AWGN) and the Rayleigh fading, and for different speeds of the receiver.

## 4.2 The Single Carrier Wireless Communication System

The relation between BER and SNR performance for BPSK modulation/demodulation types at different receiver equipment speed and for ideal channel estimation is shown in Figure 4.1.
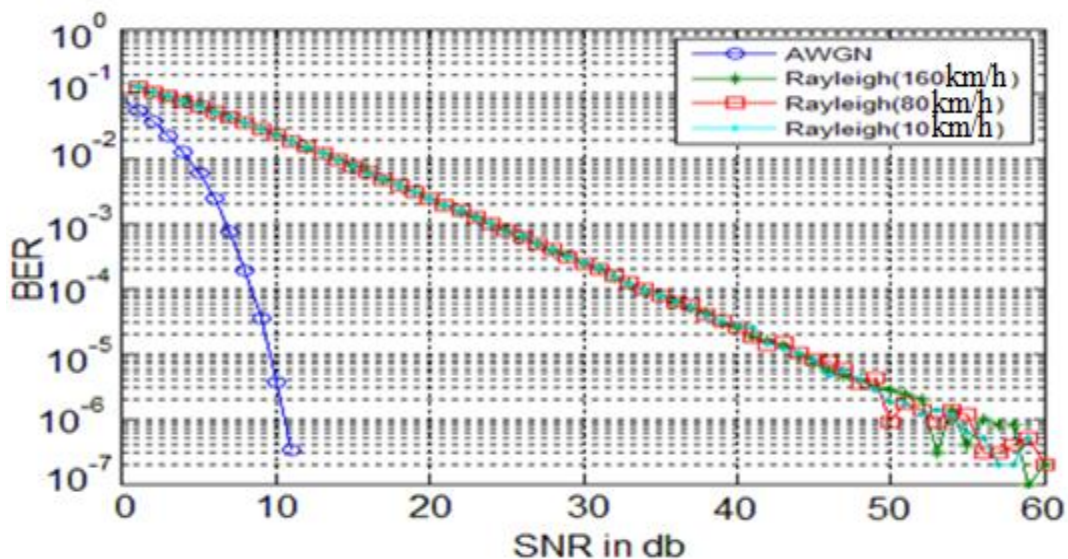


Figure 4.1 BER curves for BPSK with ideal channel estimation through Rayleigh fading channel and corrupted with AWGN.

Figure 4.1 shows that the BER performance of the moving receiver for different speeds is the same as the performance of the static receiver that is affected by the Rayleigh multipath channel with AWGN but without any effect of the Doppler frequency shift. The effect of the Doppler shift frequency on the received signal has been completely removed since the prefect Rayleigh fading channel parameters are considered in calculating the received signal. The received signal is calculated by multiplying it by the inverse of the perfect Rayleigh fading channel parameters because a flat fading channel is assumed.

The relationship between the BER and the SNR performance for (BPSK, QPSK, 16QAM, 32QAM, 64QAM, and 128QAM) modulation/demodulation types and at different receiver equipment speeds has been found by assuming 10% of the transmitted data as pilots to estimate the actual Rayleigh fading channel coefficients; this means that only 10% of the channel points are estimated and interpolated to estimate the whole channel curve (see Figures 3.3 and 3.4). The effect of the Rayleigh fading channel has been nearly removed by considering the estimated Rayleigh fading channel coefficients in the single tab equalizer. Then, the two outputs of the equalizer have been applied to a proper demodulation scheme to recover the transmitting bits with a BER as shown in Figures 4.2, 4.3, 4.4, 4.5, 4.6 and 4.7. The range of SNR is form 0dB to 60dB. The step size of SNR is set to 1dB.
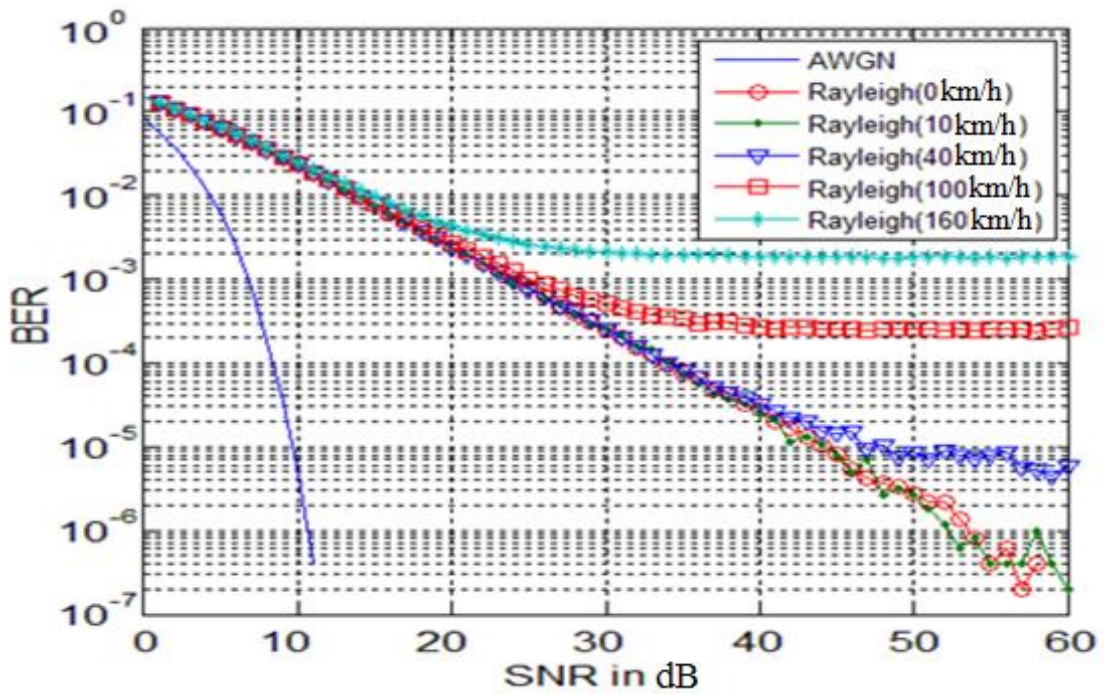
Figure 4.2: BER curves for BPSK for different speeds, 10% of transmitted data are used for channel estimation.
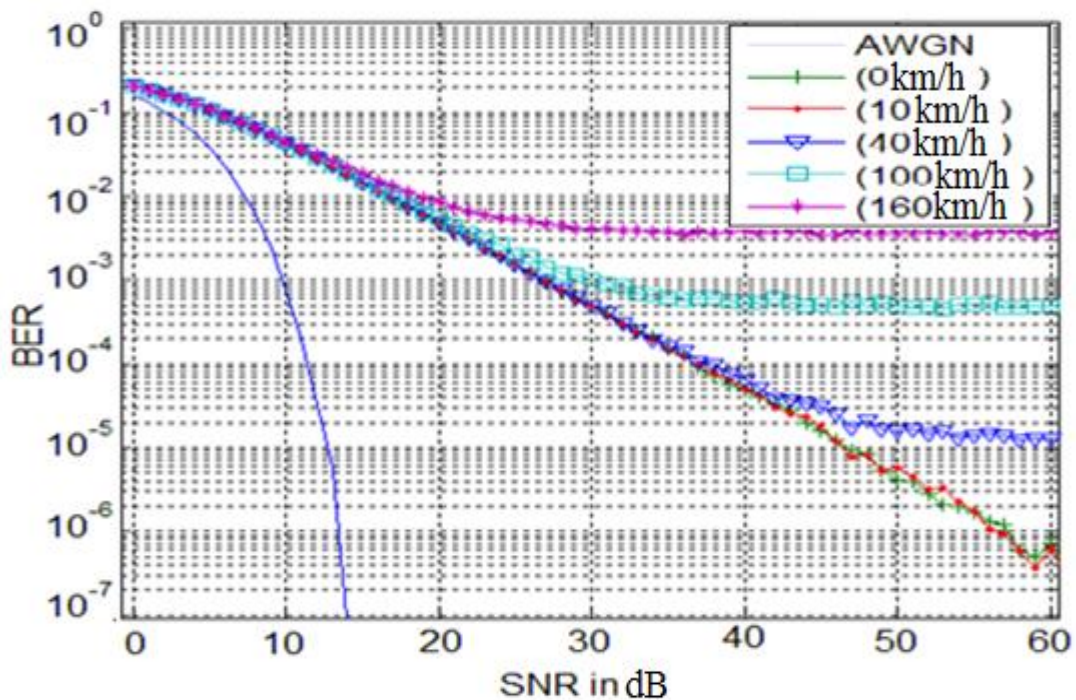


Figure 4.3: BER curves for QPSK for different speeds, 10% of transmitted data are used for channel estimation.
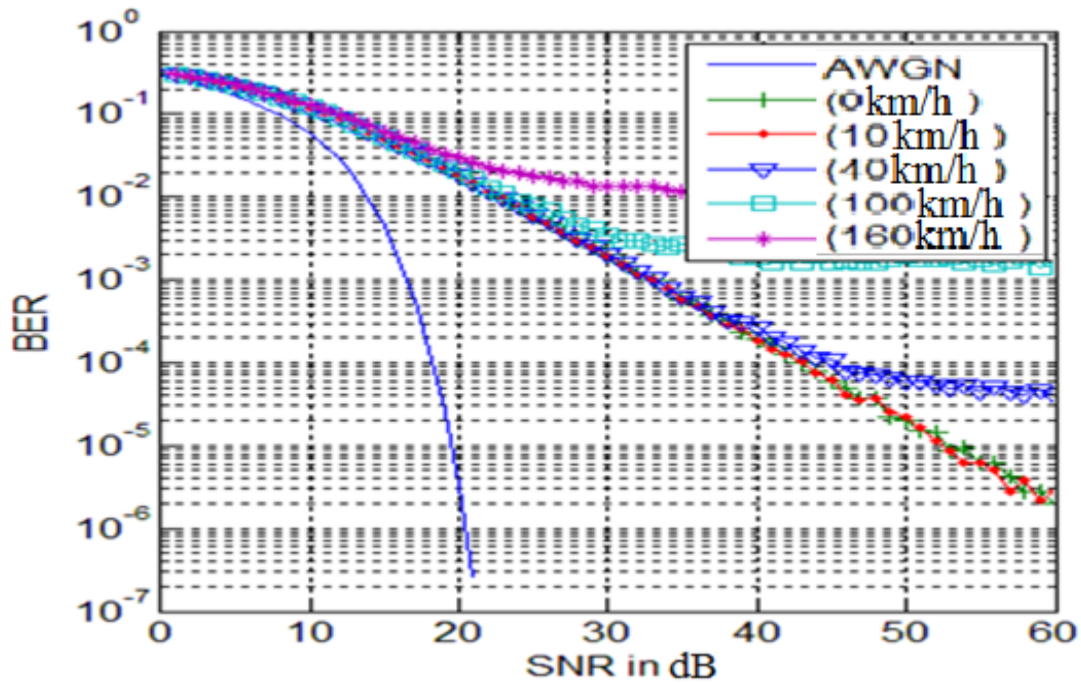
Figure 4.4: BER curves for 16QAM for different speeds, 10% of transmitted data are used for channel estimation.
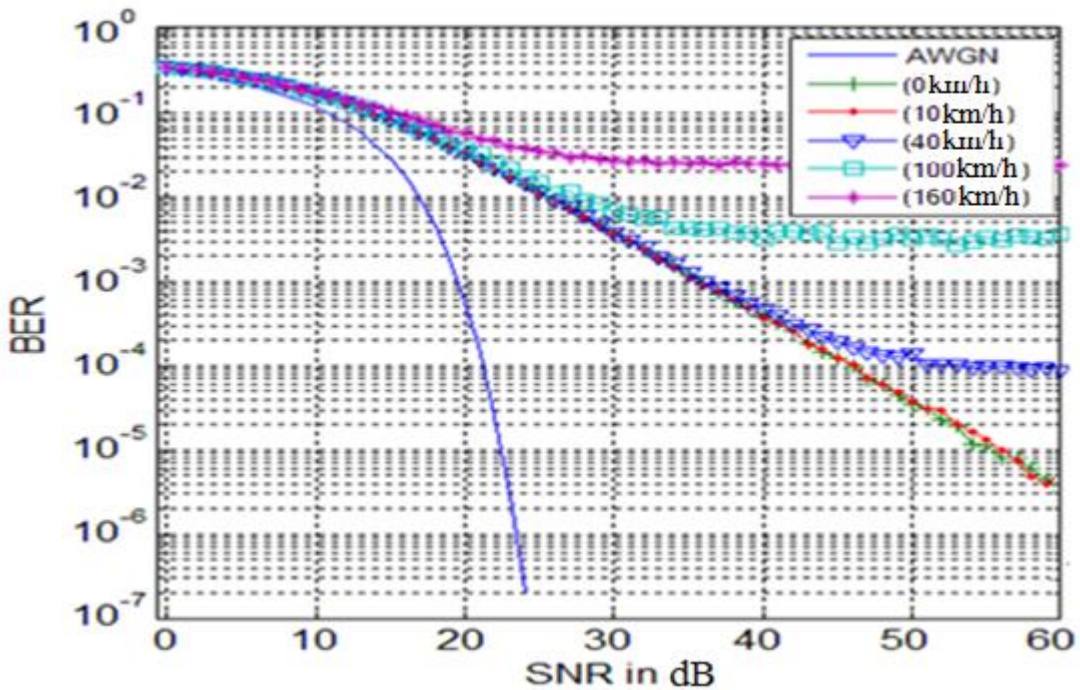


Figure 4.5: BER curves for 32QAM for different speeds, 10% of transmitted data are used for channel estimation.

86
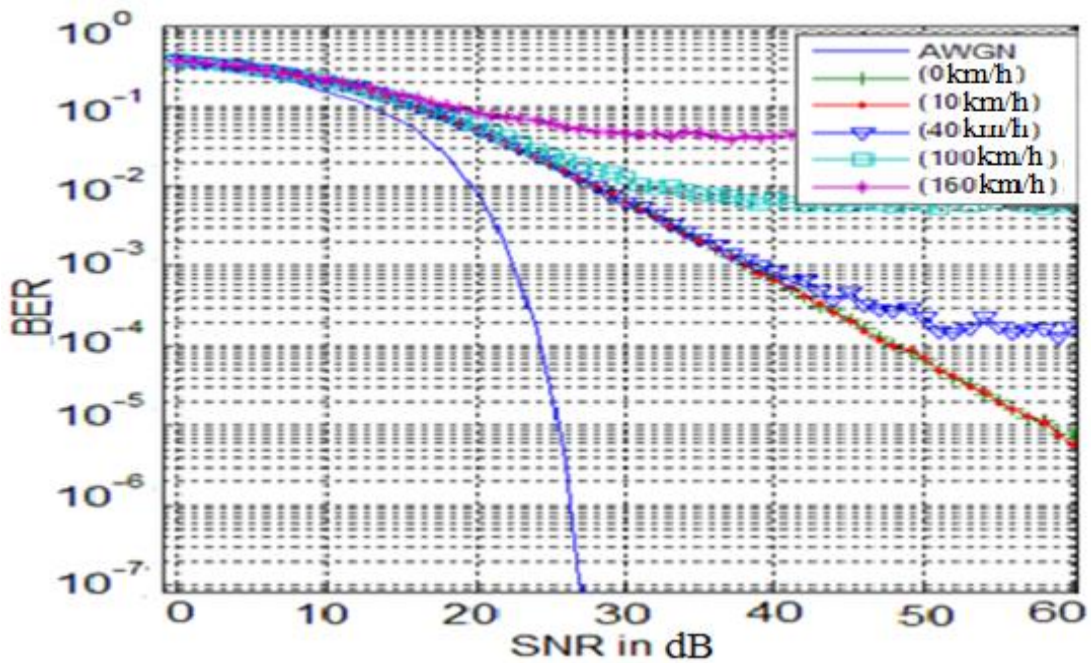
Figure 4.6: BER curves for 64QAM for different speeds, 10% of transmitted data are used for channel estimation.
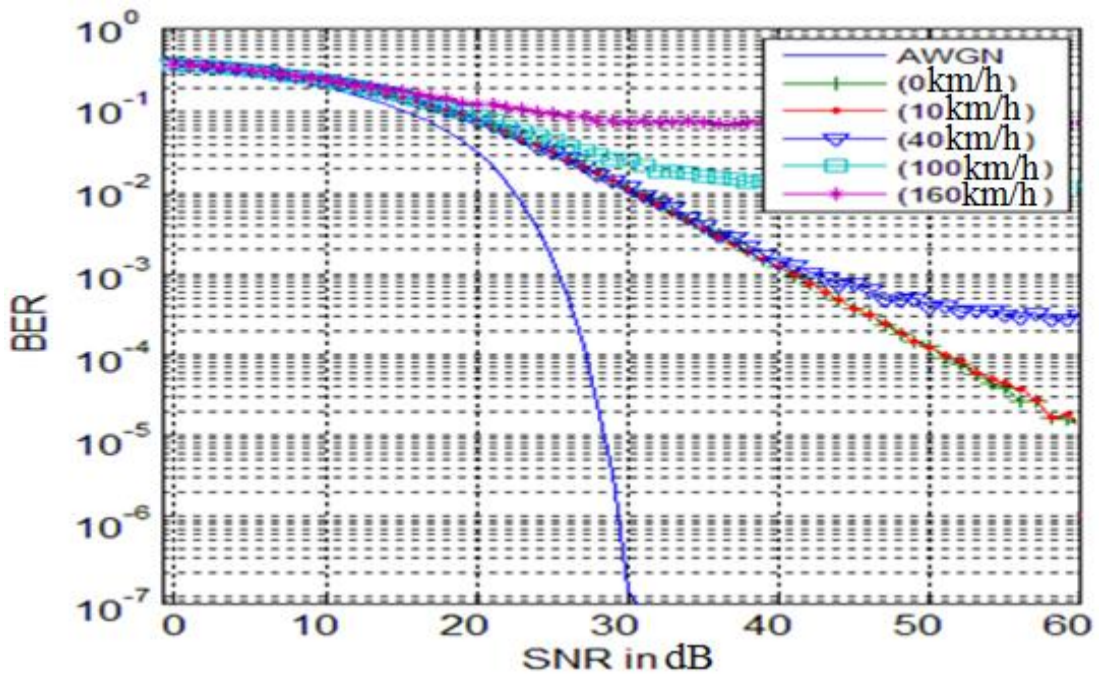


Figure 4.7: BER curves for 128QAM for different speeds, 10% of transmitted data are used for channel estimation.

Figure 4.2-4.7 show that the worst BER performances of the used modulations have occurred at the maximum moving receiver speed which is 160Km/s. The BER performance improves as the speed of the receiver equipment decreases.

The choice of best modulation scheme for the instantaneous channel conditions to achieve the desired BER depends on the values of the SNR and the Doppler frequency shifts (speed of the receiver) which are known for the receiver. The following tables show the best modulation scheme used for the instantaneous SNR and the receiver speed. For example, if it is required to decide the type of modulation for a BER of 10^-3 or less, the shaded values in the following tables specify the type of modulation scheme according to the speed of the receiver.

Table 4.1: Single carrier best BER for 0dB SNR

| Mod speed | BPSK | QPSK | 16QAM | 32QAM | 64QAM | 128QAM |
|---|---|---|---|---|---|---|
| 0km/h | 10^-0.834 | 10^-0.676 | 10^-0.494 | 10^-0.449 | 10^-0.421 | 10^-0.399 |
| 10km/h | 10^-0.837 | 10^-0.677 | 10^-0.494 | 10^-0.45 | 10^-0.421 | 10^-0.4 |
| 40km/h | 10^-0.835 | 10^-0.676 | 10^-0.494 | 10^-0.448 | 10^-0.421 | 10^-0.399 |
| 100km/h | 10^-0.835 | 10^-0.674 | 10^-0.493 | 10^-0.448 | 10^-0.42 | 10^-0.4 |
| 160km/h | 10^-0.83 | 10^-0.671 | 10^-0.489 | 10^-0.445 | 10^-0.423 | 10^-0.396 |

Table 4.2: Single carrier best BER for 10dB SNR

| Mod speed | BPSK | QPSK | 16QAM | 32QAM | 64QAM | 128QAM |
|---|---|---|---|---|---|---|
| 0km/h | 10^−1.632 | 10^−1.367 | 10^-0.926 | 10^-0.772 | 10^-0.69 | 10^-0.608 |
| 10km/h | 10^−1.642 | 10^−1.369 | 10^-0.927 | 10^-0.773 | 10^-0.691 | 10^-0.61 |
| 40km/h | 10^−1.635 | 10^−1.364 | 10^-0.924 | 10^-0.772 | 10^-0.688 | 10^-0.61 |
| 100km/h | 10^−1.628 | 10^−1.357 | 10^-0.919 | 10^-0.769 | 10^-0.679 | 10^-0.602 |
| 160km/h | 10^−1.604 | 10^−1.336 | 10^-0.896 | 10^-0.744 | 10^-0.666 | 10^-0.585 |

Table 4.3: Single carrier best BER for 20dB SNR

| Mod speed | BPSK | QPSK | 16QAM | 32QAM | 64QAM | 128QAM |
|---|---|---|---|---|---|---|
| 0km/h | 10^-2.602 | 10^-2.306 | 10^-1.733 | 10^-1.477 | 10^-1.287 | 10^-1.096 |
| 10km/h | 10^-2.644 | 10^-2.328 | 10^-1.753 | 10^-1.477 | 10^-1.293 | 10^-1.101 |
| 40km/h | 10^-2.62 | 10^-2.32 | 10^-1.731 | 10^-1.467 | 10^-1.277 | 10^-1.093 |
| 100km/h | 10^-2.567 | 10^-2.264 | 10^-1.687 | 10^-1.44 | 10^-1.226 | 10^-1.049 |
| 160km/h | 10^-2.366 | 10^-2.061 | 10^-1.533 | 10^-1.242 | 10^-1.08 | 10^-0.898 |

Table 4.4: Single carrier best BER for 30dB SNR

| Mod speed | BPSK | QPSK | 16QAM | 32QAM | 64QAM | 128QAM |
|---|---|---|---|---|---|---|
| 0km/h | 10^-3.617 | 10^-3.312 | 10^-2.701 | 10^-2.438 | 10^-2.196 | 10^-1.936 |
| 10km/h | 10^-3.601 | 10^-3.304 | 10^-2.721 | 10^-2.432 | 10^-2.203 | 10^-1.946 |
| 40km/h | 10^-3.584 | 10^-3.304 | 10^-2.693 | 10^-2.427 | 10^-2.201 | 10^-1.914 |
| 100km/h | 10^-3.287 | 10^-3.000 | 10^-2.458 | 10^-2.16 | 10^-1.897 | 10^-1.582 |
| 160km/h | 10^-2.678 | 10^-2.387 | 10^-1.865 | 10^-1.572 | 10^-1.331 | 10^-1.112 |

Table 4.5: Single carrier best BER for 40dB SNR

| Mod speed | BPSK | QPSK | 16QAM | 32QAM | 64QAM | 128QAM |
|---|---|---|---|---|---|---|
| 0km/h | 10^-4.546 | 10^-4.323 | 10^-3.715 | 10^-3.427 | 10^-3.181 | 10^-2.916 |
| 10km/h | 10^-4.623 | 10^-4.296 | 10^-3.741 | 10^-3.444 | 10^-3.178 | 10^-2.904 |
| 40km/h | 10^-4.491 | 10^-4.196 | 10^-3.572 | 10^-3.326 | 10^-3.068 | 10^-2.861 |
| 100km/h | 10^-3.577 | 10^-3.262 | 10^-2.724 | 10^-2.487 | 10^-2.15 | 10^-1.854 |
| 160km/h | 10^-2.73 | 10^-2.411 | 10^-1.94 | 10^-1.591 | 10^-1.368 | 10^-1.159 |

Table 4.6: Single carrier best BER for 50dB SNR

| Mod speed | BPSK | QPSK | 16QAM | 32QAM | 64QAM | 128QAM |
|---|---|---|---|---|---|---|
| 0km/h | 10^-5.552 | 10^-5.382 | 10^-4.694 | 10^-4.464 | 10^-4.171 | 10^-3.899 |
| 10km/h | 10^-5.584 | 10^-5.248 | 10^-4.659 | 10^-4.424 | 10^-4.153 | 10^-3.918 |
| 40km/h | 10^-5.075 | 10^-4.8 | 10^-4.226 | 10^-3.851 | 10^-3.641 | 10^-3.416 |
| 100km/h | 10^-3.586 | 10^-3.305 | 10^-2.711 | 10^-2.492 | 10^-2.217 | 10^-1.914 |
| 160km/h | 10^-2.739 | 10^-2.441 | 10^-1.94 | 10^-1.603 | 10^-1.391 | 10^-1.126 |

Table 4.7: Single carrier best BER for 60dB SNR

| Mod speed | BPSK | QPSK | 16QAM | 32QAM | 64QAM | 128QAM |
|---|---|---|---|---|---|---|
| 0km/h | ----------- | 10^-6.146 | 10^-5.698 | 10^-5.501 | 10^-5.103 | 10^-4.832 |
| 10km/h | 10^-6.698 | 10^-6.191 | 10^-5.55 | 10^-5.261 | 10^-5.223 | 10^-4.844 |
| 40km/h | 10^-5.236 | 10^-4.895 | 10^-4.389 | 10^-4.033 | 10^-3.756 | 10^-3.51 |
| 100km/h | 10^-3.576 | 10^-3.312 | 10^-2.746 | 10^-2.443 | 10^-2.196 | 10^-1.926 |
| 160km/h | 10^-2.738 | 10^-2.419 | 10^-1.924 | 10^-1.619 | 10^-1.364 | 10^-1.136 |

As noted from tables 4.1, 4.2 and 4.3, BER of $10^{-3}$ cannot be fulfilled for SNR of values 0dB, 10dB and 20dB respectively (yellow shaded values). Therefore there is no chance to select any type of modulation scheme. However, selecting the BPSK is better than disconnecting the communication link.

The present work identifies the best modulation scheme used with the instantaneous channel conditions (the SNR and the Doppler effects). Although at any SNR, the BPSK modulation is the best and the 128QAM is the worst in terms of BER, high order modulation schemes such as 32QAM 64QAM and 128QAM can be used for good channel conditions and low speed of the receiver. If the desired BER in physical layer at the receiver is $10^{-3}$, it has been found that for 160 km/h speed of the receiver, the BPSK modulation should be used. For 100 km/h, the BPSK and QPSK can be used on condition that the SNR is greater than 30dB. For 40 km/h, the 16QAM and 32 QAM can be used on condition that the SNR is greater than 40dB. For 10 km/h, the 64 QAM can be used on condition that the SNR is greater than 40 dB, and for the stationary receiver, the 128 QAM can be used on condition that SNR is around or greater than 50dB.

## 4.3 The OFDM Wireless Communication System

The relationship between the BER and the SNR performance for QPSK, 16QAM, 32QAM, 64QAM, 128QAM and 256QAM modulation/demodulation and at different receiver equipment speed has been found by assuming 10% of the transmitted data as pilots to estimate

the actual Rayleigh fading channel coefficients. The effect of the Rayleigh fading channel has been nearly removed by considering the estimated Rayleigh fading channel coefficients in the single tab equalizer. Then, the output of the equalizer has been applied to proper demodulation schemes to recover  the transmitting bits with a BER as shown in Figures 4.8, 4.9, 4.10, 4.11, 4.12 and 4.13. The range of SNR is from 0dB to 60dB. The step size of SNR is set to be 5dB in order to reduce the time of the simulation which almost needs many days of computation time on a high-speed computer (HP Workstation Z220, 3.4 GHz, Xeon E3 processors and 16 GB RAM) to get a reasonable view about the relation between the SNR and the BER. Another way to reduce the simulation time is by making the number of the transmitted bits vary according to the values of SNR, for example the number of the transmitted bits for 10dB SNR can be much smaller than the transmitted bits for 60dB SNR in order to get a distinct point for BER associated with that SNR. To measure BER accurately, each set of samples for each value of SNR is retransmitted 100-1000 times and then the average of BER for all those trials is calculated.
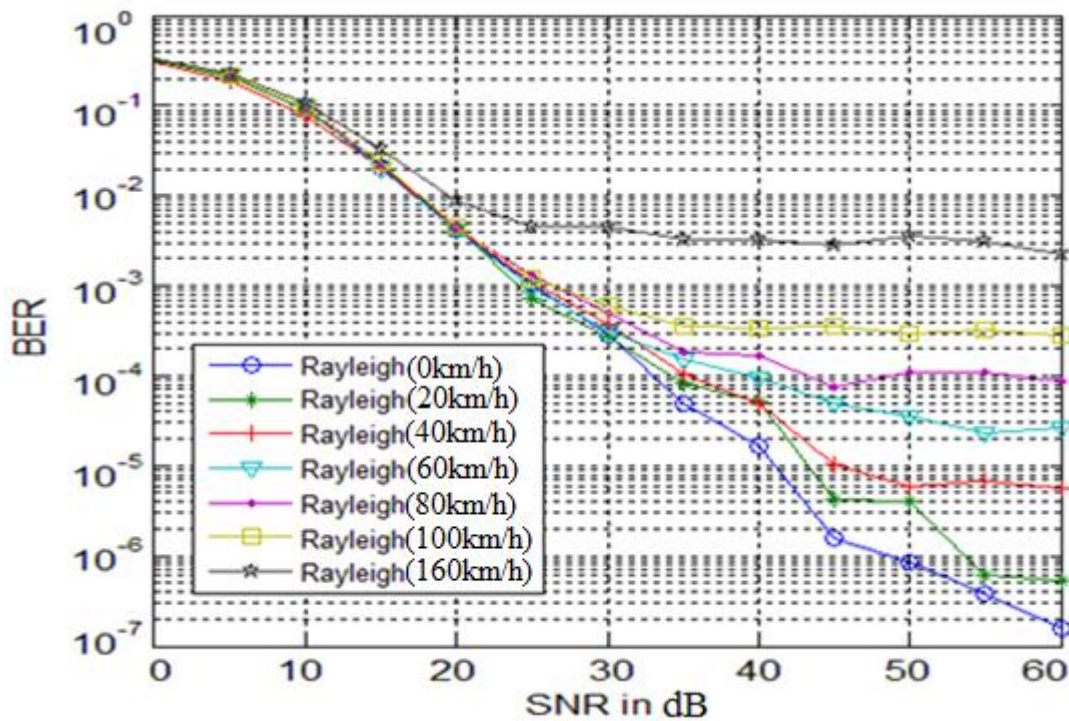
Figure 4.8: BER curves for QPSK for different speeds, 10% of transmitted data are used for channel estimation.
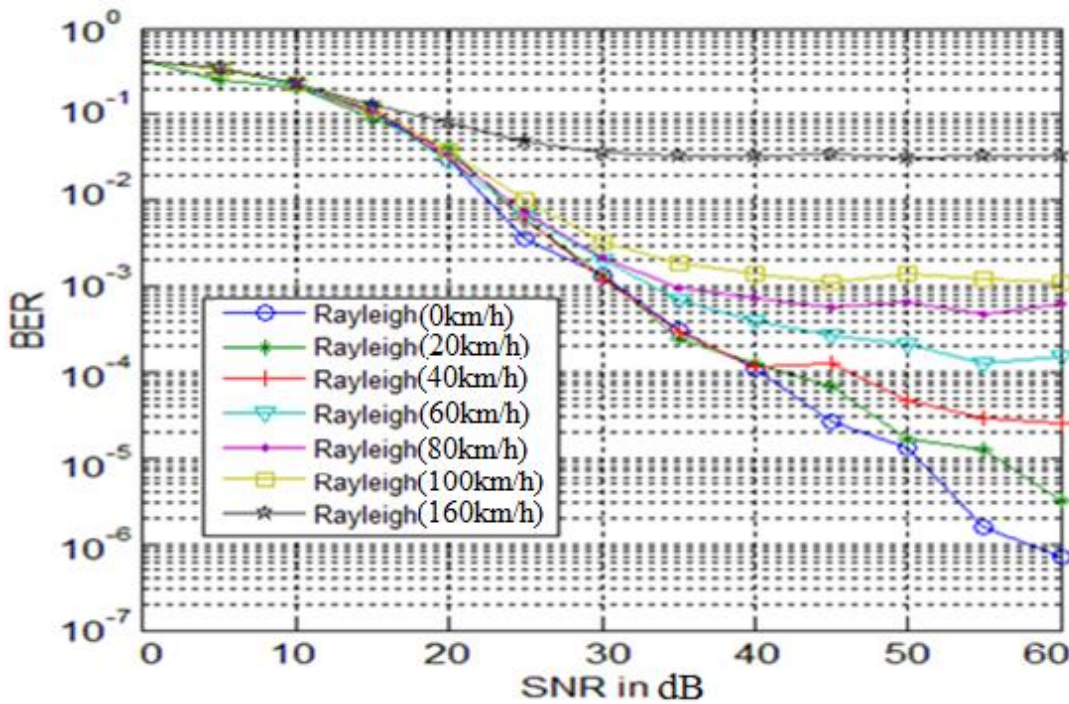


Figure 4.9: BER curves for 16QAM for different speeds, 10% of transmitted data are used for channel estimation.
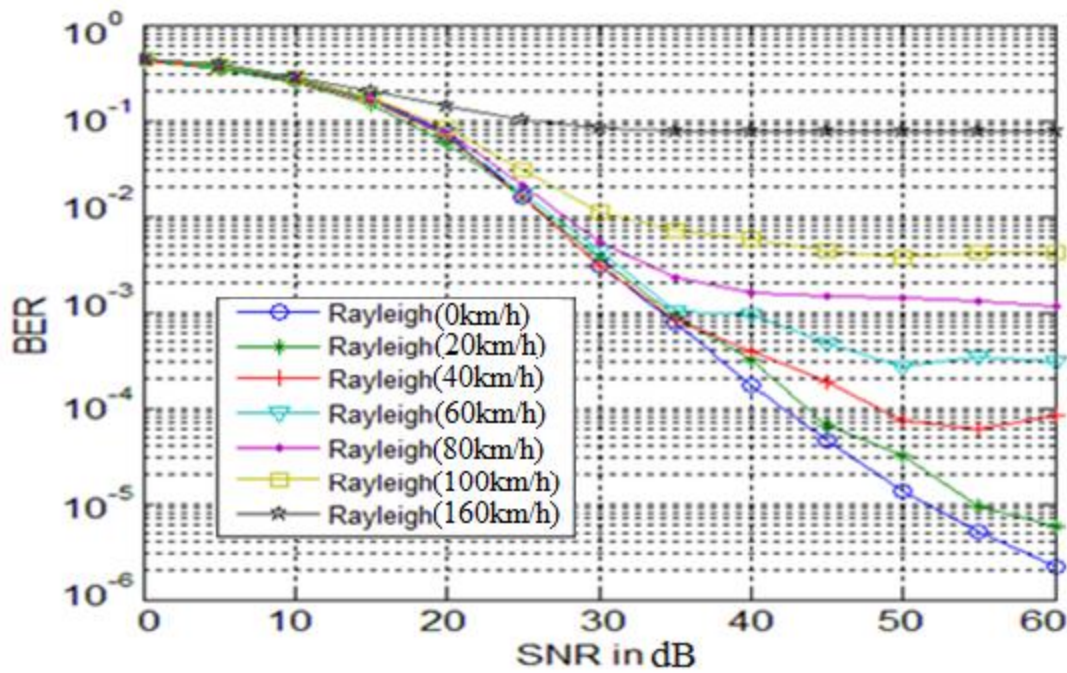
Figure 4.10: BER curves for 32QAM for different speeds, 10% of transmitted data are used for channel estimation.
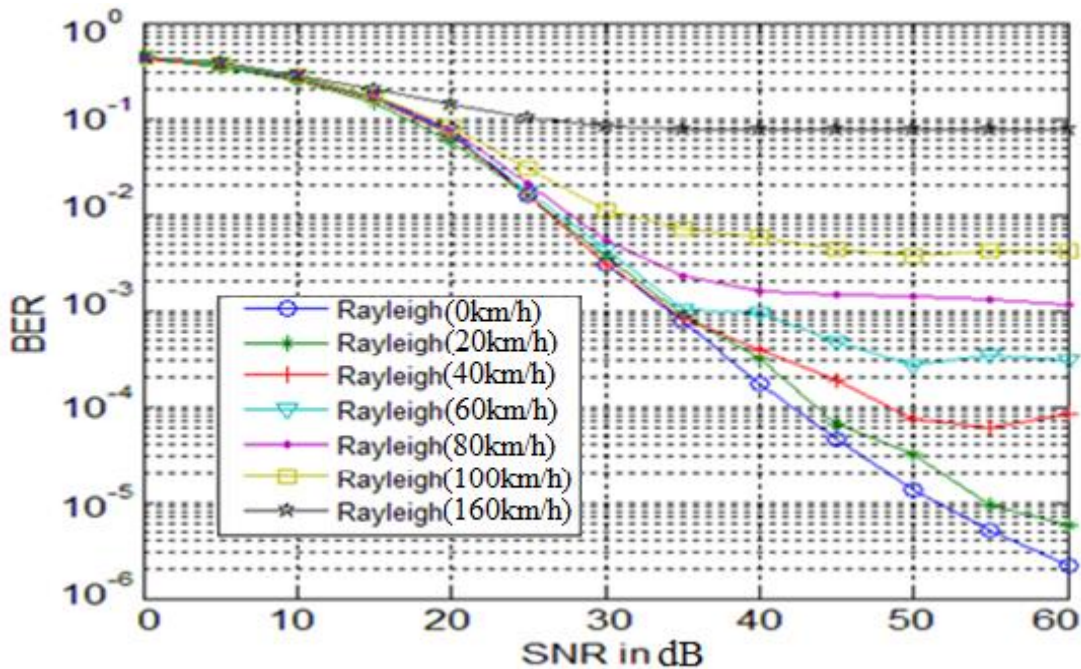


Figure 4.11: BER curves for 64QAM for different speeds, 10% of transmitted data are used for channel estimation.
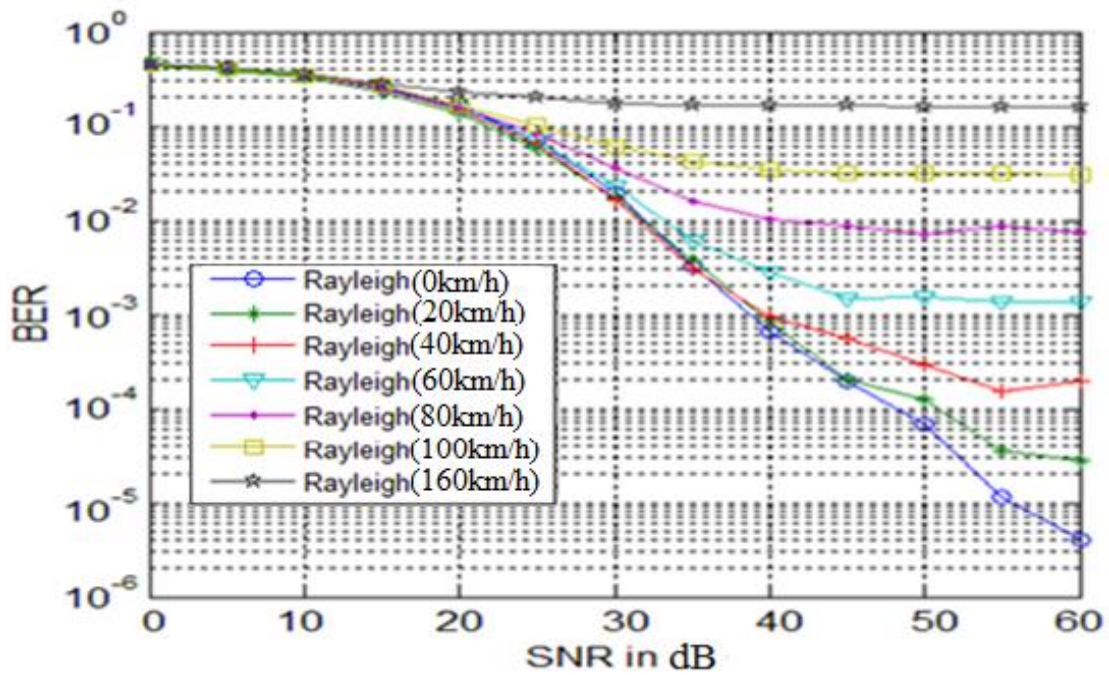
Figure 4.12: BER curves for 128QAM for different speeds, 10% of transmitted data are used for channel estimation.
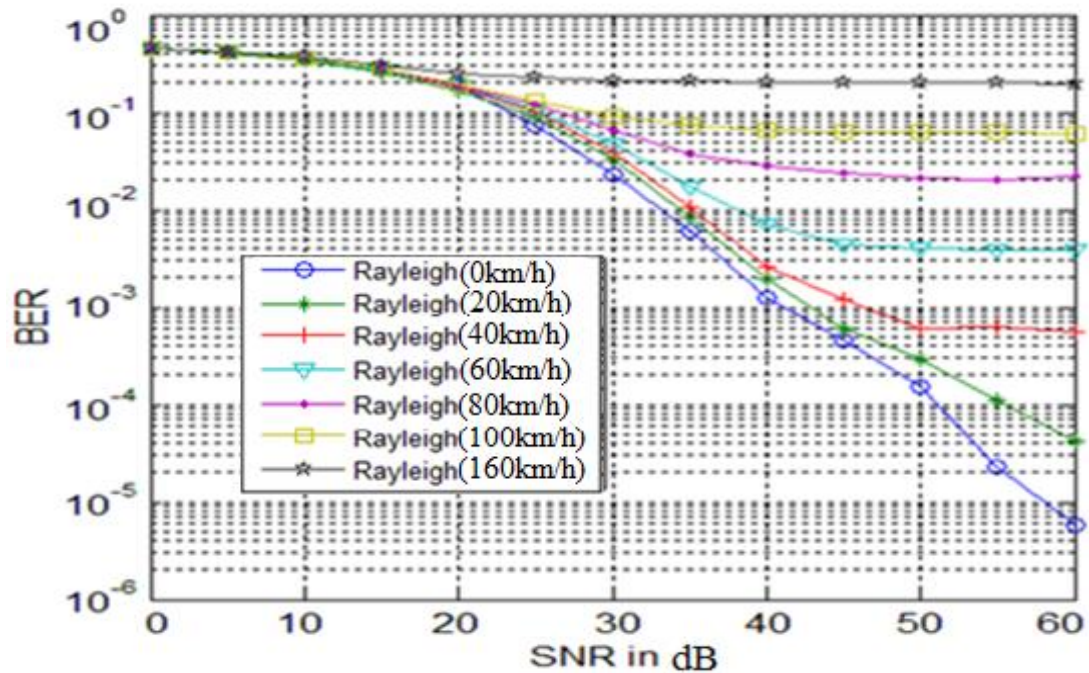


Figure 4.13: BER curves for 256QAM for different speeds, 10% of transmitted data are used for channel estimation.

94

The choice of the best modulation scheme for the instantaneous channel conditions, to achieve the desired BER, depends on the values of the SNR and the Doppler frequency shift (speed of the receiver) which are considered to be known at the receiver. The following tables are used to decide the best modulation scheme used for the instantaneous SNR and the receiver speed. For example, if it is required to decide the type of modulation for a BER of $10^{-3}$ or less, the shaded values in the following tables specify the type of modulation scheme according to the speed of the receiver.

Table 4.8: OFDM best BER for 0dB SNR

| Mod<br>speed | QPSK | 16QAM | 32QAM | 64QAM | 128QAM | 256QAM |
|---|---|---|---|---|---|---|
| 0km/h | $10^{-0.477}$ | $10^{-0.378}$ | $10^{-0.362}$ | $10^{-0.349}$ | $10^{-0.343}$ | $10^{-0.34}$ |
| 20km/h | $10^{-0.493}$ | $10^{-0.383}$ | $10^{-0.38}$ | $10^{-0.366}$ | $10^{-0.355}$ | $10^{-0.347}$ |
| 40km/h | $10^{-0.515}$ | $10^{-0.388}$ | $10^{-0.371}$ | $10^{-0.36}$ | $10^{-0.349}$ | $10^{-0.343}$ |
| 60km/h | $10^{-0.486}$ | $10^{-0.386}$ | $10^{-0.367}$ | $10^{-0.356}$ | $10^{-0.347}$ | $10^{-0.341}$ |
| 80km/h | $10^{-0.483}$ | $10^{-0.383}$ | $10^{-0.366}$ | $10^{-0.355}$ | $10^{-0.346}$ | $10^{-0.339}$ |
| 100km/h | $10^{-0.477}$ | $10^{-0.382}$ | $10^{-0.365}$ | $10^{-0.352}$ | $10^{-0.345}$ | $10^{-0.339}$ |
| 160km/h | $10^{-0.478}$ | $10^{-0.38}$ | $10^{-0.362}$ | $10^{-0.351}$ | $10^{-0.344}$ | $10^{-0.336}$ |

Table 4.9: OFDM best BER for 5dB SNR

| Mod<br>speed | QPSK | 16QAM | 32QAM | 64QAM | 128QAM | 256QAM |
|---|---|---|---|---|---|---|
| 0km/h | $10^{-0.655}$ | $10^{-0.46}$ | $10^{-0.43}$ | $10^{-0.401}$ | $10^{-0.386}$ | $10^{-0.377}$ |
| 20km/h | $10^{-0.682}$ | $10^{-0.594}$ | $10^{-0.46}$ | $10^{-0.429}$ | $10^{-0.406}$ | $10^{-0.392}$ |
| 40km/h | $10^{-0.726}$ | $10^{-0.484}$ | $10^{-0.444}$ | $10^{-0.417}$ | $10^{-0.395}$ | $10^{-0.381}$ |
| 60km/h | $10^{-0.667}$ | $10^{-0.481}$ | $10^{-0.439}$ | $10^{-0.408}$ | $10^{-0.391}$ | $10^{-0.374}$ |
| 80km/h | $10^{-0.663}$ | $10^{-0.475}$ | $10^{-0.432}$ | $10^{-0.408}$ | $10^{-0.389}$ | $10^{-0.376}$ |
| 100km/h | $10^{-0.655}$ | $10^{-0.475}$ | $10^{-0.432}$ | $10^{-0.407}$ | $10^{-0.389}$ | $10^{-0.372}$ |
| 160km/h | $10^{-0.641}$ | $10^{-0.457}$ | $10^{-0.417}$ | $10^{-0.4}$ | $10^{-0.382}$ | $10^{-0.373}$ |

Table 4.10: OFDM best BER for 10dB SNR

| Mod speed | QPSK | 16QAM | 32QAM | 64QAM | 128QAM | 256QAM |
|---|---|---|---|---|---|---|
| 0km/h | 10^−1.018 | 10^−0.642 | 10^−0.551 | 10^−0.507 | 10^−0.458 | 10^−0.432 |
| 20km/h | 10^−1.052 | 10^−0.693 | 10^−0.602 | 10^−0.549 | 10^−0.49 | 10^−0.468 |
| 40km/h | 10^−1.113 | 10^−0.673 | 10^−0.58 | 10^−0.514 | 10^−0.467 | 10^−0.45 |
| 60km/h | 10^−1.022 | 10^−0.656 | 10^−0.563 | 10^−0.517 | 10^−0.472 | 10^−0.444 |
| 80km/h | 10^−1.012 | 10^−0.65 | 10^−0.56 | 10^−0.506 | 10^−0.47 | 10^−0.442 |
| 100km/h | 10^−1.009 | 10^−0.648 | 10^−0.547 | 10^−0.506 | 10^−0.46 | 10^−0.441 |
| 160km/h | 10^−0.966 | 10^−0.638 | 10^−0.547 | 10^−0.479 | 10^−0.452 | 10^−0.423 |

Table 4.11: OFDM best BER for 15dB SNR

| Mod speed | QPSK | 16QAM | 32QAM | 64QAM | 128QAM | 256QAM |
|---|---|---|---|---|---|---|
| 0km/h | 10^−1.685 | 10^−0.941 | 10^−0.758 | 10^−0.677 | 10^−0.589 | 10^−0.567 |
| 20km/h | 10^−1.647 | 10^−1.059 | 10^−0.834 | 10^−0.738 | 10^−0.636 | 10^−0.589 |
| 40km/h | 10^−1.682 | 10^−0.986 | 10^−0.793 | 10^−0.697 | 10^−0.608 | 10^−0.564 |
| 60km/h | 10^−1.717 | 10^−0.968 | 10^−0.78 | 10^−0.694 | 10^−0.605 | 10^−0.568 |
| 80km/h | 10^−1.665 | 10^−0.942 | 10^−0.768 | 10^−0.683 | 10^−0.598 | 10^−0.546 |
| 100km/h | 10^−1.631 | 10^−0.923 | 10^−0.768 | 10^−0.667 | 10^−0.571 | 10^−0.549 |
| 160km/h | 10^−1.475 | 10^−0.88 | 10^−0.692 | 10^−0.623 | 10^−0.546 | 10^−0.513 |

Table 4.12: OFDM best BER for 20dB SNR

| Mod speed | QPSK | 16QAM | 32QAM | 64QAM | 128QAM | 256QAM |
|---|---|---|---|---|---|---|
| 0km/h | 10^−2.376 | 10^−1.524 | 10^−1.124 | 10^−0.94 | 10^−0.789 | 10^−0.728 |
| 20km/h | 10^−2.348 | 10^−1.406 | 10^−1.244 | 10^−1.029 | 10^−0.863 | 10^−0.775 |
| 40km/h | 10^−2.367 | 10^−1.507 | 10^−1.161 | 10^−1.008 | 10^−0.829 | 10^−0.742 |
| 60km/h | 10^−2.378 | 10^−1.539 | 10^−1.144 | 10^−0.978 | 10^−0.822 | 10^−0.727 |
| 80km/h | 10^−2.368 | 10^−1.464 | 10^−1.118 | 10^−0.945 | 10^−0.794 | 10^−0.724 |
| 100km/h | 10^−2.342 | 10^−1.414 | 10^−1.075 | 10^−0.909 | 10^−0.786 | 10^−0.719 |
| 160km/h | 10^−2.052 | 10^−1.1 | 10^−0.843 | 10^−0.764 | 10^−0.643 | 10^−0.6 |

Table 4.13: OFDM best BER for 25dB SNR

| Mod speed | QPSK | 16QAM | 32QAM | 64QAM | 128QAM | 256QAM |
|---|---|---|---|---|---|---|
| 0km/h | 10^−3.125 | 10^−2.447 | 10^−1.796 | 10^−1.401 | 10^−1.148 | 10^−1.138 |
| 20km/h | 10^−3.137 | 10^−2.222 | 10^−1.805 | 10^−1.494 | 10^−1.231 | 10^−1.045 |
| 40km/h | 10^−3.14 | 10^−2.224 | 10^−1.797 | 10^−1.475 | 10^−1.179 | 10^−0.998 |
| 60km/h | 10^−3.009 | 10^−2.186 | 10^−1.768 | 10^−1.425 | 10^−1.151 | 10^−0.967 |
| 80km/h | 10^−2.865 | 10^−2.136 | 10^−1.68 | 10^−1.352 | 10^−1.076 | 10^−0.928 |
| 100km/h | 10^−2.923 | 10^−1.998 | 10^−1.515 | 10^−1.258 | 10^−0.1 | 10^−0.879 |
| 160km/h | 10^−2.349 | 10^−1.321 | 10^−0.997 | 10^−0.849 | 10^−0.695 | 10^−0.644 |

Table 4.14: OFDM best BER for 30dB SNR

| Mod speed | QPSK | 16QAM | 32QAM | 64QAM | 128QAM | 256QAM |
|---|---|---|---|---|---|---|
| 0km/h | $10^{-3.551}$ | $10^{-2.868}$ | $10^{-2.516}$ | $10^{-2.146}$ | $10^{-1.714}$ | $10^{-1.64}$ |
| 20km/h | $10^{-3.577}$ | $10^{-2.872}$ | $10^{-2.449}$ | $10^{-2.129}$ | $10^{-1.77}$ | $10^{-1.482}$ |
| 40km/h | $10^{-3.435}$ | $10^{-2.914}$ | $10^{-2.519}$ | $10^{-2.148}$ | $10^{-1.785}$ | $10^{-1.412}$ |
| 60km/h | $10^{-3.517}$ | $10^{-2.689}$ | $10^{-2.368}$ | $10^{-2.067}$ | $10^{-1.634}$ | $10^{-1.329}$ |
| 80km/h | $10^{-3.304}$ | $10^{-2.669}$ | $10^{-2.28}$ | $10^{-1.854}$ | $10^{-1.455}$ | $10^{-1.193}$ |
| 100km/h | $10^{-3.215}$ | $10^{-2.494}$ | $10^{-1.961}$ | $10^{-1.588}$ | $10^{-1.227}$ | $10^{-1.037}$ |
| 160km/h | $10^{-2.346}$ | $10^{-1.451}$ | $10^{-1.071}$ | $10^{-0.883}$ | $10^{-0.764}$ | $10^{-0.683}$ |

Table 4.15: OFDM best BER for 35dB SNR

| Mod speed | QPSK | 16QAM | 32QAM | 64QAM | 128QAM | 256QAM |
|---|---|---|---|---|---|---|
| 0km/h | $10^{-4.315}$ | $10^{-3.515}$ | $10^{-3.11}$ | $10^{-2.839}$ | $10^{-2.486}$ | $10^{-2.223}$ |
| 20km/h | $10^{-4.085}$ | $10^{-3.621}$ | $10^{-3.051}$ | $10^{-2.755}$ | $10^{-2.433}$ | $10^{-2.071}$ |
| 40km/h | $10^{-3.987}$ | $10^{-3.539}$ | $10^{-3.076}$ | $10^{-2.75}$ | $10^{-2.517}$ | $10^{-1.979}$ |
| 60km/h | $10^{-3.816}$ | $10^{-3.154}$ | $10^{-2.991}$ | $10^{-2.513}$ | $10^{-2.222}$ | $10^{-1.771}$ |
| 80km/h | $10^{-3.728}$ | $10^{-3.011}$ | $10^{-2.644}$ | $10^{-2.253}$ | $10^{-1.795}$ | $10^{-1.438}$ |
| 100km/h | $10^{-3.452}$ | $10^{-2.725}$ | $10^{-2.152}$ | $10^{-1.828}$ | $10^{-1.384}$ | $10^{-1.128}$ |
| 160km/h | $10^{-2.491}$ | $10^{-1.484}$ | $10^{-1.106}$ | $10^{-0.925}$ | $10^{-0.783}$ | $10^{-0.682}$ |

Table 4.16: OFDM best BER for 40dB SNR

| Mod speed | QPSK | 16QAM | 32QAM | 64QAM | 128QAM | 256QAM |
|---|---|---|---|---|---|---|
| 0km/h | $10^{-4.780}$ | $10^{-3.96}$ | $10^{-3.762}$ | $10^{-3.519}$ | $10^{-3.176}$ | $10^{-2.897}$ |
| 20km/h | $10^{-4.282}$ | $10^{-3.906}$ | $10^{-3.508}$ | $10^{-3.336}$ | $10^{-3.085}$ | $10^{-2.71}$ |
| 40km/h | $10^{-4.31}$ | $10^{-3.936}$ | $10^{-3.414}$ | $10^{-3.342}$ | $10^{-3.026}$ | $10^{-2.584}$ |
| 60km/h | $10^{-4.027}$ | $10^{-3.398}$ | $10^{-3.03}$ | $10^{-3.002}$ | $10^{-2.559}$ | $10^{-2.151}$ |
| 80km/h | $10^{-3.78}$ | $10^{-3.141}$ | $10^{-2.791}$ | $10^{-2.408}$ | $10^{-1.985}$ | $10^{-1.561}$ |
| 100km/h | $10^{-3.478}$ | $10^{-2.861}$ | $10^{-2.237}$ | $10^{-1.927}$ | $10^{-1.464}$ | $10^{-1.176}$ |
| 160km/h | $10^{-2.483}$ | $10^{-1.475}$ | $10^{-1.12}$ | $10^{-0.935}$ | $10^{-0.783}$ | $10^{-0.699}$ |

Table 4.17: OFDM best BER for 45dB SNR

| Mod speed | QPSK | 16QAM | 32QAM | 64QAM | 128QAM | 256QAM |
|---|---|---|---|---|---|---|
| 0km/h | $10^{-5.8}$ | $10^{-4.57}$ | $10^{-4.35}$ | $10^{-3.872}$ | $10^{-3.718}$ | $10^{-3.343}$ |
| 20km/h | $10^{-5.37}$ | $10^{-4.17}$ | $10^{-4.176}$ | $10^{-3.732}$ | $10^{-3.691}$ | $10^{-3.217}$ |
| 40km/h | $10^{-4.986}$ | $10^{-3.902}$ | $10^{-3.727}$ | $10^{-3.667}$ | $10^{-3.257}$ | $10^{-2.93}$ |
| 60km/h | $10^{-4.308}$ | $10^{-3.57}$ | $10^{-3.322}$ | $10^{-3.133}$ | $10^{-2.83}$ | $10^{-2.363}$ |
| 80km/h | $10^{-4.114}$ | $10^{-3.245}$ | $10^{-2.83}$ | $10^{-2.534}$ | $10^{-2.065}$ | $10^{-1.63}$ |
| 100km/h | $10^{-3.447}$ | $10^{-2.959}$ | $10^{-2.364}$ | $10^{-1.871}$ | $10^{-1.491}$ | $10^{-1.202}$ |
| 160km/h | $10^{-2.542}$ | $10^{-1.459}$ | $10^{-1.115}$ | $10^{-0.931}$ | $10^{-0.78}$ | $10^{-0.695}$ |

Table 4.18: OFDM best BER for 50dB SNR

| Mod speed | QPSK | 16QAM | 32QAM | 64QAM | 128QAM | 256QAM |
|---|---|---|---|---|---|---|
| 0km/h | $10^{-6.07}$ | $10^{-4.88}$ | $10^{-4.87}$ | $10^{-4.53}$ | $10^{-4.162}$ | $10^{-3.808}$ |
| 20km/h | $10^{-5.39}$ | $10^{-4.783}$ | $10^{-4.5}$ | $10^{-4.19}$ | $10^{-3.906}$ | $10^{-3.53}$ |
| 40km/h | $10^{-5.239}$ | $10^{-4.336}$ | $10^{-4.128}$ | $10^{-3.915}$ | $10^{-3.541}$ | $10^{-3.219}$ |
| 60km/h | $10^{-4.448}$ | $10^{-3.671}$ | $10^{-3.578}$ | $10^{-3.186}$ | $10^{-2.817}$ | $10^{-2.402}$ |
| 80km/h | $10^{-3.955}$ | $10^{-3.18}$ | $10^{-2.859}$ | $10^{-2.565}$ | $10^{-2.147}$ | $10^{-1.678}$ |
| 100km/h | $10^{-3.524}$ | $10^{-2.85}$ | $10^{-2.424}$ | $10^{-1.911}$ | $10^{-1.508}$ | $10^{-1.208}$ |
| 160km/h | $10^{-2.437}$ | $10^{-1.499}$ | $10^{-1.115}$ | $10^{-0.936}$ | $10^{-0.791}$ | $10^{-0.697}$ |

Table 4.19: OFDM best BER for 55dB SNR

| Mod speed | QPSK | 16QAM | 32QAM | 64QAM | 128QAM | 256QAM |
|---|---|---|---|---|---|---|
| 0km/h | $10^{-6.418}$ | $10^{-5.798}$ | $10^{-5.29}$ | $10^{-5.12}$ | $10^{-4.939}$ | $10^{-4.632}$ |
| 20km/h | $10^{-6.22}$ | $10^{-4.91}$ | $10^{-4.03}$ | $10^{-4.356}$ | $10^{-4.442}$ | $10^{-3.949}$ |
| 40km/h | $10^{-5.175}$ | $10^{-4.536}$ | $10^{-4.215}$ | $10^{-4.09}$ | $10^{-3.813}$ | $10^{-3.204}$ |
| 60km/h | $10^{-4.64}$ | $10^{-3.889}$ | $10^{-3.462}$ | $10^{-3.263}$ | $10^{-2.868}$ | $10^{-2.42}$ |
| 80km/h | $10^{-3.961}$ | $10^{-3.322}$ | $10^{-2.894}$ | $10^{-2.599}$ | $10^{-2.065}$ | $10^{-1.692}$ |
| 100km/h | $10^{-3.496}$ | $10^{-2.917}$ | $10^{-2.379}$ | $10^{-1.921}$ | $10^{-1.502}$ | $10^{-1.208}$ |
| 160km/h | $10^{-2.507}$ | $10^{-1.484}$ | $10^{-1.115}$ | $10^{-0.941}$ | $10^{-0.793}$ | $10^{-0.697}$ |

Table 4.20: OFDM best BER for 60dB SNR

| Mod speed | QPSK | 16QAM | 32QAM | 64QAM | 128QAM | 256QAM |
|---|---|---|---|---|---|---|
| 0km/h | $10^{-6.799}$ | $10^{-6.145}$ | $10^{-5.65}$ | $10^{-5.32}$ | $10^{-5.391}$ | $10^{-5.23}$ |
| 20km/h | $10^{-6.28}$ | $10^{-5.487}$ | $10^{-5.24}$ | $10^{-5.11}$ | $10^{-4.56}$ | $10^{-4.37}$ |
| 40km/h | $10^{-5.24}$ | $10^{-4.6}$ | $10^{-4.075}$ | $10^{-4.133}$ | $10^{-3.71}$ | $10^{-3.252}$ |
| 60km/h | $10^{-4.58}$ | $10^{-3.81}$ | $10^{-3.51}$ | $10^{-3.22}$ | $10^{-2.86}$ | $10^{-2.41}$ |
| 80km/h | $10^{-4.07}$ | $10^{-3.211}$ | $10^{-2.933}$ | $10^{-2.63}$ | $10^{-2.133}$ | $10^{-1.6562}$ |
| 100km/h | $10^{-3.56}$ | $10^{-2.959}$ | $10^{-2.37}$ | $10^{-1.938}$ | $10^{-1.519}$ | $10^{-1.218}$ |
| 160km/h | $10^{-2.655}$ | $10^{-1.474}$ | $10^{-1.12}$ | $10^{-0.933}$ | $10^{-0.796}$ | $10^{-0.708}$ |

As noted from tables 4.8- 4.14, BER of $10^{-3}$ cannot be fulfilled for SNR of values 0dB, 5dB, 10dB, 15dB, 20dB, 25dB, 30dB respectively (yellow shaded values). Therefore there is no chance to select any type of modulation scheme. However, selecting the QPSK is better than disconnecting the communication link.

The present work identifies the best modulation scheme used with the instantaneous channel conditions (the SNR and the Doppler effects). Although at any SNR, the QPSK modulation is the best and the 256QAM is the worst in terms of BER, high-order modulation schemes such as 32QAM 64QAM, 128QAM and 256QAM can be used for good channel conditions and low speed of the receiver. If the desired BER in the physical layer at the receiver is 10^-3, it is found that for 160 km/h and 100 km/h speeds of the receiver, the QPSK modulation should be used. For 80 km/h speed, the QPSK and 16QAM can be used on condition that the SNR is equal or greater than 35dB. For 60 km/h speed, the 16QAM can be used on condition that the SNR is greater than 35dB, and the 32QAM and the 64QAM can be used on condition that the SNR is greater than 40dB. For 40 km/h speed, the 128QAM can be used on condition that the SNR is greater than 40dB and the 256QAM can be used on condition that the SNR is greater than 50dB. For 20 km/h and the stationary receiver, the 256QAM can be used on condition that the SNR is greater than 45dB.

## 4.4 The 2*2 MIMO-OFDM Wireless Communication System

The relationship between the SNR and the BER performance for QPSK, 16QAM, 32QAM, 64QAM, 128QAM and 256QAM modulation/demodulation types and at different receiver equipment speeds has been found by assuming 10% of the transmitted data as pilots to estimate (interpolate) the actual Rayleigh fading channel coefficients. The effect of the Rayleigh fading channel has been nearly removed by considering the estimated Rayleigh fading channel coefficients in the

MIMO single tab equalizer. Then the two outputs of the equalizer have been applied to a proper demodulation scheme to recover the transmitting bits with a BER as shown in Figures 4.14, 4.15, 4.16, 4.17, 4.18 and 4.19. The BER has been calculated by taking the average value of the two BERs produced for the two OFDM symbols which are transmitted from antenna 1 and antenna 2 simultaneously. The range of SNR is from 0dB to 60dB. The step size of SNR is set to 5dB in order to reduce the time of the simulation which almost needs many days of computation time on a high-speed computer to get a reasonable view about the relation between the SNR and the BER.
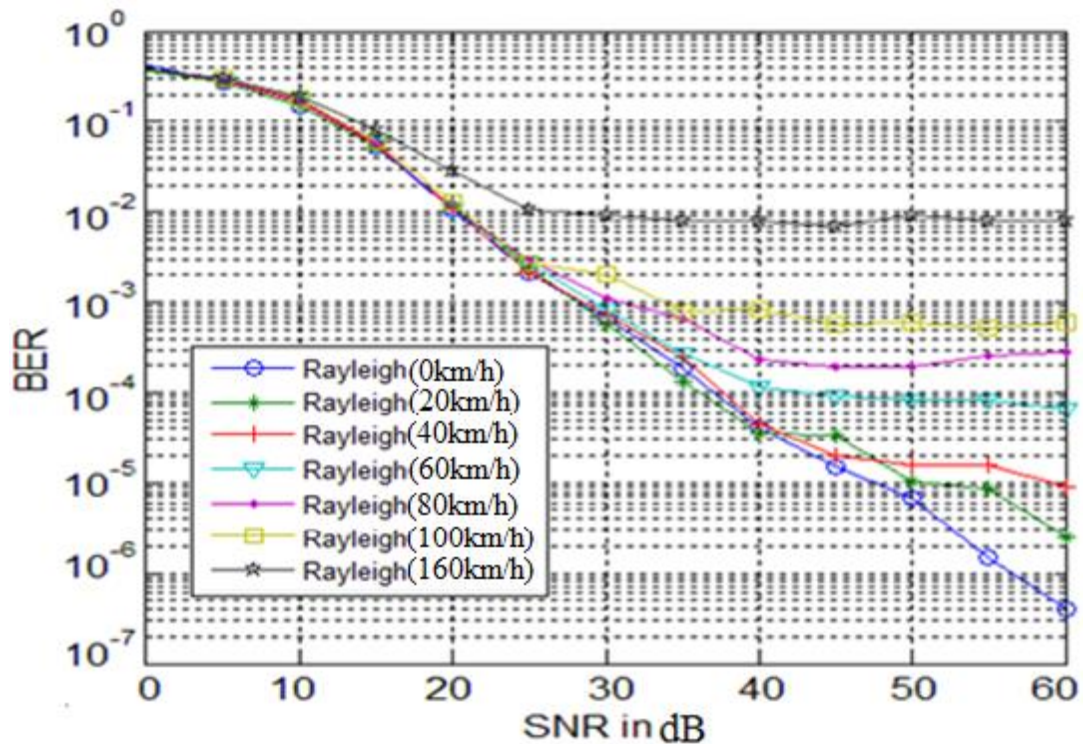


Figure 4.14: BER curves for QPSK for different speeds, 10% of transmitted data are used for channel estimation.
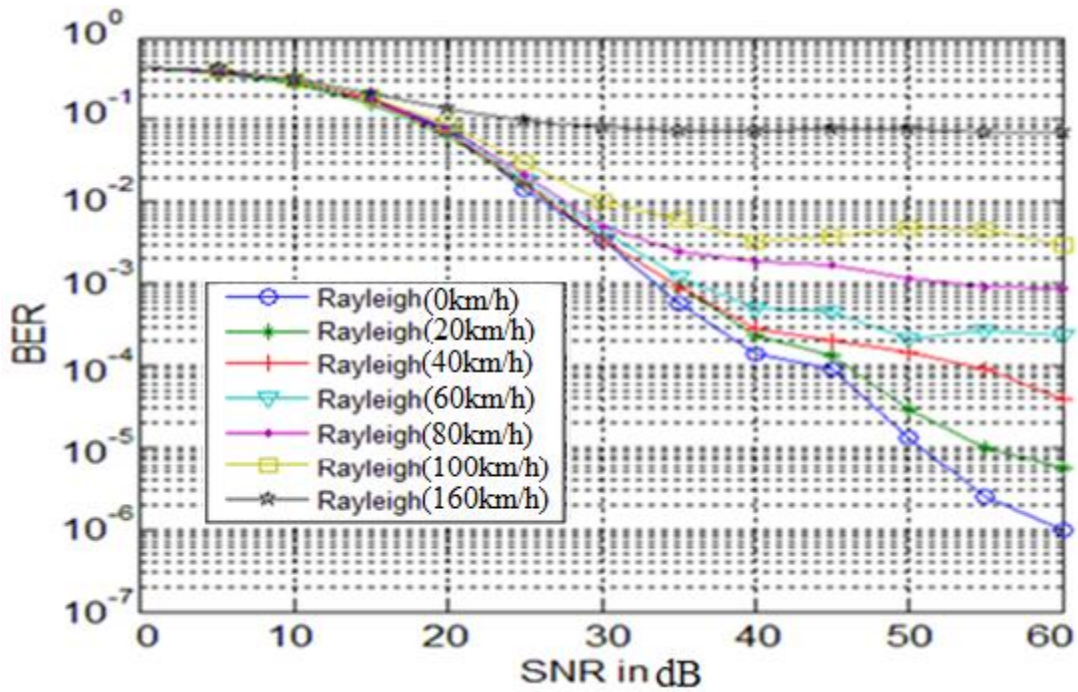
Figure 4.15: BER curves for 16QAM for different speeds, 10% of transmitted data are used for channel estimation.
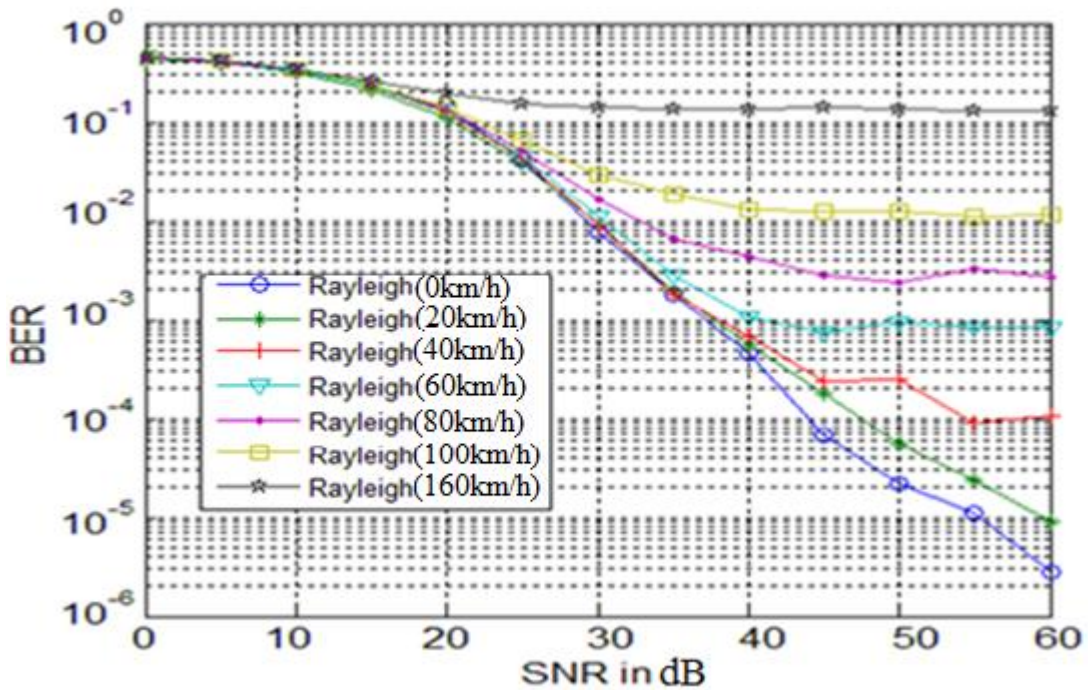


Figure 4.16: BER curves for 32QAM for different speeds, 10% of transmitted data are used for channel estimation.
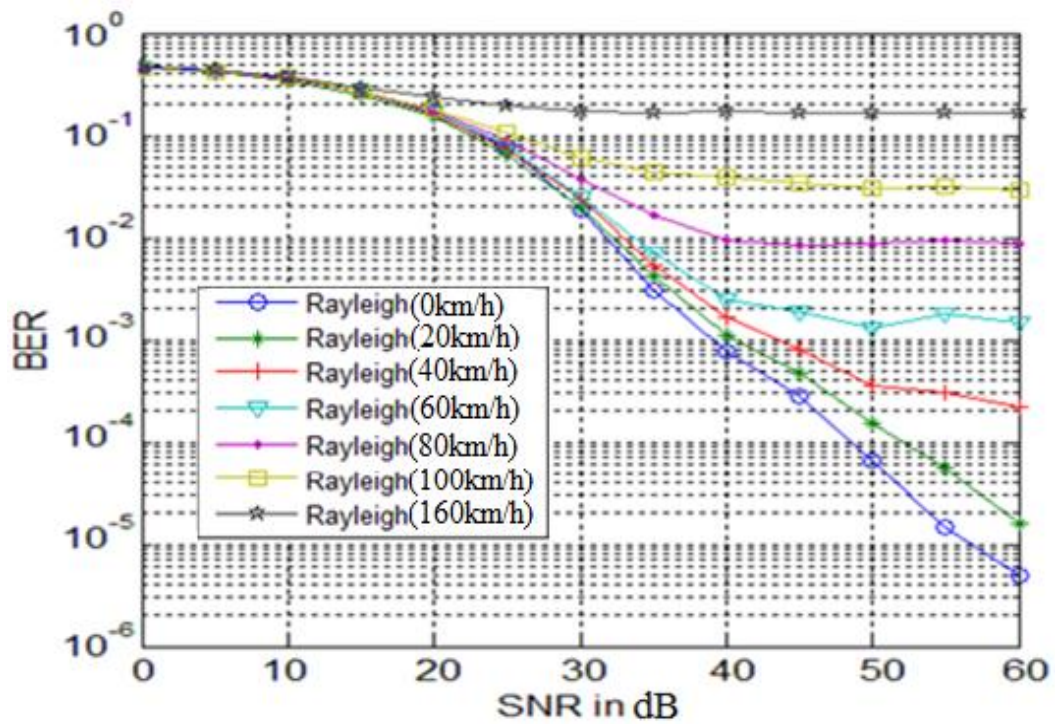
Figure 4.17: BER curves for 64QAM for different speeds, 10% of transmitted data are used for channel estimation.
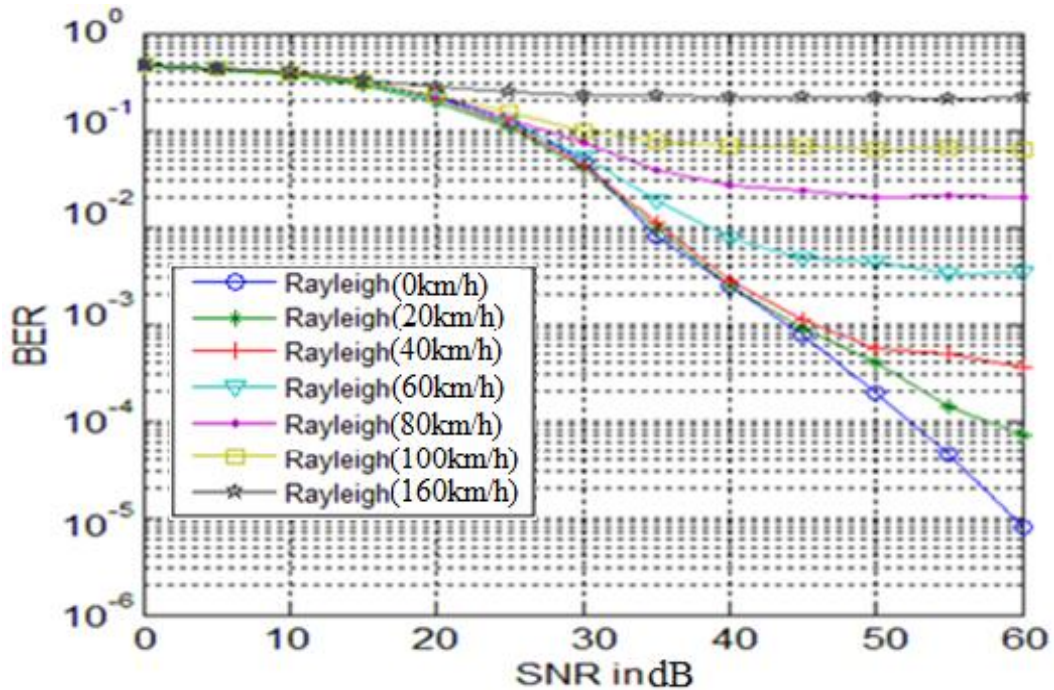


Figure 4.18: BER curves for 128QAM for different speeds, 10% of transmitted data are used for channel estimation.
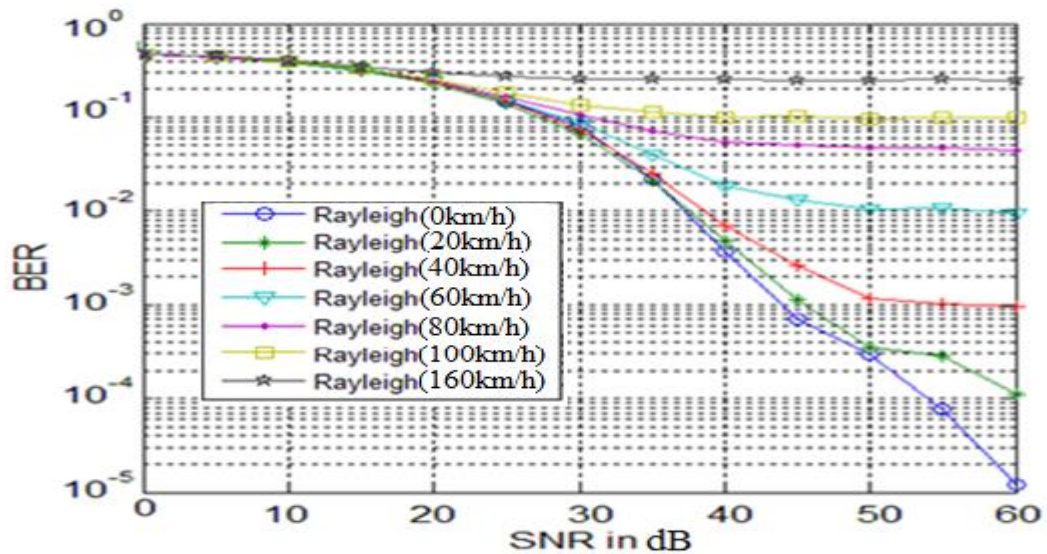
Figure 4.19: BER curves for 256QAM for different speeds, 10% of transmitted data are used for channel estimation.

The choice of the best modulation scheme for the instantaneous channel conditions, to achieve the desired BER, depends on the values of the SNR and the Doppler frequency shift (speed of the receiver) which are considered to be known at the receiver. Tables 4.21-4.33 are used to decide the best modulation scheme used according to the instantaneous SNR and the receiver speed. For example, if it is required to decide the type of modulation for a BER of 10^-3 or less, the blue shaded values specify the possibility of choosing the type of modulation scheme for the 2*2 MIMO-OFDM system according to the speed of the receiver. BER of 10^-3 for the yellow shade values cannot be fulfilled for SNR of values 0dB, 5dB, 10dB, 15dB, 20dB, 25dB, 30dB respectively. Therefore there is no chance to select any type of modulation scheme. However, selecting the QPSK is better than disconnecting the communication link. On the other hand, the green shaded values in the same tables are for extra modulation schemes when the OFDM system is considered.

103

Table 4.21: 2*2 MIMO-OFDM best BER for 0dB SNR

| Mod speed | QPSK | 16QAM | 32QAM | 64QAM | 128QAM | 256QAM |
|---|---|---|---|---|---|---|
| 0km/h | 10^-0.377 | 10^-0.353 | 10^-0.343 | 10^-0.333 | 10^-0.328 | 10^-0.325 |
| 20km/h | 10^-0.44 | 10^-0.365 | 10^-0.352 | 10^-0.342 | 10^-0.336 | 10^-0.332 |
| 40km/h | 10^-0.428 | 10^-0.358 | 10^-0.347 | 10^-0.338 | 10^-0.333 | 10^-0.328 |
| 60km/h | 10^-0.422 | 10^-0.356 | 10^-0.345 | 10^-0.336 | 10^-0.332 | 10^-0.327 |
| 80km/h | 10^-0.421 | 10^-0.355 | 10^-0.343 | 10^-0.336 | 10^-0.33 | 10^-0.327 |
| 100km/h | 10^-0.419 | 10^-0.354 | 10^-0.344 | 10^-0.334 | 10^-0.33 | 10^-0.327 |
| 160km/h | 10^-0.415 | 10^-0.354 | 10^-0.343 | 10^-0.335 | 10^-0.332 | 10^-0.326 |

Table 4.22: 2*2 MIMO-OFDM best BER for 5dB SNR

| Mod speed | QPSK | 16QAM | 32QAM | 64QAM | 128QAM | 256QAM |
|---|---|---|---|---|---|---|
| 0km/h | 10^-0.554 | 10^-0. 404 | 10^-0.382 | 10^-0.365 | 10^-0.355 | 10^-0.349 |
| 20km/h | 10^-0.57 | 10^-0.432 | 10^-0.402 | 10^-0.383 | 10^-0.367 | 10^-0.36 |
| 40km/h | 10^-0.546 | 10^-0.416 | 10^-0.392 | 10^-0.374 | 10^-0.363 | 10^-0.354 |
| 60km/h | 10^-0.539 | 10^-0.411 | 10^-0.388 | 10^-0.371 | 10^-0.36 | 10^-0.352 |
| 80km/h | 10^-0.533 | 10^-0.41 | 10^-0.387 | 10^-0.369 | 10^-0.359 | 10^-0.352 |
| 100km/h | 10^-0.53 | 10^-0.409 | 10^-0.384 | 10^-0.367 | 10^-0.359 | 10^-0.35 |
| 160km/h | 10^-0.532 | 10^-0.404 | 10^-0.383 | 10^-0.363 | 10^-0.356 | 10^-0.349 |

Table 4.23: 2*2 MIMO-OFDM best BER for 10dB SNR

| Mod speed | QPSK | 16QAM | 32QAM | 64QAM | 128QAM | 256QAM |
|---|---|---|---|---|---|---|
| 0km/h | 10^-0.836 | 10^-0.514 | 10^-0.47 | 10^-0.434 | 10^-0.404 | 10^-0.397 |
| 20km/h | 10^-0.834 | 10^-0.566 | 10^-0.45 | 10^-0.461 | 10^-0.432 | 10^-0.415 |
| 40km/h | 10^-0.787 | 10^-0.542 | 10^-0.482 | 10^-0.446 | 10^-0.42 | 10^-0.405 |
| 60km/h | 10^-0.773 | 10^-0.533 | 10^-0.476 | 10^-0.441 | 10^-0.417 | 10^-0.401 |
| 80km/h | 10^-0.768 | 10^-0.53 | 10^-0.472 | 10^-0.439 | 10^-0.414 | 10^-0.401 |
| 100km/h | 10^-0.756 | 10^-0.522 | 10^-0.468 | 10^-0.435 | 10^-0.411 | 10^-0.398 |
| 160km/h | 10^-0.727 | 10^-0.502 | 10^-0.469 | 10^-0.426 | 10^-0.399 | 10^-0.389 |

Table 4.24: 2*2 MIMO-OFDM best BER for 15dB SNR

| Mod speed | QPSK | 16QAM | 32QAM | 64QAM | 128QAM | 256QAM |
|---|---|---|---|---|---|---|
| 0km/h | 10^-1.288 | 10^-0.743 | 10^-0.627 | 10^-0.572 | 10^-0.502 | 10^-0.473 |
| 20km/h | 10^-1.289 | 10^-0.801 | 10^-0.67 | 10^-0.603 | 10^-0.537 | 10^-0.503 |
| 40km/h | 10^-1.26 | 10^-0.765 | 10^-0.644 | 10^-0.576 | 10^-0.516 | 10^-0.49 |
| 60km/h | 10^-1.237 | 10^-0.752 | 10^-0.635 | 10^-0.569 | 10^-0.511 | 10^-0.483 |
| 80km/h | 10^-1.242 | 10^-0.745 | 10^-0.628 | 10^-0.564 | 10^-0.505 | 10^-0.477 |
| 100km/h | 10^-1.224 | 10^-0.735 | 10^-0.618 | 10^-0.561 | 10^-0.505 | 10^-0.473 |
| 160km/h | 10^-1.109 | 10^-0.679 | 10^-0.583 | 10^-0.529 | 10^-0.475 | 10^-0.459 |

Table 4.25: 2*2 MIMO-OFDM best BER for 20dB SNR

| Mod<br>speed | QPSK | 16QAM | 32QAM | 64QAM | 128QAM | 256QAM |
|---|---|---|---|---|---|---|
| 0km/h | 10^-1.967 | 10^-1.132 | 10^-0.844 | 10^-0.76 | 10^-0.637 | 10^-0.601 |
| 20km/h | 10^-1.938 | 10^-1.191 | 10^-0.953 | 10^-0.82 | 10^-0.708 | 10^-0.643 |
| 40km/h | 10^-1.957 | 10^-1.151 | 10^-0.902 | 10^-0.795 | 10^-0.682 | 10^-0.622 |
| 60km/h | 10^-1.974 | 10^-1.12 | 10^-0.887 | 10^-0.781 | 10^-0.668 | 10^-0.612 |
| 80km/h | 10^-1.979 | 10^-1.093 | 10^-0.872 | 10^-0.761 | 10^-0.654 | 10^-0.603 |
| 100km/h | 10^-1.895 | 10^-1.062 | 10^-0.847 | 10^-0.752 | 10^-0.637 | 10^-0.59 |
| 160km/h | 10^-1.536 | 10^-0.866 | 10^-0.711 | 10^-0.628 | 10^-0.556 | 10^-0.523 |

Table 4.26: 2*2 MIMO-OFDM best BER for 25dB SNR

| Mod<br>speed | QPSK | 16QAM | 32QAM | 64QAM | 128QAM | 256QAM |
|---|---|---|---|---|---|---|
| 0km/h | 10^-2.662 | 10^-1.844 | 10^-1.386 | 10^-1.11 | 10^-0.892 | 10^-0.827 |
| 20km/h | 10^-2.612 | 10^-1.782 | 10^-1.404 | 10^-1.176 | 10^-0.978 | 10^-0.856 |
| 40km/h | 10^-2.664 | 10^-1.774 | 10^-1.366 | 10^-1.131 | 10^-0.935 | 10^-0.823 |
| 60km/h | 10^-2.573 | 10^-1.726 | 10^-1.346 | 10^-1.094 | 10^-0.918 | 10^-0.804 |
| 80km/h | 10^-2.526 | 10^-1.674 | 10^-1.289 | 10^-1.05 | 10^-0.881 | 10^-0.778 |
| 100km/h | 10^-2.57 | 10^-1.529 | 10^-1.176 | 10^-0.98 | 10^-0.823 | 10^-0.738 |
| 160km/h | 10^-1.98 | 10^-1.017 | 10^-0.813 | 10^-0.708 | 10^-0.605 | 10^-0.557 |

Table 4.27: 2*2 MIMO-OFDM best BER for 30dB SNR

| Mod<br>speed | QPSK | 16QAM | 32QAM | 64QAM | 128QAM | 256QAM |
|---|---|---|---|---|---|---|
| 0km/h | 10^-3.19 | 10^-2.471 | 10^-2.106 | 10^-1.727 | 10^-1.332 | 10^-1.084 |
| 20km/h | 10^-3.238 | 10^-2.465 | 10^-2.049 | 10^-1.71 | 10^-1.401 | 10^-1.18 |
| 40km/h | 10^-3.133 | 10^-2.47 | 10^-2.04 | 10^-1.616 | 10^-1.351 | 10^-1.132 |
| 60km/h | 10^-3.089 | 10^-2.362 | 10^-1.957 | 10^-1.609 | 10^-1.271 | 10^-1.067 |
| 80km/h | 10^-2.949 | 10^-2.3 | 10^-1.78 | 10^-1.423 | 10^-1.14 | 10^-0.976 |
| 100km/h | 10^-2.682 | 10^-2.002 | 10^-1.539 | 10^-1.211 | 10^-1.0078 | 10^-0.868 |
| 160km/h | 10^-2.045 | 10^-1.091 | 10^-0.856 | 10^-0.757 | 10^-0.641 | 10^-0.586 |

Table 4.28: 2*2 MIMO-OFDM best BER for 35dB SNR

| Mod<br>speed | QPSK | 16QAM | 32QAM | 64QAM | 128QAM | 256QAM |
|---|---|---|---|---|---|---|
| 0km/h | 10^-3.74 | 10^-3.235 | 10^-2.753 | 10^-2.526 | 10^-2.092 | 10^-1.657 |
| 20km/h | 10^-3.881 | 10^-3.047 | 10^-2.719 | 10^-2.369 | 10^-2.01 | 10^-1.677 |
| 40km/h | 10^-3.619 | 10^-3.036 | 10^-2.745 | 10^-2.28 | 10^-1.956 | 10^-1.597 |
| 60km/h | 10^-3.568 | 10^-2.915 | 10^-2.561 | 10^-2.153 | 10^-1.731 | 10^-1.401 |
| 80km/h | 10^-3.174 | 10^-2.617 | 10^-2.193 | 10^-1.777 | 10^-1.409 | 10^-1.153 |
| 100km/h | 10^-3.101 | 10^-2.23 | 10^-1.73 | 10^-1.368 | 10^-1.113 | 10^-0.937 |
| 160km/h | 10^-2.1 | 10^-1.137 | 10^-0.87 | 10^-0.777 | 10^-0.647 | 10^-0.598 |

Table 4.29: 2*2 MIMO-OFDM best BER for 40dB SNR

| Mod speed | QPSK | 16QAM | 32QAM | 64QAM | 128QAM | 256QAM |
|---|---|---|---|---|---|---|
| 0km/h | 10^-4.39 | 10^-3.856 | 10^-3.35 | 10^-3.119 | 10^-2.598 | 10^-2.434 |
| 20km/h | 10^-4.462 | 10^-3.625 | 10^-3.262 | 10^-2.95 | 10^-2.613 | 10^-2.32 |
| 40km/h | 10^-4.346 | 10^-3.55 | 10^-3.17 | 10^-2.789 | 10^-2.553 | 10^-2.151 |
| 60km/h | 10^-3.94 | 10^-3.307 | 10^-2.974 | 10^-2.599 | 10^-2.115 | 10^-1.735 |
| 80km/h | 10^-3.628 | 10^-2.725 | 10^-2.351 | 10^-2.026 | 10^-1.578 | 10^-1.267 |
| 100km/h | 10^-3.09 | 10^-2.477 | 10^-1.887 | 10^-1.42 | 10^-1.165 | 10^-1.005 |
| 160km/h | 10^-2.089 | 10^-1.138 | 10^-0.868 | 10^-0.772 | 10^-0.655 | 10^-0.599 |

Table 4.30: 2*2 MIMO-OFDM best BER for 45dB SNR

| Mod speed | QPSK | 16QAM | 32QAM | 64QAM | 128QAM | 256QAM |
|---|---|---|---|---|---|---|
| 0km/h | 10^-4.817 | 10^-4.05 | 10^-4.16 | 10^-3.546 | 10^-3.116 | 10^-3.151 |
| 20km/h | 10^-4.465 | 10^-3.878 | 10^-3.737 | 10^-3.331 | 10^-3.04 | 10^-2.944 |
| 40km/h | 10^-4.694 | 10^-3.696 | 10^-3.628 | 10^-3.09 | 10^-2.952 | 10^-2.588 |
| 60km/h | 10^-4.046 | 10^-3.34 | 10^-3.124 | 10^-2.726 | 10^-2.32 | 10^-1.886 |
| 80km/h | 10^-3.713 | 10^-2.769 | 10^-2.552 | 10^-2.088 | 10^-1.614 | 10^-1.295 |
| 100km/h | 10^-3.248 | 10^-2.433 | 10^-1.901 | 10^-1.471 | 10^-1.174 | 10^-0.989 |
| 160km/h | 10^-2.155 | 10^-1.124 | 10^-0.855 | 10^-0.772 | 10^-0.655 | 10^-0.604 |

Table 4.31: 2*2 MIMO-OFDM best BER for 50dB SNR

| Mod speed | QPSK | 16QAM | 32QAM | 64QAM | 128QAM | 256QAM |
|---|---|---|---|---|---|---|
| 0km/h | 10^-5.163 | 10^-4.89 | 10^-4.666 | 10^-4.19 | 10^-3.71 | 10^-3.531 |
| 20km/h | 10^-4.989 | 10^-4.527 | 10^-4.256 | 10^-3.823 | 10^-3.39 | 10^-3.454 |
| 40km/h | 10^-4.805 | 10^-3.834 | 10^-3.614 | 10^-3.441 | 10^-3.261 | 10^-2.935 |
| 60km/h | 10^-4.092 | 10^-3.666 | 10^-3.032 | 10^-2.878 | 10^-2.36 | 10^-1.988 |
| 80km/h | 10^-3.717 | 10^-2.93 | 10^-2.618 | 10^-2.064 | 10^-1.686 | 10^-1.325 |
| 100km/h | 10^-3.221 | 10^-2.321 | 10^-1.907 | 10^-1.517 | 10^-1.208 | 10^-1.012 |
| 160km/h | 10^-2.036 | 10^-1.122 | 10^-0.872 | 10^-0.778 | 10^-0.66 | 10^-0.603 |

Table 4.32: 2*2 MIMO-OFDM best BER for 55dB SNR

| Mod speed | QPSK | 16QAM | 32QAM | 64QAM | 128QAM | 256QAM |
|---|---|---|---|---|---|---|
| 0km/h | 10^-5.831 | 10^-5.59 | 10^-4.951 | 10^-4.836 | 10^-4.335 | 10^-4.108 |
| 20km/h | 10^-5.065 | 10^-5.002 | 10^-4.63 | 10^-4.262 | 10^-3.852 | 10^-3.538 |
| 40km/h | 10^-4.8 | 10^-4.05 | 10^-4.04 | 10^-3.521 | 10^-3.305 | 10^-2.991 |
| 60km/h | 10^-4.075 | 10^-3.574 | 10^-3.078 | 10^-2.751 | 10^-2.476 | 10^-1.97 |
| 80km/h | 10^-3.587 | 10^-3.048 | 10^-2.487 | 10^-2.026 | 10^-1.67 | 10^-1.325 |
| 100km/h | 10^-3.287 | 10^-2.353 | 10^-1.949 | 10^-1.498 | 10^-1.191 | 10^-1.003 |
| 160km/h | 10^-2.09 | 10^-1.152 | 10^-0.887 | 10^-0.775 | 10^-0.667 | 10^-0.598 |

Table 4.33: 2*2 MIMO-OFDM best BER for 60dB SNR

| Mod\speed | QPSK | 16QAM | 32QAM | 64QAM | 128QAM | 256QAM |
|---|---|---|---|---|---|---|
| 0km/h | 10^-6.39 | 10^-6.017 | 10^-5.555 | 10^-5.315 | 10^-5.09 | 10^-4.922 |
| 20km/h | 10^-5.59 | 10^-5.255 | 10^-5.038 | 10^-4.796 | 10^-4.152 | 10^-3.954 |
| 40km/h | 10^-5.047 | 10^-4.411 | 10^-3.976 | 10^-3.663 | 10^-3.439 | 10^-3.016 |
| 60km/h | 10^-4.18 | 10^-3.641 | 10^-3.071 | 10^-2.829 | 10^-2.472 | 10^-2.022 |
| 80km/h | 10^-3.557 | 10^-3.07 | 10^-2.575 | 10^-2.055 | 10^-1.693 | 10^-1.345 |
| 100km/h | 10^-3.22 | 10^-2.518 | 10^-1.94 | 10^-1.54 | 10^-1.199 | 10^-1.004 |
| 160km/h | 10^-2.09 | 10^-1.15 | 10^-0.888 | 10^-0.786 | 10^-0.667 | 10^-0.611 |

The 2*2 MIMO-OFDM tables identify the best modulation scheme used with the instantaneous channel conditions (the SNR and the Doppler effects). Although at any SNR, the QPSK modulation is the best and the 256QAM is the worst in terms of BER, high order modulation schemes such as 32QAM, 64QAM, 128QAM or 256QAM can be used for good channel conditions and low speed of receiver. If the desired BER in the physical layer at the receiver is $10^{-3}$, it is found that for 160 km/h and 100 km/h speeds of the receiver, only the QPSK modulation should be used. For 80 km/h speed, the QPSK and 16QAM can be used on condition that the SNR is equal or greater than 55dB. For 60 km/h speed, the 16QAM can be used on condition that the SNR is greater than 40dB, the 32QAM can be used on condition that the SNR is greater than 45dB. For 40 km/h speed, the 64QAM can be used on condition that the SNR is greater than 40dB and the 128QAM can be used on condition that the SNR is greater than 50dB. For 20 km/h speed, the 128QAM can be used on condition that the SNR is greater than 45dB and the 256QAN can be used on condition that the SNR is greater than 50dB. For the stationary receiver, the 256QAM can be used on condition that the SNR is greater than 45dB.

The 2*2 MIMO-OFDM and the OFDM tables show that, the OFDM system has a better BER factor as compared with the 2*2 MIMO-OFDM, but at the same time the data throughput of the 2*2 MIMO-OFDM system is higher. For the same example mentioned, if the desired BER in the physical layer at the receiver is $10^{-3}$, then the QPSK is the only modulation scheme choice for both OFDM and 2*2 MIMO-OFDM systems when the SNR ranges from 0 to 34dB and for all the speeds of the receiver. In addition, for a SNR greater than 35dB the green shaded values in Tables 4.28-4.33 show the type of modulation scheme which can be used for the OFDM system but which cannot be used for the 2*2 MIMO-OFDM system for the same channel conditions and for the same speed of the receiver. Another conclusion which may be drawn from Tables 4.28-4.33 is that when the SNR increases, mostly the same modulation schemes used for the OFDM system can be used for the 2*2 MIMO-OFDM system. For example, at the 35dB SNR (Table 4.28), the OFDM system can use five more choices (shaded by green color) than that the 2*2 MIMO-OFDM system can use. Moreover, for 40dB SNR, the OFDM system can use eight more choices than that the 2*2 MIMO-OFDM system can use, whereas, for 60dB SNR, the OFDM system can use only one more choice than the 2*2 MIMO-OFDM system can use.

Although it seems that the OFDM system has better BER than the BER of the 2*2 MIMO-OFDM system and sometimes may go to higher modulation order but in terms of data throughput the 2*2 MIMO-OFDM is better. For example, if the SNR is 50dB and the speed of the receiver is 40km/h, Table 4.31 shows that the OFDM system can transmit

single symbol of 256QAM modulation (8 bit per symbol) whereas the 2\*2 MIMO-OFDM system can transmit two parallel symbols of 128QAM modulation (2\*(7 bit per symbol)). This example shows that the data throughput of 2\*2 MIMO-OFDM system is higher than the data throughput of the OFDM system by 75%. Also if the speed of the receiver is 20km/k then both the two systems can use the 256QAM and as a result the data throughput of 2\*2 MIMO-OFDM system is twice the data throughput of the OFDM system.

## 4.5 Adaptation of the Modulation Scheme

The investigated communication systems can be made adaptive by enabling a choice of the modulation scheme. This choice takes into account the SNR and speed of the receiver. The results obtained in this chapter can be used to construct a look-up table containing SNR, speed of the receiver and the recommended type of modulation.

As an example, the results shown in figures 4.14-4.19, are used to construct Table 4.34. The table shows the recommended modulation scheme to achieve 10^-3 BER according to the speed of the receiver and the channel SNR.

Table 4.34: look-up table for 2\*2 MIMO-OFDM adaptive modulation

| SNR(dB)  speed | 0-30 | 35 | 40 | 45 | 50 | 55 | 60 |
|---|---|---|---|---|---|---|---|
| 0km/h | QPSK | 16QAM | 64QAM | 256QAM | 256QAM | 256QAM | 256QAM |
| 20km/h | QPSK | 16QAM | 32QAM | 128QAM | 256QAM | 256QAM | 256QAM |
| 40km/h | QPSK | 16QAM | 32QAM | 64QAM | 128QAM | 128QAM | 256QAM |
| 60km/h | QPSK | QPSK | 16QAM | 32QAM | 32QAM | 32QAM | 32QAM |
| 80km/h | QPSK | QPSK | QPSK | QPSK | QPSK | 16QAM | 16QAM |
| 100km/h | QPSK | QPSK | QPSK | QPSK | QPSK | QPSK | QPSK |
| 160km/h | QPSK | QPSK | QPSK | QPSK | QPSK | QPSK | QPSK |

The adaptive modulation in the 2*2 MIMO-OFDM systems can be easily implemented using the Table 4.34 which is searched and accordingly the type of modulation scheme is switched. Values inside this table are used to switch the mapper and the de-mapper modules (see Figure 2.12) to the appropriate modulation scheme.

# Chapter Five

## Conclusions and Suggestions for Future Work

### 5.1 Conclusions

From the results obtained, the following may be concluded:

1. The effect of the Doppler shift frequency on the received signal is completely cancelled if perfect Rayleigh fading channel parameters are considered in calculating the received signal. In this case, the relative movement between the transmitter and the receiver has no effect on the communication system. This is an ideal case.

2. The effect of the Doppler shift frequency on the received signal is nearly removed when considering the estimated Rayleigh fading channel coefficients using a single tab equalizer.

3. The worst BER performance of the used modulations usually occurs at the maximum moving receiver speed. The BER performance improves as the speed of the receiver equipment decreases.

4. The choice of the best modulation scheme for instantaneous channel conditions, to achieve the desired BER, depends on the values of the SNR and the Doppler frequency shifts (speed of the receiver).

5. For a single carrier base band transmission system, if the desired BER in physical layer at the receiver $10^{-3}$ is chosen, it is found that for 160 km/h speed of the receiver, the BPSK modulation should be used. For 100 km/h, the BPSK and QPSK can be used on

condition that the SNR is greater than 30dB. For 40 km/h, the 16QAM and 32 QAM can be used on condition that the SNR is greater than 40dB. For 10 km/h, the 64 QAM can be used on condition that the SNR is greater than 40dB. Furthermore, for the stationary receiver, the 128 QAM can be used on condition that SNR is around or greater than 50dB.

6. For OFDM system, if the desired BER in physical layer at the receiver 10^-3 is chosen, it is found that for 160 km/h and 100 km/h speed of the receiver, the QPSK modulation should be used. For 80 km/h, the QPSK and 16QAM can be used on condition that the SNR is equal or greater than 35dB. For 60 km/h, the 16QAM can be used on condition that the SNR is greater than 35dB, the 32QAM and the 64QAM can be used on condition that the SNR is greater than 40dB. For 40 km/h, the 128QAM can be used on condition that the SNR is greater than 40dB and the 256QAM can be used on condition that the SNR is greater than 50dB. For 20 km/h and the stationary receiver, the 256QAM can be used on condition that the SNR is greater than 45dB.

7. For 2*2 MIMO-OFDM, if the desired BER in physical layer at the receiver is 10^-3, it is found that for 160 km/h and 100 km/h speeds of the receiver, only the QPSK modulation should be used. For 80 km/h, the QPSK and 16QAM can be used on condition that the SNR is equal or greater than 55dB. For 60 km/h, the 16QAM can be used on condition that the SNR is greater than 40dB, and the 32QAM can be used on condition that the SNR is greater than 45dB. For 40 km/h, the 64QAM can be used on condition that the SNR is greater

than 40dB, and the 128QAM can be used on condition that the SNR is greater than 50dB. For 20 km/h, the 128QAM can be used on condition that the SNR is greater than 45dB and the 256QAN can be used on condition that the SNR is greater than 50dB. For the stationary receiver, the 256QAM can be used on condition that the SNR is greater than 45dB.

8. It may be concluded that the best and most applicable method for the IFFT zero padding to generate the OFDM symbol is the symmetric zero padding at the two sides of the IFFT inputs, which is shown in Figure 3.15. One may also conclude that the OFDM spectrum bandwidth of the real part is the same as that of the imaginary part.

9. The time spaces between the output samples of the parallel to serial convertors determine the OFDM symbol duration and consequently determine the subcarrier bandwidth.

10. If the size of the OFDM IFFT is doubled, the bandwidth needed to transmit the OFDM symbol should also be doubled on condition that the time of the OFDM symbol remains constant.

11. The bandwidth needed to transmit one OFDM symbol before and after adding CP is the same.

12. The added CP to the OFDM symbol has the same bandwidth as that of the OFDM symbol before adding the CP.

13. The BER performance of the OFDM system is better than the BER for the 2*2-MIMO-OFDM system when the equalizer used in the two systems is the ZF. On the contrary, the data throughput of the

2*2 MIMO-OFDM system is greater than that of the OFDM system.

14. Look-up tables can be easily constructed from the obtained results as a switching indexes for the adaptive modulation.

## 5.2 **Suggestions for Future Work**

The following are some suggestions for future work in this field:

1. Using the MMSE MIMO-OFDM equalizer instead of the ZF equalizer and evaluating the results in comparison to those of the ZF equalizer.

2. Increasing the number of transmitting and receiving antennas for the MIMO-OFDM system rather than 2*2 and comparing the results with the 2*2 MIMO system.

3. Using an adaptive number of pilots for channel estimation and building a table describing the best number of pilots for the instantaneous channel condition and speed of the receiver.

4. Using the Rician fading channel instead of the Rayleigh fading channel and comparing the results for all the cases.

5. Using the error detection and correction (CRC) and noticing the improvements that may occur in the system.

## References

[1] Chang-Joo Kim, Goo-Young Jeong, Young-Jo Bang, Han-Kyu Park and Sang-sam Choi, "New Rayleigh Channel Estmator Based On PSAM Channel sounding Technique," IEEE International Conference on communications ICC '97, Montreal, 1997 IEEE Explore, pp. 1518 -1520.

[2] National Instruments, "OFDM and Multi-Channel Communication Systems", report, Published on: June 19, 2013.

[3] Mohammed Aboud Kadhim, Widad Ismail, "Implementation of WIMAX IEEE802.16d Baseband Transceiver on Multi-Core Software-Defined Radio Platform", WSEAS Transaction on Communication, Issue 5, Vol. 9, May 2010.

[4] Kyongkuk Cho and Dongweon Yoon, "On the General BER Expression of One- and Two-Dimensional Amplitude Modulations," IEEE Transactions on Communications, vol. 50, no.7, pp. 1074-1080, July 2002.

[5] Larry Riche, Khalil Sujaee, and Roy George, "The performance of high order modulation QAM-OFDM in the presence multipath fading channels", IEEE Explore, 2012.

[6] S.B. Weinstein," Data Transmission by Frequency-Division Multiplexing Using the Discrete Fourier Transform", IEEE transaction on communication technology, Vol. 19, no. 5, pp. 628-634, 1971.

[7] Sridhar V., Anil Kumar M., M. Renuka, "Embedded Universal Audio Scrambler using OFDM Technique", International Journal of Engineering Research and Development, Vol. 1, Issue 2, PP. 25-28, May 2012.

[8] Kavitha K V N, Abhishek Jaiswal, Sibaram Khara, "Performance analysis of MISO-OFDM & MIMO-OFDM Systems", International Journal of Engineering and Technology (IJET), Vol. 5 no 3 June-July 2013.

[9] Oyetunji S. A and Akinninranye A. A, "Performance Evaluation Of Digital Modulation Techniques In AWGN Communication Channel," International Journal of Engineering Research & Technology (IJERT), Vol. 2, Issue 5, pp. 2100-2106, May 2013.

[10] Ahmed Ramadan, Shawki Shabaan and Abd-Elmoaty Elbadawy, "Performance Analysis of WiMAX Network for SISO-MISO Using

Adaptive Modulation and Coding", International Journal of Emerging Technology and Advanced Engineering, Vol. 4, Issue 5, May 2014.

[11] Rainer Grünheid and Hermann Rohling, "Adaptive Modulation and Multiple Access for the OFDM Transmission Technique", Wireless Personal Communications 13, Kluwer Academic Publishers, 2000.

[12] K. Seshadri Sastry and M. S. Prasad Babu, "Fuzzy logic based Adaptive Modulation Using Non Data Aided SNR Estimation for OFDM system", International Journal of Engineering Science and Technology, Vol. 2, no. 6, pp. 2384-2392, 2010.

[13] James K. Cavers, "An Analysis of Pilot Symbol Assisted Modulation for Rayleigh Fading Channels," IEEE Transaction on Vehicular Technology, Vol. 40, no. 4, pp. 686-693, November 1991.

[14] Arthur H. Ballard, "A New Multiplex Technique for Communication Systems", IEEE transactions on power apparatus and systems, Vol. 85, no.10, October-1966.

[15] Li. Zhen, Song Junde, Song Mei and Zhou Wenan, "Link adaptation of Wideband OFDM Systems in Multi-path Fading Channel", Proceedings of the 2002 IEEE Canadian Conference on Electrical & Computer Engineering, 2002.

[16] Shang Jing, Gao Yan, Li Zhen, Man Yi and Song Junde," Performance Study of Adaptive Modulation/Coding in MIMO-OFDM System", IEEE CCECE 2003. Canadian Conference on Electrical and Computer Engineering, Montreal, May-2003.

[17] Wasan M. A. Al-Tittinche, "Performance Improvement of Cellular Communication Systems Using MIMO – OFDM", M.Sc. Thesis, University of Mosul/ Electrical Engineering Department, 2006.

[18] J.Faezah, and K.Sabira, "Adaptive Modulation for OFDM Systems", International Journal of Communication Networks and Information Security (IJCNIS), Vol. 1, no. 2, pp. 1-8, August 2009.

[19] Gabriel Martorell. Felip Riera-Palou. Guillem Femenias, "Cross-Layer Fast Link Adaptation for MIMO-OFDM Based WLANs", Springer Science+Business Media, Published online: 20 April 2010.

[20] Sami H. O. Salih and Mamoun M. A. Suliman, "Implementation of Adaptive Modulation and Coding Technique using Matlab" International Journal of Scientific & Engineering Research Vol. 2, Issue 5, pp. 1-4, May-2011.

[21] Salima El Makhtari, Mohamed Moussaoui and Hassan Samadi, "Performance Evaluation of AMC turbo Coded OFDM for 3GPP Long Term Evolution downlink system", International Conference on Multimedia Computing and Systems (ICMCS), 2012 IEEE.

[22] T. S. Harivikram, Dr. R. Harikumar and Dr. C. Ganesh Babu, P.Murugamanickam, "Adaptive Modulation and Coding Rate for OFDM Systems", International Journal of Emerging Technology and Advanced Engineering, Vol. 3, Issue 2, February 2013.

[23] Dinesh B. Bhoyar, Dr. C. G. Dethe, Dr. M. M. Mushrif and Abhishek P. Narkhede, "Leaky Least Mean Square (LLMS) Algorithm For Channel Estimation In BPSK-QPSK-PSK MIMO-OFDM System", International Conference on Automation, Computing, Communication, Control and Compressed Sensing (iMac4s), 2013 IEEE.

[24] Varun Sharma and Hemant Dalal, "Implementation of MIMO-OFDM Using Adaptive Modulation Detection with Different Modulation Techniques", International Journal of Emerging Technologies and Engineering (IJETE) Vol. 1 Issue 5, June 2014.

[25] Evgenii Krouk and Sergei Semenov, "Modulation and Coding Techniqes in Wireless Communication," John Wiley & Sons Ltd, 2011.

[26] Bernard Sklar, "Digital Communication Fundamentals and Applications," Second Edition, Prentice Hall, January 2001.

[27] Raymond Chan, "Channel Prediction for Adaptive Modulation in Wireless Communications", M.Sc. thesis in Electrical Engineering, Virginia Polytechnic and State University, 2003.

[28] Tanvir Ahmed, M. M. Ali and M. Z. I. Sarkar, "BER Performance Analysis of Rayleigh Fading Channel in an Outdoor Environment With MLSE Equalizer", International Conference on Electrical and Computer Engineering, Dhaka, Bangladesh, 20-22, December, 2012.

[29] Waslon T. A. Lopes, WambertoJ.L.Queiroz, Francisco Madeiro and Marcelo S. Alencar, "Bit Error Probability of M-QAM and I $\times$ J-QAM Modulation Schemes in Nakagami Fading" IEEE Transactions on communication, Vol. 50, no. 7, pp. 1074-1080, July 2002.

[30] P. J. Lee. "Computation of the Bit Error Rate of Coherent M-ary PSK with Gray Code Bit Mapping", IEEE Transactions on Communications, Vol. 34, no. 5, pp. 488–491, May 1986.

[31] Theodore S. Rappaport, "Wirless Communication Principles and Practice," 2nd edition, Prentice Hall PTR, 1996.

[32] Lajos Hanzo, Yosef (Jos) Akhtman and Li Wang, "MIMO-OFDM for LTE, Wi-Fi and WiMAX", A John Wiley and Sons, Ltd, Publication, 2011.

[33] Erik Dahlman, Stefan Parkvall, Johan Skold and Per Beming, "3G Evolution HSPA and LTE for Mobile Broadband", Published by Elsevier, 2008.

[34] Mitalee Agrawal, Yudhishthir Raut, "BER Analysis of MIMO OFDM System for AWGN & Rayleigh Fading Channel", International Journal of Computer Applications, Vol. 34, no. 9, November 2011.

[35] Yong Soo Cho, Jaekwon Kim ,Won Young Yang ,Chung G. Kang, "MIMO-OFDM Wireless Communication With Matlab", John Wiley & Sons (Asia) Pte Ltd, 2010.

[36] Ramkumar Gowrishankar, "Adaptive Modulation Based MIMO Systems", M.Sc. thesis in Electrical Engineering, University of Hawai'i, 2005.

[37] Christopher Cox, "An Introduction to LTE", A John Wiley & Sons, Ltd., 2012.

[38] Krzysztof Wesolowski, "Mobile Communication Systems", John Wiley & Sons, Ltd, 2002.

## إقرار المشرف

أشهد بان الرسالة الموسومة بـ "التضمينين التكيفي لمنظومة هوائيات متعددة الإدخال متعددة الإخراج ذات الوصول المتعدد للترددات المتعامدة" قد جرى تحت إشرافي في جامعة الموصل وهي جزء من متطلبات نيل شهادة الماجستير في هندسة الاتصالات.
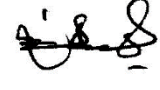
التوقيع :

المشرف : د. يونس محمود عبوش

التاريخ : 30 / 11 / 2014


## إقرار المقيم اللغوي

أشهد بأني قمت بمراجعة الرسالة الموسومة بـ " التضمين التكيفي لمنظومة هوائيات متعددة الإدخال متعددة الإخراج ذات الوصول المتعدد للترددات المتعامدة" من الناحية اللغوية وتصحيح ما ورد فيها من اخطاء لغوية وتعبيرية وبذلك أصبحت الرسالة مؤهلة للمناقشة بقدر تعلق الأمر بسلامة الأسلوب وصحة التعبير.

التوقيع :

المقوم اللغوي : أ. د. عباس جودة رحيم

التاريخ : ٥ / ١٢ / ٢٠١٤م


## إقرار رئيس لجنة الدراسات العليا

بناءً على التوصيات المقدمة من قبل المشرف والمقوم اللغوي أرشح هذه الرسالة للمناقشة .

التوقيع :

الاستاذ الدكتور:

التاريخ : / /


## إقرار رئيس القسم

بناءً على التوصيات التي تقدم بها المشرف والمقوم اللغوي ورئيس لجنة الدراسات العليا أرشح هذه الرسالة للمناقشة .

التوقيع :

الدكتور: محمود أحمد محمود

التاريخ : / /

1

**الخلاصة**

في السنوات القليلة الماضية، شهدت تقنية الإتصالات اللاسلكية تطوراً كبيراً فتح باباً للكثير من التطبيقات الجديدة التي أدت إلى إرسال و إستلام البيانات بسرعة عالية بعيداً عن تحديدات الموقع و سرعة جهاز الإستقبال.

لقد ثبت مؤخراً أن من أنجح الطرق التي تؤدي إلى متعدد الإشارات الحاملة هو نظام الوصول المتعدد للترددات المتعامدة (OFDM) الذي لا يقوم بتحقيق سرع عالية لنقل البيانات فحسب بل يقوم أيضا بتركيزها موقعياً وبالتالي مضاعفة البيانات المنقولة أضعافا كثيرة. ولغرض زيادة كفاءة المنظومة تم استخدام هوائيات متعددة لكل من الإرسال و الإستقبال و المسماة هوائيات متعددة الإدخال متعددة الإخراج (MIMO).

فضلاً عن تقنية هوائيات متعددة الإدخال متعددة الإخراج (MIMO) و تقنية الوصول المتعدد للترددات المتعامدة (OFDM) فإن تقنية تكييف التضمين (Adaptive Modulation) تعد تقنية مهمة أخرى لزيادة كمية و سرعة نقل البيانات. ويمكن تحقيق ذلك بنسبة خطأ مقبولة للبتات المنقولة (BER) و بأعلى إنتاجية لنقل البيانات (Data Throughput) اذا ما تم احتساب نسبة الإشارة إلى الضوضاء (SNR) و زحف تردد دوبلر بشكل جيد. لذلك فإن ما تم إنجازه في هذه الرسالة هو تقدير أفضل تركيبة لنوعيات التضمين اعتماداً على تمثيل قناة النقل موصوفة بخفوت رايلي و مشوهة بإضافة الضوضاء البيضاء ذات توزيع كاوسي و لسرع متعددة لجهاز الإستقبال. لقد تم في هذا البحث دراسة و تقييم ثلاث منظومات للإتصالات هي: منظومة الحامل المنفرد للإرسال و منظومة الوصول المتعدد للترددات المتعامدة (OFDM) و منظومة متعددة الإدخال متعددة الإخراج للوصول المتعدد للترددات المتعامدة (MIMO-OFDM 2*2). لقد شملت دراسة و تقييم هذه المنظومات الثلاث كلاً من نسبة خطأ البتات المنقولة (BER) و إنتاجية البيانات (Data Throughput) و لسرع مختلفة لجهاز الإستقبال، و على أساس ذالك تم تقرير نوع التكييف للتضمين (Modulation Adaptation). إن تبديل نوع التضمين الى الافضل اعتمادا على الظروف الأنية لقناة الأتصال لتحقيق نسبة خطأ مقبولة للبتات المنقولة يعتمد بشكل أساس على نسبة الإشارة إلى الضوضاء و إنحراف ترددات دوبلر و يتم ذلك عن طريق جدول تم إحتسابه لهذا الغرض.

التضمين التكيفي لمنظومة هوائيات متعددة الإدخال متعددة الإخراج ذات الوصول المتعدد للترددات المتعامدة

رسالة تقدم بها

# محمد باسل شكر
**(بكالوريوس هندسة إتصالات)**

إلى

مجلس كلية هندسة الالكترونيات في جامعة الموصل

وهي جزء من متطلبات نيل شهادة ماجستير علوم في هندسة الاتصالات

بإشراف

# الدكتور يونس محمود عبوش

1436 هـ                              2015م

جامعة الموصل

كلية هندسة الالكترونيات

# التضمين التكيفي لمنظومة هوائيات متعددة الإدخال متعددة الإخراج ذات الوصول المتعدد للترددات المتعامدة

## محمد باسل شكر
### (بكالوريوس هندسة إتصالات)

## رسالة ماجستير علوم في هندسة الاتصالات

## بإشراف
## الدكتور يونس محمود عبوش